Title: Proteomic Architecture of Human Coronary and Aortic Atherosclerosis

Authors:

Herrington David M[1*], Mao Chunhong[2], Parker Sarah[3], Fu Zongming[4], Yu Guoqiang[5], Chen Lulu[5], Venkatraman Vidya[3], Fu Yi[5], Wang Yizhi[5], Howard Tim[6], Goo Jun[7], Zhao CF[1], Liu Yongming[8], Saylor Georgia[1], Athas Grace[9], Troxclair Dana[9], Hixson James[7*], Vander Heide Richard[9*], Wang Yue[4*],Van Eyk Jennifer[3*]

Affiliations:

[1]Section on Cardiovascular Medicine, Dept. of Medicine, Wake Forest School of Medicine; Winston Salem NC 27157 USA

[2]Virginia Bioinformatics Institute, Virginia Tech, Blacksburg, VA 24061, USA

[3]Advanced Clinical Biosystems Research Institute, The Heart Institute, and Department of Medicine, Cedars-Sinai Medical Center, Los Angeles, California 90048, USA

[4]Johns Hopkins Medical Institute, Baltimore MD 21287 USA

[5]Department of Electrical and Computer Engineering, Virginia Polytechnic Institute and State University, Arlington, VA 22203, USA

[6]Center for Genomics and Personalized Medicine Research, Wake Forest School of Medicine; Winston Salem NC 27157 USA

[7]Department of Epidemiology, Human Genetics and Environmental Sciences, Human Genetics Centre, School of Public Health, University of Texas Health Science Center at Houston, Houston Tx 77225 USA

[8]Department of Epidemiology, Division of Public Health Sciences, Wake Forest School of Medicine; Winston Salem NC 27157 USA

[9]Department of Pathology, Louisiana State Health Science Center, New Orleans, Louisiana 70112 USA

* Co-senior author

Corresponding Author Information:

David Herrington, MD, MHS, Dalton McMichael Chair in Cardiovascular Medicine
Department of Internal Medicine
Medical Center Boulevard \ Winston-Salem, NC 27157
336.716.4950 (office), dherring@wakehealth.edu

Summary

The inability to detect premature atherosclerosis significantly hinders implementation of personalized therapy to prevent coronary heart disease. A comprehensive understanding of arterial protein networks and how they change in early atherosclerosis could identify new biomarkers for disease detection and improved therapeutic targets. Here we describe the human arterial proteome and the proteomic features strongly associated with early atherosclerosis based on mass-spectrometry analysis of coronary artery and aortic specimens from 100 autopsied young adults (200 arterial specimens). Convex analysis of mixtures, differential dependent network modeling and bioinformatic analyses defined the composition, network re-wiring and likely regulatory features of the protein networks associated with early atherosclerosis. Among other things the results reveal major differences in mitochondrial protein mass between the coronary artery and distal aorta in both normal and atherosclerotic samples – highlighting the importance of anatomic specificity and dynamic network structures in in the study of arterial proteomics. The publicly available data resource and the description of the analysis pipeline establish a new foundation for understanding the proteomic architecture of atherosclerosis and provide a template for similar investigations of other chronic diseases characterized by multi-cellular tissue phenotypes.

Keywords

Proteomics, human atherosclerosis, mass-spectrometry, network modelling, coronary artery, aorta

Highlights

- LC MS/MS analysis performed on 200 human aortic or coronary artery samples
- Numerous proteins, networks, and regulatory pathways associated with early atherosclerosis
- Mitochondrial proteins mass and selected metabolic regulatory pathways vary dramatically by disease status and anatomic location
- Publically available data resource and analytic pipeline are provided or described in detail

Introduction

At the molecular level atherosclerosis can be defined as an assembly of hundreds of intra- and extra-cellular proteins that jointly alter cellular processes and produce characteristic remodeling of the local vascular environment. Ultimately, these proteomic changes produce the lesions responsible for most ischemic cardiovascular events. Unfortunately, current methods to treat and prevent cardiovascular disease focus on antecedent risk factors that are not deterministic of these changes, or on anatomic manifestations of disease that are only evident long after these proteomic changes are underway. To improve early disease detection, and to interrupt the disease process before clinical consequences occur, it is necessary to recognize and understand the specific patterns and dynamic features of arterial protein networks that constitute the molecular signatures of healthy and atherosclerotic arterial tissues.

Previous studies have described features of the arterial proteome in murine [1-3] and cell models of atherosclerosis [4,5] and in limited numbers of human arterial samples with and without atherosclerosis [6-18] . To date there has not been a comprehensive survey of the human arterial proteome based on a large number of human coronary and aortic samples, using contemporary LC-MS/MS technology and subsequent identification of the proteins that signify presence of pre-clinical atherosclerosis. Accordingly, we established a tissue acquisition, mass-spectrometry analysis and statistical and bioinformatic pipeline to characterize the human coronary and distal aortic arterial proteome and to identify those proteins, networks and pathways most strongly associated with early atherosclerotic lesions. Detailed analyses of the detected proteins reveal several key features of the coronary and aortic proteome in health and disease as outlined below, and demonstrate how the data resource may be used to guide more targeted functional research concerning the proteomics of early atherosclerosis.

Results

Global Analysis of Coronary and Abdominal Aortic Proteomes Identifies Novel Arterial Proteins and Scale-Free Network Topologies

Based on stringent quality control and calling criteria a total of 1925 unambiguous protein groups (hereinafter referred to as “proteins”) were identified in one or more left anterior descending (LAD) or distal abdominal aorta (AA) samples, including 974 proteins present in 50% or more of the LAD or AA samples (**Supplementary**

Table 1). The 974 proteins represent a wide range of biological processes, molecular functions, cellular components and canonical pathways[19] (**Supplemental Figs. 1a-c and Supplemental Tables 2-5**). Of the 1925 proteins, 274 have not been previously described in twelve prior studies that directly analyzed protein content of human arterial tissues (**Supplemental Table 1**); including 52 proteins present in more than 50% of either the LAD or AA samples. (All but one of these 52 proteins were, nevertheless, predicted based on RNASeq analysis of human coronary and aortic transcriptional databases (GTEX)).

The 944 unique proteins identified in the LAD exhibited a scale-free network topology typically seen in complex adaptive networks of molecular or cellular constituents from a variety of living organisms [20-22] (**Fig. 1**). Furthermore, these proteins included several distinct and reproducible co-expression modules that roughly correlated with specific cellular functions and locations such as mitochondrial proteins involved with cellular respiration (Red module), nuclear proteins involved with chromatin assembly and organization (Turquoise module), and extra cellular matrix proteins (Brown module). A similar scale-free topology and functional modular structure was also evident in the protein data from the AA (**Supplemental Fig. 2**.) A scale-free topology suggests that the arterial proteome may arise from a complex adaptive system with properties such as self-organized criticality, emergence, and resilience.[21,23,24] Complex adaptive systems such as this are uniquely well-suited for description using graph theory and network or non-linear dynamic modelling to reveal functional insights that may be less evident from more conventional linear conceptual models and methods [25-27]

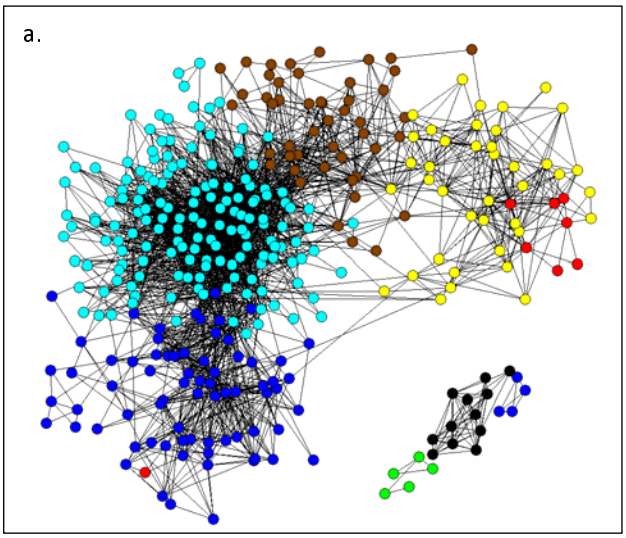

d.

Module (# of Proteins)	GO:Process (- log corr p-value)	GO:Function (log corr p-value)	GO:Component (log corr p-value)	Exemplar Protein
Green (n=54)	cellular localization (5.97)	protein complex binding (6.11)	vesicle (24.36)	Plastin-2
Yellow (n=104)	protein activation cascade (56.24)	immunoglobulin receptor binding (16.10)	blood microparticle (111.36)	Complement C3
Brown (n=109)	extracellular matrix organization (28.99)	extracellular matrix structural constituent (11.85)	extracellular region (61.77)	Biglycan
Blue (n=209)	oxidation-reduction process (32.09)	oxidoreductase activity (13.68)	extracellular vesicular exosome (61.99)	Long-chain-fatty-acid--CoA ligase 1
Red (n=35)	generation of precursor metabolites and energy (6.53)	H ion transmembrane transporter activity (5.75)	extracellular vesicular exosome (14.72)	ATP synthase subunit d, mitochondrial
Turquoise (n=376)	cell component organization or biogenesis (69.37)	protein binding (126.71)	extracellular vesicular exosome (211.89)	Prelamin-A/C
Black (n=34)	small molecule metabolic process (11.96)	oxygen transporter activity (9.09)	extracellular vesicular exosome (19.56)	Hemoglobin subunit delta

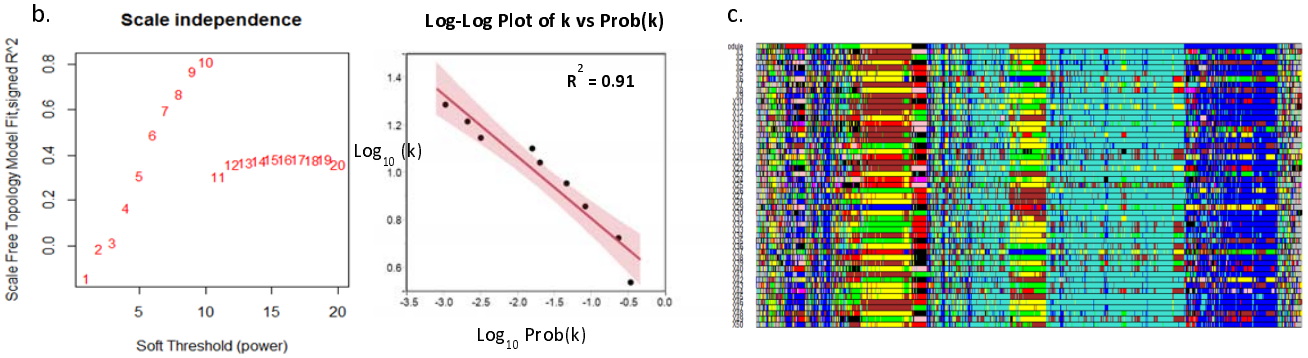

Figure 1. Weighted Co-Expression Network Analysis of Human LAD Proteins a. Adjacency map of LAD proteins color coded by module assignment based on hierarchical clustering of the topological overlap matrix (TOM)-based dissimilarity measure. For clarity of presentation only nodes (proteins) with at least one edge (adjacency measure (k)) > 97.5%tile are shown. b. Left panel shows that scale-free topology is best approximated when the adjacency power parameter β= 10. Right panel shows the log-log plot of adjacency (k) vs prob(k) with β= 10, confirming the power-law relationship in the connectivity of the expressed proteins. c. Module assignment for fifty 90% random samples of the data illustrating the overall stability of the modular structure of the protein expression patterns. Colors are assigned according cluster size which may vary with each random sample. As a result actual color assignment may vary from run to run, but module membership remains relatively stable. d. Top non-redundant GO Terms with Bonferroni corrected p-values and an exemplar protein for each module.

Comparison of Normal Coronary and Aortic Proteomes Reveal Significant Differences in Mitochondrial Protein Mass

Several hundred proteins were detected in the LAD but not in the AA samples (**Supplemental Figure 3**). This pattern was observed when limiting the analysis to completely normal samples (n=30 in each territory) or when limiting the proteins to those present in ≥ 50% of the LAD and/or AA samples. GO term analysis of the proteins exclusively detected in the LAD indicated significant enrichment of mitochondrial proteins (p-value range $1.7x10^{-6}$ to $1.8x10^{-28}$).

To confirm this apparent differential abundance of mitochondrial proteins between LAD and AA samples we performed a more sensitive data independent acquisition MS (SWATH) analysis of entirely normal samples (n=30 in each location), focusing on n=114 mitochondrial proteins involved with fatty acid metabolism, oxidative phosphorylation, TCA cycle and mitochondrial biogenesis. To account for possible site and sample differences in cellular material or protein extraction yields the quantitative results were adjusted for several housekeeping proteins, a smooth muscle cell specific marker protein and age and sex of the autopsied cases. Overall, mitochondrial proteins were 1.98-fold more abundant in the LAD compared with the AA ($p<0.001$) including a 2.25 fold increase in oxidative phosphorylation proteins ($p<0.001$) and an isolated >10-fold excess of inorganic pyrophosphatase ($p<0.001$; **Figure 2)**. A similar comparison of extracellular matrix proteins revealed only a small, albeit statistically significant ($p=0.01$) 6% excess in ECM proteins in the AA samples compared with the LAD (**Supplemental Figure 4**). (A notable exception was tenascin which had a >10-fold excess in AA samples compared with LAD ($p<0.0001$).)

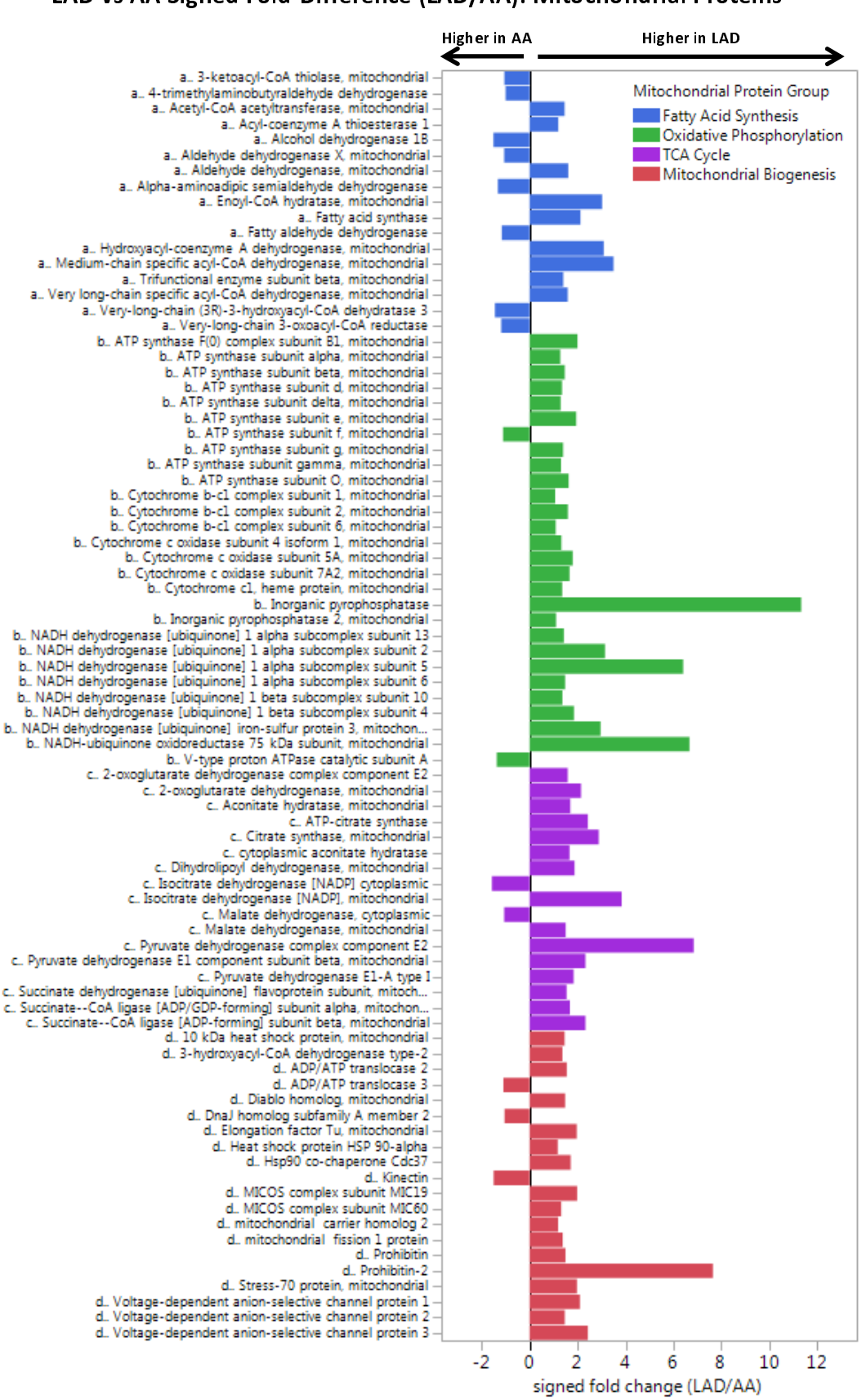

Figure 2. Comparison of Mitochondrial Proteins in Normal LAD and AA Samples. Data independent MS (SWATH) analysis of completely normal LAD and AA samples (n=30 from each anatomic location) with adjustment for age, sex, MYH11, RABA7A, TERA, G6PI. LAD vs AA MANOVA p-values by proteins class: fatty acid metabolism, $p = 0.04$, oxidative phosphorylation $p < 0.0001$, TCA $p < 0.0001$, mitochondrial biogenesis $p < 0.0001$.

These data suggest fundamental differences in mitochondrial mass and potential aerobic capacity between LAD and AA tissues, possibly reflecting the differing energy requirements of these two arterial tissue types. This is exemplified by the dramatic excess of inorganic pyrophasphatase in the LAD compared to the aorta suggesting enhanced capacity to initiate fatty acid oxidation. This heterogeneity in the proteomic profile of two arterial tissues emphasize the need for arterial anatomic specificity when characterizing the proteomics and functional biology of arterial tissues – especially if considering mechanisms or interventions that involve metabolic pathways (see below)

Atherosclerotic tissues in both the LAD and AA present a proteomic profile consistent with TNF activation; however, the LAD also provides evidence of inhibition of PPAR-α, PPAR-γ, and insulin receptor regulated proteins, a pattern that is not evident in the AA.

To define the proteomic profile of early atherosclerosis two complementary phenotyping strategies were used. First, each sample was graded by a vascular histopathologist according to %surface area involvement of normal intima (NL), fatty streak (FS) or fibrous plaque (FP). Extensive regression analyses (MANOVA, GLM, Ordinal Regression, Elastic Net) were performed to identify proteins individually or jointly associated with %FP in the LAD and AA samples (**Supplemental Tables 6-7, Supplemental Figure 5**). The internal validity of these data is evidenced by the presence and consistency across anatomic locations of several known protein markers of atherosclerosis from model systems among the top hits (e.g. Apo B-100, Ig mu chain C, CD5 antigen-like, Plastin-2, Tenascin, Thrombospondin-1, Cathepsin B, and Vitronectin.) [1]

Separately, convex analysis of mixtures[22] (CAM) was used to de-convolve the global protein profiles from individual samples into data-derived tissue phenotypes and to identify marker proteins associated with each data-derived tissue phenotype (**LAD: Figure 3, AA: Supplemental Figure 6**). This approach has the advantage of incorporating information about tissue phenotype from the global protein profiles that is independent of the pathologist visual inspection of the arterial samples. The data-derived tissue phenotypes, and associated FP marker proteins roughly correlated with results based on pathologic assessment of extent of disease, but retained sufficient variation from pathology based results to suggest complementary information was present (**Supplemental Figure 7**).

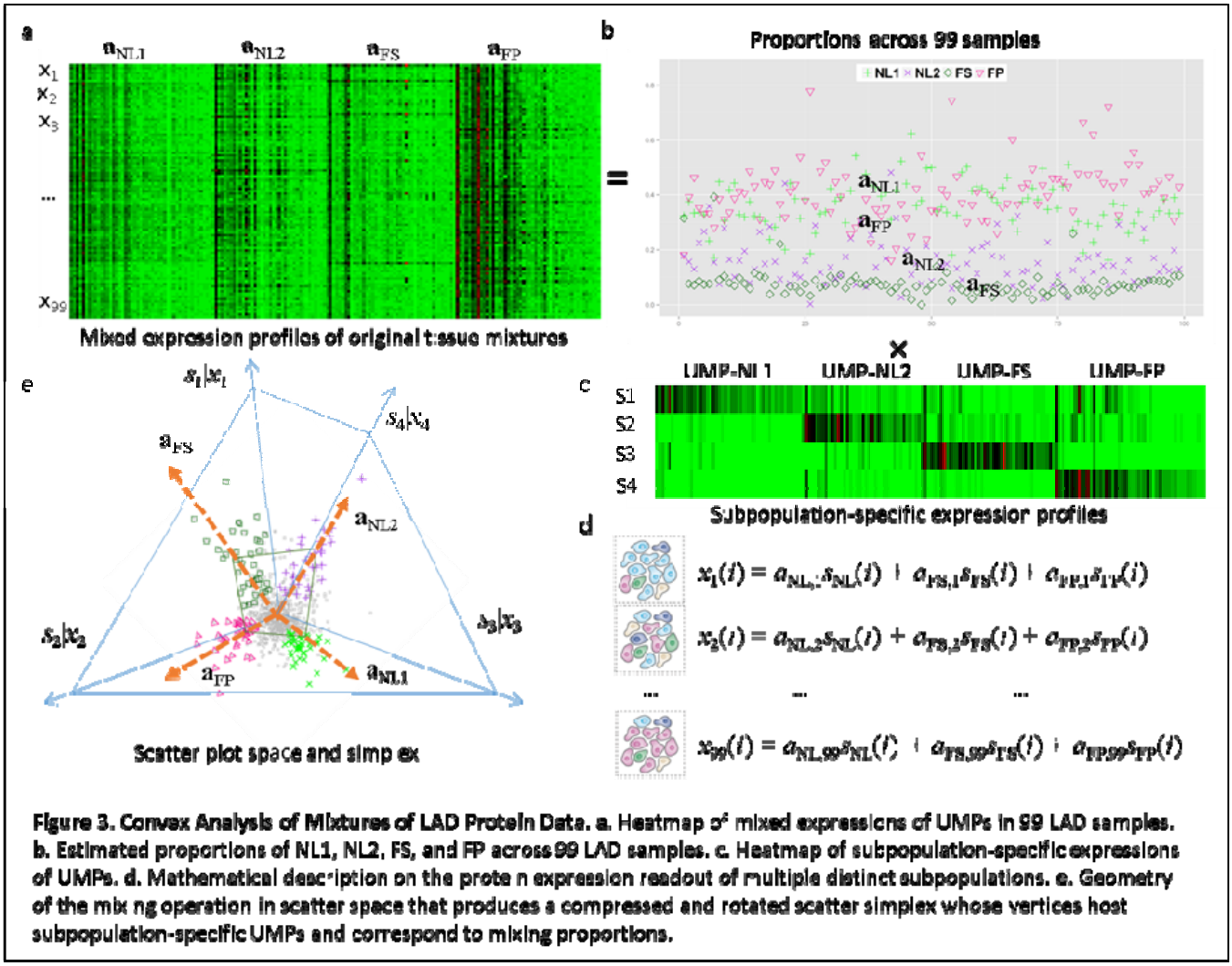

Figure 3. Convex Analysis of Mixtures of LAD Protein Data. a. Heatmap of mixed expressions of UMPs in 99 LAD samples. **b.** Estimated proportions of NL1, NL2, FS, and FP across 99 LAD samples. **c.** Heatmap of subpopulation-specific expressions of UMPs. **d.** Mathematical description on the protein expression readout of multiple distinct subpopulations. **e.** Geometry of the mixing operation in scatter space that produces a compressed and rotated scatter simplex whose vertices host subpopulation-specific UMPs and correspond to mixing proportions.

To take full advantage of both phenotyping strategies we used principal component analysis and hierarchical clustering of the pathologist- and CAM-derived phenotype data to produce a patho-proteomic classification for each LAD sample (**Fig. 4**). The clusters at the extremes of the first principle component identified samples highly enriched with FP or NL tissue (FP: n=15; NL: n=30) with little or no confounding from fatty streaks from either a gross pathology or global proteomic perspective. Comparing these FP and NL enriched samples identified eighty-nine (n=89) individual proteins with ≥ (+/-) 1.7 fold-difference and a t-test q-value of ≤0.05 for FP vs NL (**Supplemental Tables 8 and 9)**. Bioinformatic functional analysis of these atherosclerosis associated proteins revealed a pattern consistent with activation of the TNF-α pathway (p=2.64E-07), but also inhibition of insulin receptor, PPAR-α and PPAR-γ pathways (p=4.22E-10, 2.42E-13, 8.56E-16 respectively) (**Fig. 4, Supplemental Table 10**). A similar analysis of the atherosclerosis proteins in the AA samples (FP: n= 9, NL: N= 18) confirmed a core group of n=19 early atherosclerosis-associated proteins that were shared

across both anatomic territories (**Supplemental Table 11-13**) and also produced a pattern consistent with TNF activation similar to the LAD (p=1.92E-05). However, in the AA sample proteomes there was no evidence of inhibition of the insulin receptor, PPAR-α or PPAR-γ pathways (**Supplemental Tables 10**).

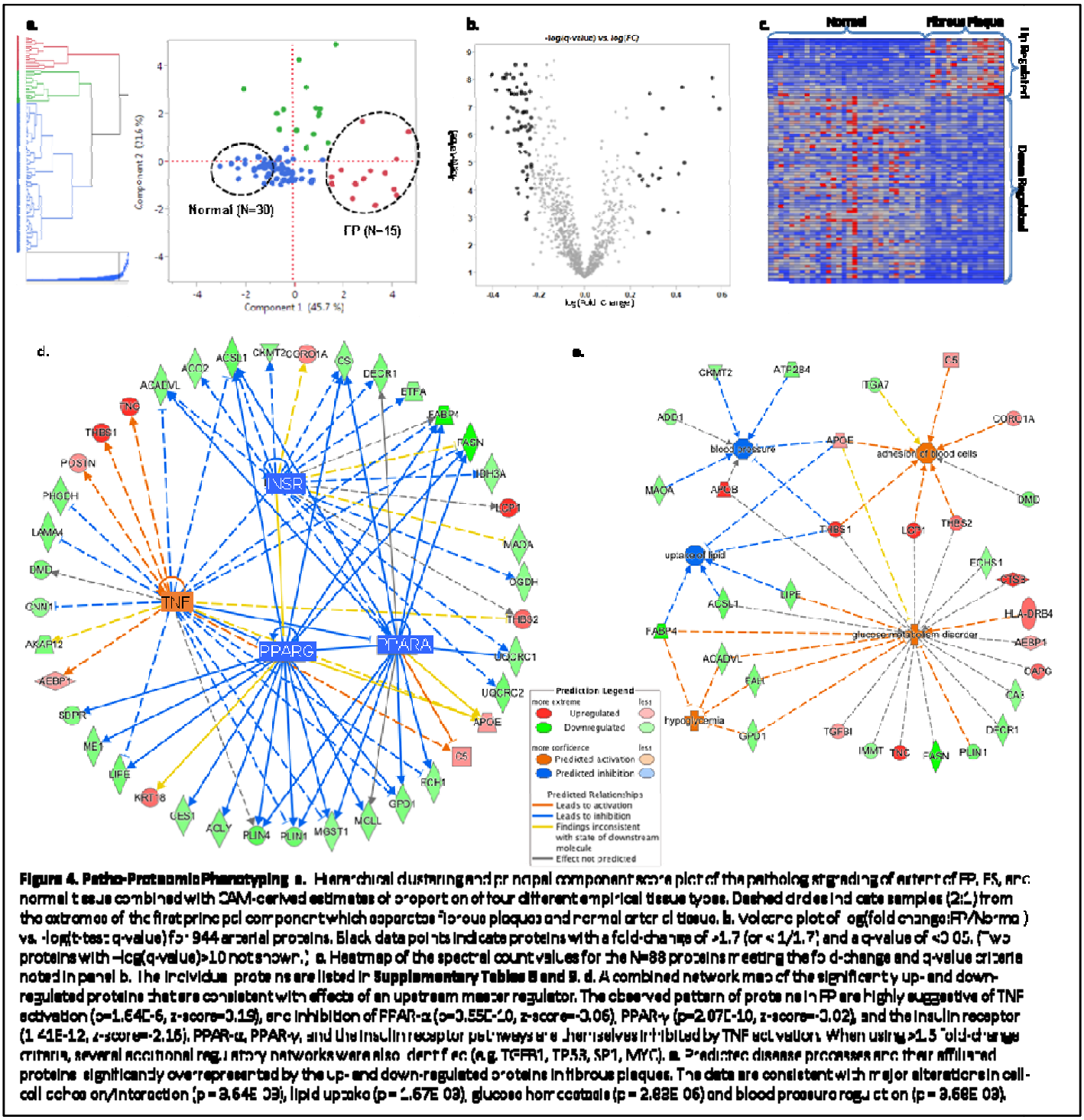

Figure 4. Patho-Proteomic Phenotyping a. Hierarchical clustering and principal component score plot of the pathological grading of artery of FP, FS, and normal tissue combined with CAM-derived estimates of proportion of four different empirical tissue types. Dashed circles indicate samples (2:1) from the extremes of the first principal component which separates fibrous plaques and normal arterial tissue. **b.** Volcano plot of log(fold change:FP/Normal) vs. -log(t-test q-value) for 944 arterial proteins. Black data points indicate proteins with a fold-change of >1.7 (or < 1/1.7) and a q-value of <0.05. (Two proteins with -log(q-value)>10 not shown.) **c.** Heatmap of the spectral count values for the N=88 proteins meeting the fold-change and q-value criteria noted in panel b. The individual proteins are listed in **Supplementary Tables 8 and 9. d.** A combined network map of the significantly up- and down-regulated proteins that are consistent with effects of an upstream master regulator. The observed pattern of proteins in FP are highly suggestive of TNF activation (p=1.64E-6, z-score=3.19), and inhibition of PPAR-α (p=3.55E-10, z-score=-3.06), PPAR-γ (p=2.07E-10, z-score=-3.02), and the insulin receptor (1.41E-12, z-score=-2.15). PPAR-α, PPAR-γ, and the insulin receptor pathways are themselves inhibited by TNF activation. When using >1.5 fold-change criteria, several additional regulatory networks were also identified (e.g. TGFB1, TP53, SP1, MYC). **e.** Predicted disease processes and their affiliated proteins significantly over-represented by the up- and down-regulated proteins in fibrous plaques. The data are consistent with major alterations in cell-cell adhesion/interaction (p = 3.64E-03), lipid uptake (p = 1.67E-03), glucose homeostasis (p = 2.63E-06) and blood pressure regulation (p = 3.66E-03).

Differential network analysis of coronary and aortic proteomes indicate divergent mitochondrial dynamics in the setting of atherosclerosis characterized by reduced mitochondrial mass in coronary arteries that is not evident in in the distal abdominal aorta.

An important feature of complex adaptive systems is the potential for network topologies to change under different conditions. Accordingly, we used differential dependent network (DDN) analysis of the FP-associated proteins identified above to select proteins that were pivotal in the re-wiring of the network structure between NL and FP in the LAD samples (**Figure 5**). Analysis of n=26 re-wiring hub proteins revealed significant enrichment of TCA proteins ($p=4.8x10^{-6}$). Subsequent analysis of individual TCA proteins documented an average 60% reduction in TCA proteins in FP enriched samples vs. NL.

a.

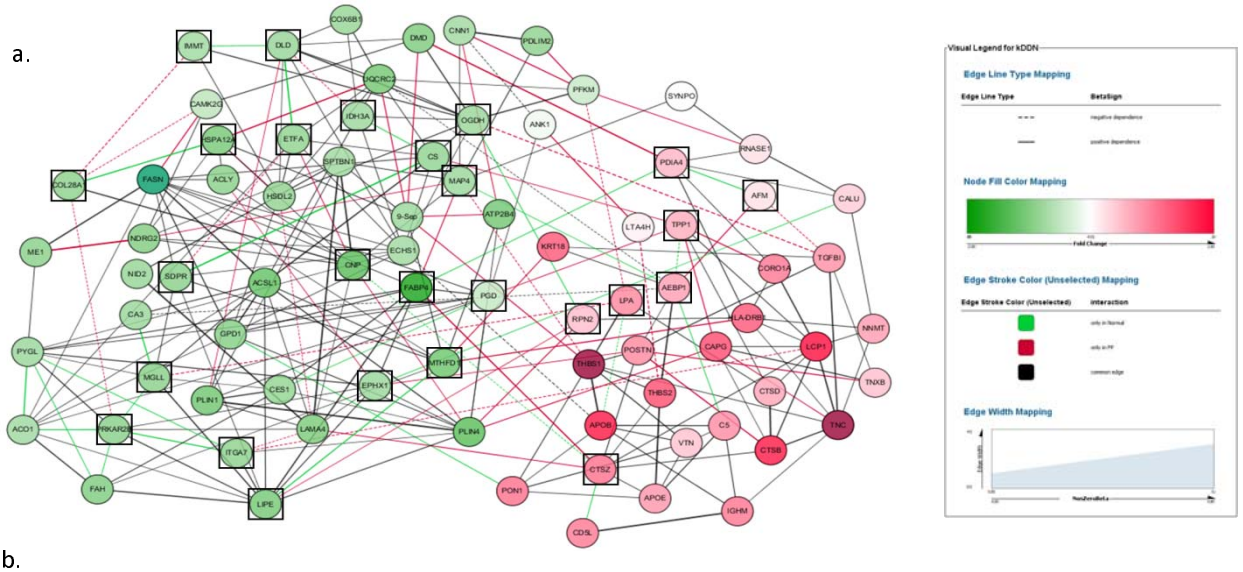

b.

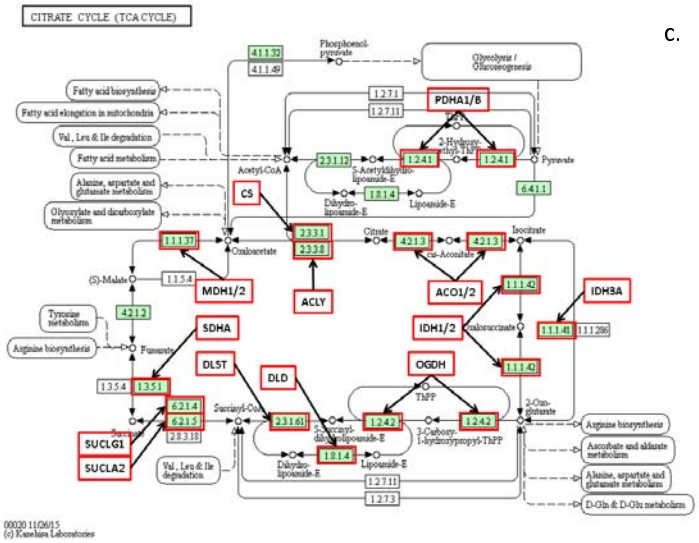

c.

Uniprot ID	Protein Name	Gene Symbol	FP/NL	p-value	q-value
O75390	Citrate synthase, mitochondrial	CS	0.532422	2.96E-04	1.88E-03
P53396	ATP-citrate synthase	ACLY	0.512504	3.66E-04	2.06E-03
Q99798	Aconitate hydratase, mitochondrial	ACO2	0.555556	2.16E-06	1.96E-04
P21399	Cytoplasmic aconitate hydratase	ACO1	0.584052	2.18E-03	7.94E-03
O75874	Isocitrate dehydrogenase [NADP] cytoplasmic	IDH1	0.982143	8.30E-01	3.90E-01
P48735	Isocitrate dehydrogenase [NADP], mitochondrial	IDH2	0.596685	3.34E-03	1.02E-02
P50213	Isocitrate dehydrogenase [NAD] subunit alpha, mitochondrial	IDH3A	0.573422	1.18E-03	5.06E-03
Q02218	2-oxoglutarate dehydrogenase, mitochondrial	OGDH	0.563903	4.88E-03	1.24E-02
P36957	Dihydrolipoyllysine-residue succinyltransferase component of 2-oxoglutarate dehydrogenase complex, mitochondrial	DLST	0.603627	1.08E-04	9.80E-04
P09622	Dihydrolipoyl dehydrogenase, mitochondrial	DLD	0.555556	1.90E-05	3.88E-04
P53597	Succinyl-CoA ligase [ADP/GDP-forming] subunit alpha, mitochondrial	SUCLG1	0.866039	7.81E-02	7.88E-02
Q9P2R7	Succinyl-CoA ligase [ADP-forming] subunit beta, mitochondrial	SUCLA2	0.754927	3.42E-02	4.43E-02
P31040	Succinate dehydrogenase [ubiquinone] flavoprotein subunit, mitochondrial	SDHA	0.651365	3.67E-03	1.08E-02
P40925	Malate dehydrogenase, cytoplasmic	MDH1	0.776119	3.31E-03	1.02E-02
P40926	Malate dehydrogenase, mitochondrial	MDH2	0.811429	3.06E-02	4.18E-02
P08559	Pyruvate dehydrogenase E1 component subunit alpha, somatic form, mitochondrial	PDHA1	0.618138	9.32E-04	4.18E-03
P11177	Pyruvate dehydrogenase E1 component subunit beta, mitochondrial	PDHB	0.557034	1.33E-04	1.08E-03

Figure 5 Differential Network Analysis of FP Associated Proteins in the LAD **a.** Plot depicts the re-wiring of protein networks between FP and NL samples. Green nodes are up-regulated and red nodes are down-regulated in FP samples. Green edges indicate significant correlation in normal samples not present in FP samples. Red edges indicate significant correlation in FP samples not present in normal samples. Black squares indicate differential network "hub proteins" (ie. proteins with different couplings to network partners in both FP and NL samples). Go term analysis of the differential network hub proteins indicated significant enrichment of TCA proteins (p=4.8x10-6). **b**. TCA cycle proteins with MS data available for additional analysis. Every protein indicated by a red box was quantitatively lower in FP samples after adjustment for housekeeping proteins, age and sex. **c**. Statistical comparison of TCA proteins in FP vs NL LAD samples.

To confirm and extend this observation, SWATH analysis of a broad-based panel of n=114 mitochondrial proteins was performed comparing FP vs NL in the LAD (**Figure 6**). The results documented a consistent reduction of a wide range of mitochondrial proteins in the FP samples compared to NL samples after adjustment for housekeeping and vascular smooth muscle cell marker proteins, age and sex. In contrast, a similar analysis of the same proteins in AA samples revealed a much less consistent and non-statistically

significant pattern of mitochondrial protein suppression. To determine if this was a mitochondrial specific phenomenon we also performed targeted SWATH analysis of a panel of ECM proteins (n=77) and found a modest atherosclerosis-associated increase of ECM proteins in both territories (LAD mean fold-increase = 1.25, MANOVA p-value= 0.02; AA mean fold increase = 1.78 fold increase, p-value = 0.017); although there were specific examples of anatomic discordance that deserve further study (e.g. laminins and nidogens) (**Supplemental Figure 8**).

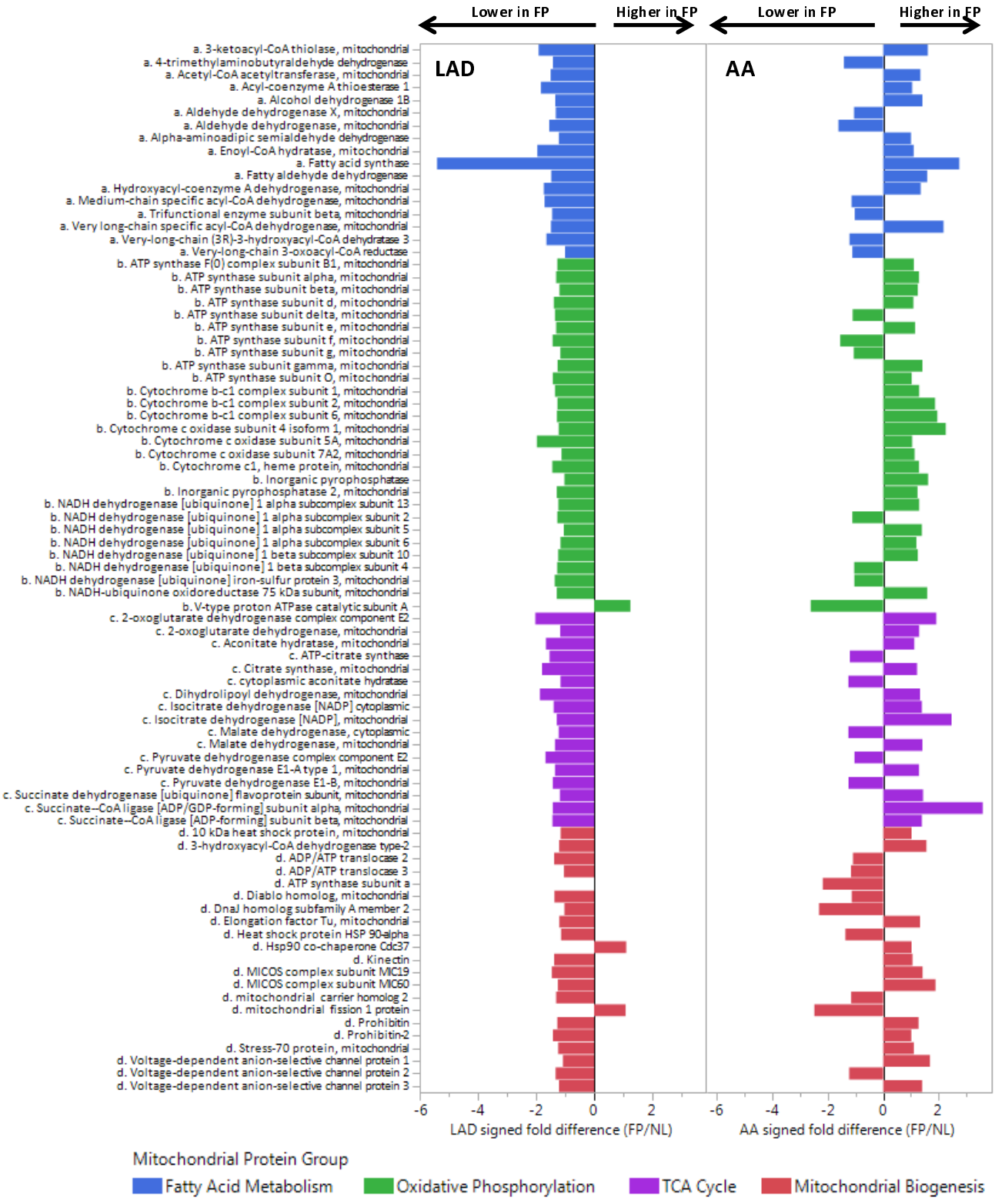

Figure 6. Comparison of Mitochondrial Proteins in FP vs NL Samples from the LAD and AA Data independent acquisition (SWATH) analysis was used to compare a targeted set of mitochondrial proteins in n=15 FP and n=30 NL LAD samples after adjustment for age, sex, MYH11, RABA7A, TERA, G6PI. Histogram bars indicate relative difference between FP and NL samples in each anatomic location. LAD MANOVA p-value for each mitochondrial protein group: p <0.0001 for each group; AA MANOVA p-values for each mitochondrial protein group: p = n.s. for each group.

Discussion

The results here provide a comprehensive survey of human coronary and aortic proteins and identify individual proteins, protein networks and regulatory pathways indicative of early atherosclerosis. These data can be distinguished from prior work because of the number and diversity of proteins identified, the fact that these proteins were obtained from a large number of human coronary and aortic arterial samples where the effects of local tissue context, natural variation in human subjects, and a range of arterial tissue phenotypes from normal to early atherosclerosis are manifest. Several analytic methods were used to illuminate complex networks involving many proteins that jointly signify arterial health and disease. Importantly, the publicly accessible data generated by this work, and the analytic methods depicted here represent foundational resources that could lead to a wide range of future research concerning human arterial protein biology.

There are several notable findings among the many results reported here. First, the human arterial proteome exhibits features consistent with a complex adaptive network, reiterating the concept that complex adaptive networks are an overarching organizational feature common to many biologic systems[28]. Looking at the arterial proteome through the lens of complexity theory including concepts such a scale-invariance (as documented here), self-organized criticality, emergence, and resiliency [21,23,24] may produce insights that have escaped more narrowly focused investigations of a smaller number of proteins or a more linear and deterministic framework. The differential dependent networks presented here emphasize this point by defining dynamic features of complex protein networks that signify normal versus atherosclerotic arteries and using key elements of these dynamic networks to discover important aspects of the proteome in atherosclerosis that were not initially evident by other means.

Second, the data document significant anatomic variation in the abundance of mitochondrial proteins in normal arterial samples, suggesting that coronary arteries likely have considerably greater aerobic capacity than the distal aorta. This fits our understanding of the different embryology[28] and normal physiologic roles of these distinct regions of the arterial system with the coronary arteries having greater energy requirements associated with regulation of coronary blood flow compared to the distal aorta which serves primarily as passive conduit for blood delivery to the lower extremities. To our knowledge this substantial variation in mitochondrial protein mass between coronary and aortic tissues in humans has not been previously documented.

Third, the data indicate profound anatomic differences in key metabolic regulatory pathways and mitochondrial dynamics in the setting of atherosclerosis. Specifically, the data reveal a broad-based reduction of mitochondrial protein mass and a proteomic pattern consistent with inhibition of PPAR-α, PPAR-γ, and insulin receptor regulated pathways in atherosclerotic coronary arteries, but not in similarly diseased distal abdominal aortic samples. These provide critical anatomic specificity to the growing body of evidence that mitochondrial dysfunction and altered mitochondrial dynamics are also central features of atherosclerosis [29 15 30], and may provide a mechanistic framework to explain the anatomic dimorphism between coronary and peripheral arterial disease with respect to conventional and genetic risk factors for atherosclerosis [31,32] It remains to be determined whether the reduction in mitochondrial protein mass in coronary atherosclerosis is a consequence of oxidative, or Ca^{++}-mediated mitochondrial damage and mitophagy or impaired mitochondrial biogenesis, or both. It is interesting to note that the concurrent increases in the lysosomal proteases cathepsin B, D and Z in the atherosclerotic samples may signify enhanced lysosomal biogenesis useful for targeted degradation of damaged mitochondria [29].

The data also reassuringly highlight numerous individual proteins and a global proteomic pattern of TNF activation in the FP samples consistent with several decades of research documenting the role of inflammation in the pathogenesis of atherosclerosis. [33] However, even the more familiar indicators of TNF activation and inflammation exhibited substantial anatomic variation from LAD to distal aorta in our data, an observation that was made possible by the extended proteomic depth of coverage in the current study.

Recognizing the anatomic heterogeneity with respect to metabolic enzyme profiles and mitochondrial function has important implications for research on arterial health and disease. Many of the pathogenic mechanisms and targeted therapies for atherosclerosis are directly related to fatty acid metabolism or aerobic energy biosynthesis and redox homeostasis [34]. Unfortunately, a great deal of our understanding of arterial biology has been generated without regard to anatomic distribution. For instance many animal models of atherosclerosis rely on aortic, femoral or carotid manifestations of disease with the assumption that findings are generalizable to human coronary arteries. Likewise the overwhelming majority of contemporary human arterial proteomic data have been generated from carotid arteries – typically severely diseased endarterectomy specimens. The current data suggest that a complete understanding of the pathogenesis and prevention of human coronary

artery atherosclerosis, especially as it relates to metabolic mechanisms and mitochondrial function, may require more anatomically specific methods of interrogation. It is also interesting to consider whether anatomic variations in the arterial proteome may be illuminating about other forms of arterial disease that have distinct anatomic distributional features (e.g. Marfan's syndrome, Kawasaki disease, fibromuscular dysplasia, etc).

Several limitations in the current work should be considered. First, although a comprehensive analysis of 200 human arterial specimens is a considerable technical accomplishment resulting in much greater power to discern real patterns in the data, and despite the fact that we used stringent statistical methods and other information theoretical considerations to minimize false positives (generally to $\leq$ 5%), there remains the possibility of residual confounding or limited statistical power which could obscure both positive and negative associations. This is especially true for the AA samples where the number of significantly diseased arterial samples was more limited than in the LAD. The fact that many of the sentinel findings generated by the initial data dependent MS approach were subsequently confirmed and strengthened by a separate data independent acquisition MS method (which typically utilizes different peptides for protein identification) provides further support for the validity of the findings. Second, the fact that the samples were all collected post-mortem raises questions about possible effects of death on the stability of individual proteins or specific cellular functional processes. If such effects are differentially manifest in normal versus atherosclerotic tissues, this could give the appearance of differences by disease status that are not present during life. It is reassuring that many of the individual proteins identified here overlap with findings from animal models of atherosclerosis and *in-vitro* studies where the effects of post-mortem hypoxia and cessation of cellular metabolic activity are more easily minimized. Third, the observed differences in the proteome between normal and diseased samples represent a unique, albeit macroscopic view of the proteomic architecture of human coronary and distal aortic atherosclerosis based on analysis of hundreds of proteins. Much more work is required to clarify the functional role of the specific proteins, protein networks and pathways identified here, and to establish if there is therapeutic value in manipulating them – perhaps even in an anatomically specific manner.

In summary, these data represent the most comprehensive description of the human coronary and aortic proteome to date and reveal numerous proteins, networks and pathways that are strongly indicative of early atherosclerosis. They also indicate fundamental differences in mitochondrial dynamics between the coronary

artery and the distal aorta in both normal and atherosclerotic conditions. The data analyses highlight the value of new methods to extricate tissue phenotypes from heterogeneous tissue samples and depict dynamic features of protein networks that vary as a function of disease state and anatomic location. These data and methods establish a new foundation for future research to better understand the human arterial proteomic architecture in health and disease.

Author Contributions:

D.H., J.V.E., Yue W., R.V.H., J.H. designed the project, supervised the execution of the research plan, and made significant contributions to the interpretation and presentation of the results; C.M. and S.P. provided critical project management and scientific direction concerning specific aspects of the data acquisition and bioinformatic analyses; Z.F. and V.V. were primarily responsible for generation and annotation of the mass-spectrometry data; G.Y, L.C, Y.F., Y.W., J.G., G.S. performed data analysis; T.H. and Y.L. contributed to genomic analyses and interpretation; D.T. and G.A. and were responsible for collecting, grading, storing and shipping the pathologic specimens.

Acknowledgments:

This work was supported by 1R01HL111362 from the, National Heart, Lung and Blood Institute of the National Institutes of Health

Methods

Arterial Sample Acquisition and Pathology Grading Methods

Male and female cases of any race, aged 18-50 years (men) or 18-60 years (women) with no ante mortem clinical suspicion of coronary disease autopsied < 24 hours of death were eligible for inclusion. This report includes data from the first 100 adult coroner cases included in the study (age range:15-55 yrs., 75% males, 67% White, 26% Black, 7% Other). The Medico-Legal Death Investigators obtain signed family consent for retrieval of anatomic specimens prior to the autopsy. During the autopsy the pathologist dissects the aorta (ligamentum arteriosum to aortic bifurcation) and LAD and removes branching arteries and adventitial or epicardial adipose tissue. Both the aorta and LAD are opened longitudinally, cleansed of blood and photographed (**Supplemental Fig. 9a and b**). In each of the regions to be sampled, the pathologist inspects the intimal surface and categorizes the type and percent involvement of the following atherosclerotic changes: a) fatty streaks (FS); b) fibrous plaques (FP); c) complicated lesions (CL); and d) calcified lesions (CO), and records the data on a data collection form. Consistent with the age and cause of death (trauma), the fibrous plaques were almost exclusively early lesions - only one specimen had any macroscopic evidence of calcification and <3% of samples had any evidence of plaque hemorrhage, ulceration or thrombosis. Next the pathologist collects up to 1 gram of tissue from each of three standardized sections of the thoracic and abdominal aorta and two sections from the coronary artery [35] (**Supplemental Fig. 9c and d**). The specimens are snap frozen in cryotubes with liquid nitrogen and remain in a 34L VWR Cryogenic Dewar until transferred to a -80 freezer equipped with temperature alarms and automated generator back-up systems in the Department of Pathology at LSU. Additionally, targeted “pure” samples of grossly normal (non-lesion) and, if available, grossly atherosclerotic (lesion) are taken and divided into three 100mg portions and 1.) snap frozen, 2.) placed in RNALater solution and frozen, and 3.) placed in formalin and stored at room temperature for possible future immunohistochemistry analyses. A 50 gram sample of liver is also collected and frozen for future studies. All samples received at LSU are checked for label accuracy and entered in a database using an unlinked anonymous code for further processing, analyses and storage.

Protein Extraction, MS Analysis and Protein Identification

Aorta and LAD tissues were pulverized in liquid nitrogen and homogenized in 8M urea, 2M thiourea, 4% CHAPs and 1% DTT using Dounce homogenizer for 100 strokes, centrifuged at 16000 rpm for 20 mins . Protein concentration of the supernatant was assessed by CB-X assay kit (G-Biosciences MO, USA). 100 µg of protein was precipitated using 2-D clean-up kit (GE Healthcare MA, USA) and then reconstitute in 6M urea, 50mM ammonium bicarbonate. The protein was reduced, alkylated and digested with trypsin (1:20). Peptides were desalted using Oasis HLB 96-well Plate (Waters MA, USA). A total of 2.0 µg of peptides per sample were then analyzed using label-free quantification on a reversed-phase liquid chromatography tandem mass spectrometry (RPLC–MS/MS) online with an Orbitrap Elite mass spectrometer (Thermo Scientific, USA) coupled to an Easy-nLC 1000 system (Thermo Scientific, USA). Peptides concentrated on a C18 trap column (Acclaim PepMap 100, 300 µm × 5 mm, C18, 5 µm, 100 Å; maximum pressure 800bar) in 0.1% TFA, then separated on a C18 analytical column (Acclaim PepMap RSLC, 75 µm × 15 cm, nano Viper, C18, 2 µm, 100 Å) using a linear gradient from 5% to 35% solvent B over 155 mins (solvent A: 0.1% aqueous formic acid and solvent B: 0.1% formic acid in acetonitrile; flow rate 350 nL/min; column oven temperature 45 °C). The analysis was operated in a data-dependent mode with full scan MS spectra acquired at a resolution of 60,000 in the Orbitrap analyzer, followed by tandem mass spectra of the 20 most abundant peaks in the linear ion trap after peptide fragmentation by collision-induced dissociation (CID).

To eliminate batch effect, the same parameters were used for mass spectra acquisition and the peptides from each individual were analyzed randomly in one batch. To minimize cross contamination, a blank run was performed between each sample. To monitor column performance, 200fmol BSA digested peptides were analyzed to make sure elution time of same peptide were within 0.2 minutes and signal intensity and total spectra counts variation were less than 10%. One LAD and one AA sample (from different subjects) were excluded because of poor protein yield leaving n=99 samples from each territory for analysis.

The MS/MS data obtained from the Orbitrap Elite were converted to mzXML and mgf format using Msconvert version 3.0.3858 from ProteoWizard [36] for peaklist generation. All data were searched using the X!Tandem [37] algorithm version 2009.10.01.1 and OMSSA [38] algorithm version 2.1.9. The dataset was searched against the concatenated target/decoy [39] Human Uniprot [40] database as of July 24, 2015, with only reviewed and canonical

sequences used. The search parameters were as follows: Fixed modification of Carbamidomethyl (C) and variable modifications of Oxidation (M), Phosphorylation (STY); Enzyme: Trypsin with 2 maximum missed cleavages; Parent Tolerance: 0.050.08 Da; Fragment tolerance: 1.00 Da. Post-search analysis was performed using Trans Proteomic Pipeline [41] version v4.6, rev 1 with protein group and peptide probability thresholds set to 90% and 90%, respectively, and one or more distinct peptide required for identification. PeptideProphet [42] was used for peptide validation from each individual search algorithm and iProphet [43] was used to merge results from the separate algorithms and further refine the identification probabilities. Lastly, ProteinProphet [44] was then used to infer protein identifications from the resulting combined peptide list and perform grouping of ambiguous hits. Protein Group and Peptide False Discovery Rates were calculated automatically using a target-decoy method for the above probability thresholds (0.72% and 0.06% respectively). Protein isoforms were only reported if a peptide comprising an amino acid sequence that was unique to the isoform was identified. Label-free quantification of each protein was performed using weighted spectral counting [45]. The distribution of protein spectral counts for each data file was inspected to verify equivalence in sample loading and instrument performance between files. Based on this analysis, a median normalization (adjustment of the raw spectral counts for each protein of a given file to the median of all spectral counts observed for the same file) was performed (**Supplemental Fig. 10**).

The final non-redundant protein groups were analyzed through the use of IPA (Ingenuity® Systems, www.ingenuity.com) to generate network, functional and pathway analyses. The MS/MS proteomics data have been deposited to the ProteomeXchange Consortium (http://www.proteomexchange.org) via the PRIDE partner repository [46] with the dataset identifier (# to be added at the time of publication).

Post-processing Quality Control and Data Imputation

A total of 1925 unambiguous proteins were detected in one or more of the 99 LAD samples. Of these proteins 944 had $\leq$50% missingness and 375 had no missingness in all 99 samples (**Supplemental Fig. 11a, d**). PCA analysis of the 375 proteins with complete data from every sample failed to identify significant sample outliers or important batch effects (**Supplemental Fig. 11c**). Missing values for the 944 proteins with $\leq$ 50% missingness were imputed using a low rank approximation derived from non-linear iterative partial least squares (NIPALS) PCA [47] (**Supplemental Fig. 11b**). All subsequent analyses including regression, WCNA,

and CAM were performed on this imputed data set. Exploratory regression analysis of proteins with > 50% missingness using missingness encoding failed to identify proteins with compelling association with disease and these proteins were subsequently dropped from further consideration. In a similar manner the AA samples revealed 1495 unambiguous proteins including 725 with ≤50% missingness and no important batch effects or extreme outliers.

Analysis of Association with Extent of Atherosclerosis

Three orthogonal strategies (regression, weighted co-expression analysis, convex analysis of mixtures) were employed to identify proteins individually or jointly associated with extent of disease.

Regression Models: MANOVA models with adjustment for age, sex, and race were used to model the joint distributions of % intimal surface demonstrating fibrous plaque (FP), streaks (FS), and normal (NL) intima as a function of each individual protein. To account for possible differences in tissue sample volumes, cellular composition or protein yields the models were also adjusted for several housekeeping proteins (Proteasome subunit beta type-2, Small nuclear ribonucleoprotein Sm D3, Receptor expression-enhancing protein 5, Ras-related protein Rab-7a) and Myosin-11 (a vascular smooth muscle cell marker protein). Separately, generalized linear models (GLM) were used to examine the association between individual proteins and %FP or %NL after adjustment for age, sex, race and the same set of housekeeping and VSMC genes. In the models of %FP the reference was, by definition, the % intimal surface demonstrating fatty streaks or normal intima. In contrast, in models of %NL the reference was, by definition, the % intimal surface demonstrating fatty streaks or fibrous plaques. Accordingly we developed separate models using each trait (%FP or %NL) as the dependent variable with the expectation that direction of effect would be inversely related depending on the dependent variable used. Proteins with beta coefficients in the same direction for both %FP and %NL were excluded from further consideration. In a similar manner ordinal regression was also used to examine the association between individual proteins and % FP or % NL treated as three level ordinal variables (FP: 0%, 1-59%, ≥60%; NL: 100%, 99-61%, <60%). Exploratory models using robust GLM with logit link produced qualitatively similar lists of significantly associated proteins (data not shown).

Weighted Co-Expression Network Modelling: The WGCNA package in R was used to identify distinct protein modules among the 94 proteins used for analysis [48]. A weighted power adjacency matrix was constructed using signed bi-correlations between proteins and mapping the results onto the 0-1 interval. The power parameter was selected such that the topological overlap connectivity (k) of the entire network approximated a scale-free topology. The topological overlap was used to create a dissimilarity matrix for hierarchical clustering to identify modules. To assess stability of module assignments, 50 bootstrap samples of the data were created and each one interrogated using identical WCGNA parameters. Once the modules were determined, regression models were developed to examine the association between module eigengenes and the arterial phenotypes (%FP and % NL) after adjustment for age, sex, and race.

Convex Analysis of Mixtures and Protein Expression Differences in Complex Tissues Analysis

Tissue heterogeneity is present in our samples where multiple tissue types are variably mixed and co-exist [49,50], representing a major confounder when studying tissue-specific disease markers [51-53]. We have recently devised CAM, a fully unsupervised data deconvolution method that exploits the strong parallelism between a latent variable model and the theory of convex sets [54]. With the newly-proven mathematical theorems, we showed that the simplex of mixed expressions is a rotated and compressed version of the simplex of tissue expressions in scatter space [55] (**Fig. 3**). The vertices of the scatter simplex, characterized by the molecular markers whose expressions are maximally enriched in a particular tissue, define the optimal data-derived distinctive tissue types present in the heterogeneous samples.

CAM works by geometrically identifying the vertices (and their resident molecular markers) of the scatter simplex of globally measured expressions (**Fig. 3a**), *i.e.*, determining the multifaceted simplex that most tightly encloses the mixed expression profiles (**Fig. 3d**), and subsequently estimate the proportions and specific expression profiles of constituent subpopulations [55] (**Fig. 3b**). Tissue samples to be analyzed by CAM contain unknown number and varying proportions of molecularly distinctive (including novel) tissue types (**Fig. 3e**). Molecular expression in a specific tissue is modeled as being linearly proportional to the abundance of that tissue and the number of tissues present is determined by the newly-derived minimum description length (MDL) criterion [55].

We first eliminate proteins whose signal intensity (vector norm) is lower than 5% (noise) or higher than 95% (outlier) of the mean value over all proteins. The signals from these proteins are unreliable and could have a negative impact on the subsequent deconvolution. Second, dimension reduction is performed on the raw measurements using principal component analysis with 10 PCs. To further reduce the impact of noise/outlier data points and permit appropriate parameterization of the MDL criterion to determine the number of tissues, we aggregate protein vectors into representative clusters using affinity propagation clustering (APC) [56-58, 22]. As an initialization-free and near-global-optimum clustering method, APC simultaneously considers all protein vectors as potential exemplars and recursively exchanges real-valued 'messages' between protein vectors until a high-quality set of exemplars and corresponding clusters gradually emerge. CAM detected four tissues from LAD simplex (**Fig. 3d**) and three tissues from AA simplex (**Supplemental Fig. 6c**). On the basis of the expression levels of tissue-specific marker proteins detected by CAM, the relative proportions of constituent tissues are estimated using standardized averaging that are then used to deconvolute the mixed expressions into tissue-specific profiles by non-negative least-square regression techniques[55]. Upregulated maker proteins associated with specific tissues can be detected by One-Versus-Everyone (OVO) fold change thresholding, e.g., currently set to 2 for FP tissue.

GO Term and Pathway Enrichment Analysis

GO Term and pathway enrichment analyses using GO Term Finder [59], and IPA (Ingenuity Pathway Analysis, Ingenuity Systems, Redwood City, CA) tools were used to characterize the evaluable proteins obtained from the arterial samples (**Supplemental Tables 1-4**). For the GO term enrichment analysis, clustering based on semantic similarity was used to indicate which child nodes could be represented by higher level parent nodes [60]. For the pathway analysis, the significant differentially expressed proteins with |fold change| >=1.7 and the false discovery rate (FDR) corrected p-value of 0.05 were analyzed with IPA for pathways, upstream regulators, and associated diseases and biological functions. The following parameters were used for these analyses: 1) Human genes in the Ingenuity Knowledge Base were used as the reference set; 2) Both the direct and indirect relationships were considered; 3) The confidence level was set to be "Experimentally Observed" and "High predicted" with high confidence scores; 4) The following selected tissues/cell types were used: heart, smooth muscle, fibroblasts, cardiomyocytes, endothelial cells, smooth muscle cells, and macrophages. The p-

values for the identified canonical pathways, disease associations and functions were calculated using Fisher's exact test. The Benjamini-Hochberg method was used to estimate the false discovery rate, and an FDR-corrected p-value of 0.05 was used to select significantly enriched pathways. The significant upstream regulators were selected using p-value <=0.05 and |Z-score| >=2.

Differential Dependent Network Analyses

Modeling biological networks is an important tool in systems biology to study the orchestrated activities of gene products in cells [26]. Significant rewiring of these networks provides a unique perspective on phenotypic transitions that can occur in biological systems [61]. Thus, instead of asking "which genes are differentially expressed", a more interesting question is "which genes are differentially connected?" [26,62]. To systematically characterize selectively activated or deactivated regulatory components and mechanisms, the modeling tools must effectively distinguish significant rewiring from random background fluctuations. We have developed an integrated molecular network learning method, within a well-grounded mathematical framework, to construct differential dependency networks with significant rewiring [23, 63]. This knowledge-fused differential dependency networks (kDDN) method, implemented as a Java Cytoscape app, can be used to optimally integrate prior biological knowledge with measured data to simultaneously construct both common and differential networks [64,65].

kDDN algorithm jointly learns the shared biological network and statistically significant rewiring across different phenotypes. Phenotype-specific data and prior knowledge are quantitatively fused via an extended Lasso model with l_1 regularized convex optimization formulation [64]. Based on the unique nature of the problem, we derive an efficient closed-form solution for the embedded sub-problem solved by the block-wise coordinate descent (BCD) algorithm. Since existing knowledge is often nonspecific or imperfect, kDDN uses a "minimax" strategy to maximize the benefit of prior knowledge while confining its negative impact under the worst-case scenario. Furthermore, kDDN matches the values of model parameters to the expected false positive rates on network edges at a specified significance level, and assesses edge-specific p-values on each of the differential connections [64].

We use kDDN to construct the network and detect significant network rewiring between FP and NL groups, where an extended Lasso-based sparse Gaussian graphic model is used to capture the network structure. The

network rewiring under different phenotypes is inferred jointly by performing the BCD algorithms sequentially for all nodes. We then used permutation-based significance test to estimate p-values of the detected differential dependence edges [63,64]. Those detected differential dependence edges with p-values larger than 0.05 were filtered out for control of false positive rate. We used different colors to distinguish differential dependency edges under each phenotype, and use solid/dashed lines to indicate positive/negative dependences between nodes. The linewidths of edges correspond to the dependency strength to give a straightforward illustration and a better comparison within the network.

Proteomic Architecture of Human Coronary and Aortic Atherosclerosis

Herrington David M[1]*, Mao Chunhong[2], Parker Sarah[3], Fu Zongming[4], Yu Guoqiang[5], Chen Lulu[5], Venkatraman Vidya[3], Fu Yi[5], Wang Yizhi[5], Howard Tim[6], Goo Jun[7], Zhao CF[1], Liu Yongming[8], Saylor Georgia[1], Athas Grace[9], Troxclair Dana[9], Hixson James[7]*, Vander Heide Richard[9]*, Wang Yue[4]*,Van Eyk Jennifer[3]* (*contributed equally)

Supplemental Tables

Table of Contents

Supplemental Table 1. Human Arterial Proteins from Left Anterior Descending (LAD) Coronary Artery (N=99) and Distal Abdominal Aortic (AA) (N=99) Samples

<Data can be viewed at Peptide Atlas http://www.peptideatlas.org/PASS/PASS01066>

Supplemental Table 2a Human LAD Protein GO Terms: Biologic Processes (top 100 GO Terms)

GO Term ID	Description	# of proteins	log(p-value)*
GO:0044710	single-organism metabolic process	490	-69.46
GO:0044699	single-organism process	807	-62.11
GO:0044281	small molecule metabolic process	293	-53.18
GO:0044763	single-organism cellular process	737	-47.07
GO:0009987	cellular process	821	-41.91
GO:0071840	cellular component organization or biogenesis	445	-40.94
GO:0016192	vesicle-mediated transport	181	-40.34
GO:0030198	extracellular matrix organization	91	-40.29
GO:0043062	extracellular structure organization	91	-40.16
GO:0008152	metabolic process	661	-38.93
GO:0019752	carboxylic acid metabolic process	146	-36.47
GO:0006082	organic acid metabolic process	156	-35.83
GO:0006810	transport	341	-35.55
GO:0055114	oxidation-reduction process	110	-33.01
GO:0006950	response to stress	329	-32.61
GO:1901564	organonitrogen compound metabolic process	227	-32.56
GO:0006897	endocytosis	111	-32.55
GO:0071704	organic substance metabolic process	615	-32.36
GO:0051179	localization	390	-32.34
GO:0065008	regulation of biological quality	274	-31.59
GO:0009056	catabolic process	218	-31.57
GO:0009611	response to wounding	130	-30.88
GO:0044707	single-multicellular organism process	349	-27.85
GO:0006091	generation of precursor metabolites and energy	85	-27.46
GO:0050896	response to stimulus	513	-27.35
GO:0072376	protein activation cascade	61	-26.78
GO:0009605	response to external stimulus	201	-24.80
GO:0042060	wound healing	101	-24.20
GO:0050817	coagulation	92	-23.59
GO:0071822	protein complex subunit organization	167	-22.67
GO:0032501	multicellular organismal process	383	-22.47
GO:0022607	cellular component assembly	199	-21.77
GO:0002576	platelet degranulation	36	-21.35
GO:0002253	activation of immune response	99	-21.31
GO:0044238	primary metabolic process	565	-21.23
GO:0050878	regulation of body fluid levels	95	-21.10
GO:0042221	response to chemical	295	-20.70
GO:0006956	complement activation	51	-20.35
GO:0050778	positive regulation of immune response	104	-19.57
GO:0000904	cell morphogenesis involved in differentiation	111	-19.30
GO:0044237	cellular metabolic process	562	-19.28
GO:0044085	cellular component biogenesis	201	-19.08
GO:0030162	regulation of proteolysis	91	-19.07
GO:0051641	cellular localization	218	-18.51
GO:0006959	humoral immune response	61	-18.28
GO:0032502	developmental process	305	-17.68
GO:0006952	defense response	174	-17.37
GO:0006898	receptor-mediated endocytosis	65	-17.33
GO:0009141	nucleoside triphosphate metabolic process	49	-17.01
GO:0002376	immune system process	211	-16.81
GO:0072524	pyridine-containing compound metabolic process	35	-16.63

GO:0048584	**positive regulation of response to stimulus**	181	-16.60
GO:0046496	**nicotinamide nucleotide metabolic process**	34	-16.58
GO:0033036	**macromolecule localization**	185	-16.54
GO:0008104	**protein localization**	165	-16.03
GO:0048518	**positive regulation of biological process**	339	-15.70
GO:0061024	**membrane organization**	116	-15.42
GO:0019538	**protein metabolic process**	350	-15.32
GO:0046907	**intracellular transport**	160	-14.83
GO:0048583	**regulation of response to stimulus**	265	-14.71
GO:0040011	**locomotion**	145	-14.58
GO:0051128	**regulation of cellular component organization**	163	-14.39
GO:0006928	**cellular component movement**	157	-14.38
GO:0005975	**carbohydrate metabolic process**	101	-14.34
GO:0006508	**proteolysis**	128	-14.21
GO:0005996	**monosaccharide metabolic process**	48	-14.20
GO:0002252	**immune effector process**	93	-14.14
GO:0051186	**cofactor metabolic process**	54	-14.02
GO:0044711	**single-organism biosynthetic process**	148	-14.01
GO:0065007	**biological regulation**	582	-13.93
GO:0031589	**cell-substrate adhesion**	46	-13.71
GO:0002682	**regulation of immune system process**	149	-13.70
GO:0080134	**regulation of response to stress**	135	-13.56
GO:0044282	**small molecule catabolic process**	53	-13.12
GO:0070887	**cellular response to chemical stimulus**	207	-13.07
GO:0030029	**actin filament-based process**	72	-13.03
GO:0050789	**regulation of biological process**	553	-12.87
GO:0045087	**innate immune response**	128	-12.85
GO:0002673	**regulation of acute inflammatory response**	23	-12.80
GO:0032879	**regulation of localization**	166	-12.67
GO:0051130	**positive regulation of cellular component organization**	101	-12.60
GO:0006793	**phosphorus metabolic process**	212	-12.59
GO:0043086	**negative regulation of catalytic activity**	86	-12.58
GO:0006457	**protein folding**	40	-12.45
GO:0009636	**response to toxic substance**	32	-12.42
GO:1901135	**carbohydrate derivative metabolic process**	120	-12.26
GO:0061615	**glycolytic process through fructose-6-phosphate**	17	-12.10
GO:0051246	**regulation of protein metabolic process**	191	-12.05
GO:0019637	**organophosphate metabolic process**	99	-11.94
GO:0007010	**cytoskeleton organization**	96	-11.92
GO:0002526	**acute inflammatory response**	26	-11.89
GO:0034446	**substrate adhesion-dependent cell spreading**	24	-11.87
GO:0006935	**chemotaxis**	89	-11.84
GO:0048468	**cell development**	136	-11.83
GO:0022610	**biological adhesion**	109	-11.72
GO:0006955	**immune response**	155	-11.61
GO:0001775	**cell activation**	88	-11.51
GO:0072350	**tricarboxylic acid metabolic process**	18	-11.43
GO:1901657	**glycosyl compound metabolic process**	53	-11.26
GO:0052547	**regulation of peptidase activity**	52	-11.17

* Bonferroni corrected p-value

Supplemental Table 2b. Human LAD Protein GO Terms: Molecular Functions (adj. p-value < 0.05*)

GO Term ID	Description	# of proteins	log(p-value)*
GO:0005515	protein binding	719	-50.25
GO:0005488	binding	780	-49.47
GO:0044822	poly(A) RNA binding	160	-29.24
GO:0005198	structural molecule activity	94	-24.83
GO:0003723	RNA binding	169	-24.82
GO:0032403	protein complex binding	101	-24.66
GO:0043167	ion binding	165	-23.14
GO:0008092	cytoskeletal protein binding	86	-21.19
GO:0043168	anion binding	113	-17.67
GO:0097367	carbohydrate derivative binding	89	-17.58
GO:0003779	actin binding	46	-16.90
GO:0016491	oxidoreductase activity	79	-16.89
GO:0097159	organic cyclic compound binding	253	-15.65
GO:0003824	catalytic activity	310	-14.77
GO:0016209	antioxidant activity	23	-13.55
GO:1901363	heterocyclic compound binding	241	-13.24
GO:0005539	glycosaminoglycan binding	32	-12.80
GO:0005200	structural constituent of cytoskeleton	26	-12.64
GO:0016616	oxidoreductase activity, acting on the CH-OH group of donors, NAD or NADP as acceptor	26	-12.47
GO:0042802	identical protein binding	107	-11.64
GO:0036094	small molecule binding	81	-11.00
GO:0016614	oxidoreductase activity, acting on CH-OH group of donors	26	-10.98
GO:0004857	enzyme inhibitor activity	47	-10.48
GO:0005201	extracellular matrix structural constituent	20	-9.54
GO:0061135	endopeptidase regulator activity	28	-9.34
GO:0019899	enzyme binding	127	-9.25
GO:0030234	enzyme regulator activity	75	-8.88
GO:1901681	sulfur compound binding	29	-8.80
GO:0043169	cation binding	82	-8.74
GO:0046872	metal ion binding	75	-7.98
GO:0016787	hydrolase activity	141	-7.76
GO:0034987	immunoglobulin receptor binding	13	-7.27
GO:0050839	cell adhesion molecule binding	29	-7.08
GO:0016684	oxidoreductase activity, acting on peroxide as acceptor	14	-7.08
GO:0008289	lipid binding	53	-6.88
GO:0005102	receptor binding	104	-6.75
GO:0003676	nucleic acid binding	187	-6.62
GO:0008201	heparin binding	20	-6.30
GO:0044548	S100 protein binding	9	-6.24
GO:0005518	collagen binding	16	-6.24
GO:0004601	peroxidase activity	13	-6.13
GO:0001948	glycoprotein binding	18	-6.02
GO:0009055	electron carrier activity	20	-6.00
GO:0005178	integrin binding	19	-5.58
GO:0017111	nucleoside-triphosphatase activity	59	-5.27
GO:0005509	calcium ion binding	34	-5.26
GO:0048306	calcium-dependent protein binding	14	-5.15
GO:1901265	nucleoside phosphate binding	53	-4.84
GO:0048037	cofactor binding	23	-4.69
GO:0016817	hydrolase activity, acting on acid anhydrides	60	-4.59
GO:0000166	nucleotide binding	52	-4.46
GO:0070325	lipoprotein particle receptor binding	9	-4.00
GO:0051082	unfolded protein binding	15	-4.00

GO:0005496	**steroid binding**	15	-3.34
GO:0019900	**kinase binding**	46	-3.28
GO:0016853	**isomerase activity**	20	-3.20
GO:0046983	**protein dimerization activity**	64	-3.16
GO:0001848	**complement binding**	7	-2.98
GO:0008307	**structural constituent of muscle**	11	-2.98
GO:0017166	**vinculin binding**	6	-2.82
GO:0042803	**protein homodimerization activity**	53	-2.77
GO:0046914	**transition metal ion binding**	38	-2.75
GO:0003823	**antigen binding**	34	-2.74
GO:0043178	**alcohol binding**	14	-2.67
GO:0002020	**protease binding**	16	-2.53
GO:0016835	**carbon-oxygen lyase activity**	11	-2.52
GO:0051087	**chaperone binding**	13	-2.50
GO:0031625	**ubiquitin protein ligase binding**	29	-2.49
GO:0016860	**intramolecular oxidoreductase activity**	10	-2.43
GO:0044389	**small conjugating protein ligase binding**	29	-2.38
GO:0019003	**GDP binding**	11	-2.31
GO:0023026	**MHC class II protein complex binding**	7	-2.28
GO:0043394	**proteoglycan binding**	7	-2.28
GO:0055102	**lipase inhibitor activity**	6	-2.21
GO:0016667	**oxidoreductase activity, acting on a sulfur group of donors**	10	-2.09
GO:0016801	**hydrolase activity, acting on ether bonds**	5	-2.06
GO:0008233	**peptidase activity**	42	-1.99
GO:0004175	**endopeptidase activity**	30	-1.98
GO:0019001	**guanyl nucleotide binding**	18	-1.95
GO:0004064	**arylesterase activity**	4	-1.75
GO:0004301	**epoxide hydrolase activity**	4	-1.75
GO:0023023	**MHC protein complex binding**	7	-1.74
GO:0019865	**immunoglobulin binding**	5	-1.72
GO:0016903	**oxidoreductase activity, acting on the aldehyde or oxo group of donors**	10	-1.60
GO:0015485	**cholesterol binding**	9	-1.56
GO:0032561	**guanyl ribonucleotide binding**	17	-1.44
GO:0044325	**ion channel binding**	14	-1.38
GO:0060090	**binding, bridging**	19	-1.33

* Bonferroni corrected p-value

Supplemental Table 2c. Human LAD Protein GO Terms: Cellular Component (adj. p-value < 0.05*)

GO Term ID	Description	# of proteins	log(p-value)*
GO:0031982	vesicle	694	-300.00
GO:0070062	extracellular vesicular exosome	671	-300.00
GO:0005925	focal adhesion	142	-84.66
GO:0044444	cytoplasmic part	633	-81.64
GO:0043226	organelle	857	-77.12
GO:0043227	membrane-bounded organelle	825	-73.16
GO:0072562	blood microparticle	92	-71.56
GO:0005829	cytosol	352	-64.45
GO:0031012	extracellular matrix	98	-60.94
GO:0005737	cytoplasm	712	-55.97
GO:0030054	cell junction	154	-53.69
GO:0015629	actin cytoskeleton	83	-26.96
GO:0005578	proteinaceous extracellular matrix	45	-22.33
GO:0005856	cytoskeleton	165	-20.83
GO:0032991	macromolecular complex	309	-19.25
GO:0060205	cytoplasmic membrane-bounded vesicle lumen	31	-17.64
GO:0031983	vesicle lumen	31	-17.44
GO:0016020	membrane	473	-16.77
GO:0044424	intracellular part	763	-15.51
GO:0043234	protein complex	259	-14.65
GO:0005622	intracellular	768	-14.65
GO:0005788	endoplasmic reticulum lumen	38	-12.37
GO:0043228	non-membrane-bounded organelle	252	-12.26
GO:0044422	organelle part	511	-11.60
GO:0044433	cytoplasmic vesicle part	65	-11.38
GO:0044437	vacuolar part	52	-10.91
GO:0044446	intracellular organelle part	500	-10.79
GO:0031091	platelet alpha granule	22	-10.39
GO:0045121	membrane raft	34	-10.18
GO:0034358	plasma lipoprotein particle	13	-8.87
GO:0032994	protein-lipid complex	13	-8.21
GO:0044449	contractile fiber part	27	-8.16
GO:0005832	chaperonin-containing T-complex	8	-7.80
GO:0005885	Arp2/3 protein complex	8	-7.80
GO:0005811	lipid particle	17	-7.67
GO:0043292	contractile fiber	27	-7.38
GO:0043229	intracellular organelle	639	-7.26
GO:0042571	immunoglobulin complex, circulating	12	-6.87
GO:0044429	mitochondrial part	75	-6.87
GO:0012505	endomembrane system	225	-6.71
GO:0019814	immunoglobulin complex	12	-6.61
GO:0005773	vacuole	56	-6.55
GO:0009986	cell surface	63	-6.12
GO:0098589	membrane region	61	-6.12
GO:0044448	cell cortex part	19	-6.09
GO:0005581	collagen trimer	12	-5.69
GO:0044445	cytosolic part	32	-5.65
GO:0044853	plasma membrane raft	16	-5.53
GO:0005739	mitochondrion	114	-5.44
GO:0098552	side of membrane	46	-5.42
GO:0005759	mitochondrial matrix	43	-5.13
GO:0009897	external side of plasma membrane	24	-5.11
GO:0045259	proton-transporting ATP synthase complex	10	-5.10
GO:0048471	perinuclear region of cytoplasm	43	-5.06
GO:0005577	fibrinogen complex	7	-4.96

GO:0005783	**endoplasmic reticulum**	109	-4.68
GO:0005839	**proteasome core complex**	9	-4.60
GO:0001725	**stress fiber**	12	-4.60
GO:0032432	**actin filament bundle**	12	-4.44
GO:0098644	**complex of collagen trimers**	9	-4.10
GO:0005623	**cell**	818	-4.08
GO:0044464	**cell part**	817	-4.06
GO:0000502	**proteasome complex**	15	-3.90
GO:0042641	**actomyosin**	12	-3.74
GO:0005938	**cell cortex**	21	-3.74
GO:0044432	**endoplasmic reticulum part**	76	-3.63
GO:0042383	**sarcolemma**	12	-3.26
GO:0031090	**organelle membrane**	157	-3.11
GO:0005874	**microtubule**	25	-3.04
GO:0071944	**cell periphery**	273	-2.98
GO:0005884	**actin filament**	12	-2.63
GO:0036019	**endolysosome**	7	-2.59
GO:0030175	**filopodium**	12	-2.54
GO:0031252	**cell leading edge**	26	-2.49
GO:0030529	**ribonucleoprotein complex**	54	-2.42
GO:0016469	**proton-transporting two-sector ATPase complex**	10	-2.41
GO:0044455	**mitochondrial membrane part**	22	-2.27
GO:0005886	**plasma membrane**	265	-2.21
GO:0001527	**microfibril**	5	-2.15
GO:0042995	**cell projection**	71	-1.98
GO:0005768	**endosome**	55	-1.91
GO:0005796	**Golgi lumen**	15	-1.85
GO:0030496	**midbody**	16	-1.83
GO:0031975	**envelope**	67	-1.80
GO:0001726	**ruffle**	15	-1.62
GO:0005743	**mitochondrial inner membrane**	33	-1.40
GO:0001772	**immunological synapse**	7	-1.39

* Bonferroni corrected p-value

Supplemental Table 3a. Human Distal Aortic Protein GO Terms: Biologic Process (top 100 GO Terms)

GO Term ID	Description	# of proteins	log(p-value)*
GO:0044699	single-organism process	619	-48.11
GO:0044763	single-organism cellular process	563	-36.27
GO:0016192	vesicle-mediated transport	153	-35.49
GO:0071840	cellular component organization or biogenesis	341	-33.98
GO:0030198	extracellular matrix organization	65	-31.62
GO:0043062	extracellular structure organization	65	-31.50
GO:0009987	cellular process	627	-30.47
GO:0065008	regulation of biological quality	217	-29.55
GO:0006897	endocytosis	91	-28.49
GO:0009611	response to wounding	93	-27.77
GO:0051179	localization	312	-27.74
GO:0044710	single-organism metabolic process	305	-27.74
GO:0051234	establishment of localization	273	-27.69
GO:0044707	single-multicellular organism process	269	-25.07
GO:0072376	protein activation cascade	53	-24.66
GO:0050896	response to stimulus	394	-24.21
GO:0006950	response to stress	227	-23.16
GO:0009056	catabolic process	166	-22.89
GO:0022607	cellular component assembly	168	-22.02
GO:0032501	multicellular organismal process	299	-21.59
GO:0042060	wound healing	66	-20.86
GO:0002576	platelet degranulation	35	-20.30
GO:0051128	regulation of cellular component organization	154	-19.28
GO:0002253	activation of immune response	79	-18.96
GO:0050817	coagulation	55	-18.75
GO:0044085	cellular component biogenesis	172	-18.56
GO:0006956	complement activation	44	-18.46
GO:0071822	protein complex subunit organization	132	-18.41
GO:0030029	actin filament-based process	70	-18.28
GO:0050778	positive regulation of immune response	84	-17.99
GO:0048518	positive regulation of biological process	284	-17.96
GO:0044767	single-organism developmental process	237	-17.90
GO:0032502	developmental process	241	-17.11
GO:0002376	immune system process	164	-16.96
GO:0072524	pyridine-containing compound metabolic process	32	-16.94
GO:0048584	positive regulation of response to stimulus	146	-16.83
GO:0022610	biological adhesion	102	-16.71
GO:0006959	humoral immune response	52	-16.68
GO:0007155	cell adhesion	101	-16.42
GO:0065007	biological regulation	470	-16.36
GO:0050878	regulation of body fluid levels	58	-16.28
GO:0006457	protein folding	38	-15.70
GO:0050789	regulation of biological process	450	-15.68
GO:0046496	nicotinamide nucleotide metabolic process	29	-15.42
GO:0008152	metabolic process	464	-15.20
GO:0007010	cytoskeleton organization	87	-14.69
GO:0034446	substrate adhesion-dependent cell spreading	24	-14.53
GO:0061621	canonical glycolysis	17	-14.49
GO:0048583	regulation of response to stimulus	216	-14.37
GO:0006909	phagocytosis	49	-14.10
GO:0051130	positive regulation of cellular component organization	89	-13.45

GO:0002673	**regulation of acute inflammatory response**	22	-13.44
GO:0080134	**regulation of response to stress**	111	-13.32
GO:0030036	**actin cytoskeleton organization**	56	-13.31
GO:0002252	**immune effector process**	78	-13.28
GO:0002526	**acute inflammatory response**	25	-13.27
GO:0032879	**regulation of localization**	142	-13.25
GO:0002682	**regulation of immune system process**	114	-12.82
GO:0030162	**regulation of proteolysis**	68	-12.73
GO:0055114	**oxidation-reduction process**	58	-12.73
GO:0006928	**cellular component movement**	113	-12.60
GO:0051641	**cellular localization**	167	-12.51
GO:0009605	**response to external stimulus**	121	-12.35
GO:0048522	**positive regulation of cellular process**	233	-12.27
GO:0044281	**small molecule metabolic process**	132	-12.26
GO:0048519	**negative regulation of biological process**	225	-12.14
GO:1901564	**organonitrogen compound metabolic process**	146	-11.89
GO:0006955	**immune response**	116	-11.72
GO:0006508	**proteolysis**	110	-11.63
GO:0071704	**organic substance metabolic process**	428	-11.53
GO:0043086	**negative regulation of catalytic activity**	71	-11.48
GO:0006165	**nucleoside diphosphate phosphorylation**	21	-11.30
GO:0003012	**muscle system process**	44	-11.18
GO:0033036	**macromolecule localization**	141	-10.70
GO:0051246	**regulation of protein metabolic process**	149	-10.69
GO:0046939	**nucleotide phosphorylation**	21	-10.65
GO:0006952	**defense response**	105	-10.41
GO:0034329	**cell junction assembly**	31	-10.36
GO:0006796	**phosphate-containing compound metabolic process**	166	-10.31
GO:0006082	**organic acid metabolic process**	81	-10.23
GO:0008104	**protein localization**	125	-10.21
GO:0032101	**regulation of response to external stimulus**	74	-10.17
GO:0042221	**response to chemical**	192	-10.11
GO:0010941	**regulation of cell death**	92	-10.08
GO:0019752	**carboxylic acid metabolic process**	74	-9.90
GO:0009205	**purine ribonucleoside triphosphate metabolic process**	34	-9.73
GO:0044092	**negative regulation of molecular function**	80	-9.69
GO:0016052	**carbohydrate catabolic process**	26	-9.64
GO:0009888	**tissue development**	91	-9.63
GO:0050794	**regulation of cellular process**	408	-9.60
GO:0034330	**cell junction organization**	34	-9.47
GO:0006793	**phosphorus metabolic process**	166	-9.44
GO:0021762	**substantia nigra development**	17	-9.42
GO:0051716	**cellular response to stimulus**	308	-9.32
GO:0070887	**cellular response to chemical stimulus**	143	-9.31
GO:0046907	**intracellular transport**	123	-9.31
GO:0051604	**protein maturation**	40	-9.17
GO:0065009	**regulation of molecular function**	152	-9.02
GO:0009132	**nucleoside diphosphate metabolic process**	21	-8.86
GO:0061024	**membrane organization**	80	-8.81

* Bonferroni corrected p-value

Supplemental Table 3b Human Distal Aortic Protein GO Terms: Molecular Function (adj. p-value < 0.05*)

GO Term ID	Description	# of proteins	log(p-value)*
GO:0005515	protein binding	583	-55.54
GO:0005488	binding	622	-50.52
GO:0032403	protein complex binding	88	-24.65
GO:0005198	structural molecule activity	82	-24.37
GO:0008092	cytoskeletal protein binding	78	-23.01
GO:0044822	poly(A) RNA binding	124	-22.28
GO:0043167	ion binding	133	-19.83
GO:0003723	RNA binding	132	-19.13
GO:0003779	actin binding	40	-15.67
GO:0097367	carbohydrate derivative binding	73	-15.32
GO:0043168	anion binding	88	-13.33
GO:0097159	organic cyclic compound binding	202	-13.19
GO:0005201	extracellular matrix structural constituent	22	-12.89
GO:0019899	enzyme binding	116	-12.87
GO:0005200	structural constituent of cytoskeleton	23	-12.12
GO:0004857	enzyme inhibitor activity	42	-11.07
GO:1901363	heterocyclic compound binding	191	-10.72
GO:0005102	receptor binding	95	-10.09
GO:0005539	glycosaminoglycan binding	25	-9.33
GO:0042802	identical protein binding	82	-8.64
GO:0016616	oxidoreductase activity, acting on the CH-OH group of donors, NAD or NADP as acceptor	22	-8.62
GO:0030234	enzyme regulator activity	67	-8.46
GO:0003824	catalytic activity	252	-8.28
GO:0050839	cell adhesion molecule binding	27	-8.14
GO:0036094	small molecule binding	63	-8.00
GO:0043169	cation binding	67	-7.86
GO:0046872	metal ion binding	62	-7.49
GO:0016614	oxidoreductase activity, acting on CH-OH group of donors	22	-7.44
GO:0016209	antioxidant activity	16	-7.42
GO:0034987	immunoglobulin receptor binding	12	-7.41
GO:0016787	hydrolase activity	125	-6.60
GO:0016491	oxidoreductase activity	52	-6.36
GO:0003924	GTPase activity	24	-5.80
GO:0004866	endopeptidase inhibitor activity	20	-5.73
GO:0008289	lipid binding	43	-5.68
GO:0044548	S100 protein binding	8	-5.64
GO:0005178	integrin binding	17	-5.56
GO:0004175	endopeptidase activity	43	-5.41
GO:1901681	sulfur compound binding	21	-5.15
GO:0003676	nucleic acid binding	147	-4.95
GO:0005518	collagen binding	13	-4.86
GO:0019901	protein kinase binding	39	-4.80
GO:0016817	hydrolase activity, acting on acid anhydrides	51	-4.75
GO:0008201	heparin binding	16	-4.71
GO:0051082	unfolded protein binding	14	-4.65
GO:0048306	calcium-dependent protein binding	12	-4.57
GO:0051920	peroxiredoxin activity	5	-4.38
GO:0001948	glycoprotein binding	14	-4.19
GO:0016835	carbon-oxygen lyase activity	13	-4.03
GO:0005509	calcium ion binding	27	-4.02
GO:0005496	steroid binding	14	-4.02
GO:0001848	complement binding	7	-3.81
GO:0016684	oxidoreductase activity, acting on peroxide as acceptor	10	-3.78
GO:1901265	nucleoside phosphate binding	42	-3.56

GO:0032561	**guanyl ribonucleotide binding**	18	-3.45
GO:0019001	**guanyl nucleotide binding**	18	-3.40
GO:0046914	**transition metal ion binding**	33	-3.25
GO:0008233	**peptidase activity**	47	-3.22
GO:0017171	**serine hydrolase activity**	31	-3.20
GO:0008307	**structural constituent of muscle**	10	-3.17
GO:0001882	**nucleoside binding**	33	-3.03
GO:0016829	**lyase activity**	18	-2.94
GO:0046983	**protein dimerization activity**	52	-2.88
GO:0070325	**lipoprotein particle receptor binding**	7	-2.71
GO:0016853	**isomerase activity**	17	-2.69
GO:0031625	**ubiquitin protein ligase binding**	25	-2.67
GO:0048037	**cofactor binding**	17	-2.64
GO:0044389	**small conjugating protein ligase binding**	25	-2.58
GO:0019003	**GDP binding**	10	-2.56
GO:0015485	**cholesterol binding**	9	-2.53
GO:0042803	**protein homodimerization activity**	43	-2.45
GO:0043178	**alcohol binding**	12	-2.32
GO:0044325	**ion channel binding**	13	-2.01
GO:0023026	**MHC class II protein complex binding**	6	-1.87
GO:0060228	**phosphatidylcholine-sterol O-acyltransferase activator activity**	4	-1.80
GO:0097493	**structural molecule activity conferring elasticity**	4	-1.80
GO:0001846	**opsonin binding**	5	-1.80
GO:0044183	**protein binding involved in protein folding**	5	-1.80
GO:0048407	**platelet-derived growth factor binding**	5	-1.80
GO:0005507	**copper ion binding**	8	-1.70
GO:0017127	**cholesterol transporter activity**	5	-1.58
GO:0003823	**antigen binding**	26	-1.58
GO:0008426	**protein kinase C inhibitor activity**	3	-1.52
GO:0070653	**high-density lipoprotein particle receptor binding**	3	-1.52
GO:0050998	**nitric-oxide synthase binding**	4	-1.44
GO:0023023	**MHC protein complex binding**	6	-1.42
GO:0016860	**intramolecular oxidoreductase activity**	8	-1.34
GO:0019843	**rRNA binding**	8	-1.34

* Bonferroni corrected p-value

Supplemental Table 3c. Human Distal Aortic Protein GO Terms: Cellular Component (adj. p-value < 0.05*)

GO Term ID	Description	# of proteins	log(p-value)*
GO:0070062	extracellular vesicular exosome	527	-290.88
GO:0031982	vesicle	542	-260.54
GO:0005576	extracellular region	566	-257.72
GO:0005925	focal adhesion	133	-90.24
GO:0072562	blood microparticle	85	-71.70
GO:0030054	cell junction	145	-61.99
GO:0044444	cytoplasmic part	491	-61.48
GO:0031012	extracellular matrix	87	-58.30
GO:0005829	cytosol	289	-54.61
GO:0043226	organelle	654	-52.71
GO:0043227	membrane-bounded organelle	631	-50.45
GO:0005737	cytoplasm	548	-40.32
GO:0015629	actin cytoskeleton	76	-29.42
GO:0005856	cytoskeleton	149	-26.01
GO:0060205	cytoplasmic membrane-bounded vesicle lumen	37	-24.40
GO:0031983	vesicle lumen	37	-24.22
GO:0005578	proteinaceous extracellular matrix	41	-22.83
GO:0032991	macromolecular complex	250	-17.78
GO:0005788	endoplasmic reticulum lumen	37	-15.26
GO:0043228	non-membrane-bounded organelle	214	-15.03
GO:0044433	cytoplasmic vesicle part	62	-13.77
GO:0043234	protein complex	210	-13.72
GO:0016020	membrane	370	-13.17
GO:0031091	platelet alpha granule	23	-12.06
GO:0045121	membrane raft	31	-11.05
GO:0044449	contractile fiber part	27	-10.63
GO:0044424	intracellular part	587	-10.34
GO:0043292	contractile fiber	27	-9.83
GO:0005622	intracellular	591	-9.44
GO:0044437	vacuolar part	60	-8.97
GO:0005885	Arp2/3 protein complex	8	-8.76
GO:0005773	vacuole	81	-8.73
GO:0044422	organelle part	399	-8.62
GO:0005581	collagen trimer	13	-8.35
GO:0012505	endomembrane system	192	-8.34
GO:0034358	plasma lipoprotein particle	11	-7.38
GO:0044446	intracellular organelle part	387	-7.24
GO:0009986	cell surface	55	-7.05
GO:0032994	protein-lipid complex	11	-6.86
GO:0042571	immunoglobulin complex, circulating	11	-6.86
GO:0098589	membrane region	53	-6.82
GO:0048471	perinuclear region of cytoplasm	40	-6.76
GO:0098644	complex of collagen trimers	10	-6.51
GO:0005832	chaperonin-containing T-complex	7	-6.44
GO:0019814	immunoglobulin complex	11	-6.40
GO:0042383	sarcolemma	13	-5.30
GO:0044448	cell cortex part	16	-5.21
GO:0009897	external side of plasma membrane	21	-5.11
GO:0098552	side of membrane	38	-4.85
GO:0001725	stress fiber	11	-4.80
GO:0005884	actin filament	13	-4.72
GO:0032432	actin filament bundle	11	-4.66
GO:0071944	cell periphery	228	-4.54
GO:0043229	intracellular organelle	492	-4.40
GO:0042995	cell projection	66	-4.36
GO:0044853	plasma membrane raft	13	-4.31

GO:0005811	**lipid particle**	12	-4.09
GO:0005577	**fibrinogen complex**	6	-4.01
GO:0042641	**actomyosin**	11	-4.01
GO:0005874	**microtubule**	23	-3.96
GO:0044445	**cytosolic part**	25	-3.91
GO:0005886	**plasma membrane**	221	-3.64
GO:0031252	**cell leading edge**	24	-3.54
GO:0005938	**cell cortex**	18	-3.53
GO:0005768	**endosome**	49	-3.01
GO:0005783	**endoplasmic reticulum**	85	-2.95
GO:0001527	**microfibril**	5	-2.75
GO:0044464	**cell part**	635	-2.69
GO:0005623	**cell**	635	-2.58
GO:0005796	**Golgi lumen**	14	-2.50
GO:0045259	**proton-transporting ATP synthase complex**	7	-2.46
GO:0001726	**ruffle**	14	-2.33
GO:0005769	**early endosome**	25	-2.23
GO:0001772	**immunological synapse**	7	-2.16
GO:0044432	**endoplasmic reticulum part**	60	-2.10
GO:0098643	**banded collagen fibril**	5	-1.88
GO:0005882	**intermediate filament**	9	-1.69
GO:0031838	**haptoglobin-hemoglobin complex**	3	-1.60
GO:0030904	**retromer complex**	6	-1.37

* Bonferroni corrected p-value

Supplemental Table 4. Enriched Ingenuity Canonical Pathways Among 944 Human LAD Proteins (FDR<0.001)

	-log(B-H p-value)		-log(B-H p-value)
Acute Phase Response Signaling	23.60	α-Adrenergic Signaling	5.21
LXR/RXR Activation	22.00	ERK/MAPK Signaling	4.90
Complement System	19.00	Regulation of Cellular Mechanics by Calpain Protease	4.76
Clathrin-mediated Endocytosis Signaling	17.80	Protein Kinase A Signaling	4.71
FXR/RXR Activation	16.80	Noradrenaline and Adrenaline Degradation	4.64
Integrin Signaling	16.40	Phospholipase C Signaling	4.57
Mitochondrial Dysfunction	14.20	HIPPO signaling	4.57
Glycolysis I	13.60	Dopamine Receptor Signaling	4.46
Actin Cytoskeleton Signaling	13.50	Paxillin Signaling	4.38
RhoGDI Signaling	13.00	Extrinsic Prothrombin Activation Pathway	4.36
Signaling by Rho Family GTPases	11.90	IL-12 Signaling and Production in Macrophages	4.34
RhoA Signaling	11.60	Breast Cancer Regulation by Stathmin1	4.31
Regulation of Actin-based Motility by Rho	11.00	PI3K/AKT Signaling	4.31
Remodeling of Epithelial Adherens Junctions	10.10	Germ Cell-Sertoli Cell Junction Signaling	4.25
Actin Nucleation by ARP-WASP Complex	9.65	Glutaryl-CoA Degradation	4.12
NRF2-mediated Oxidative Stress Response	9.21	EIF2 Signaling	4.08
Coagulation System	9.21	Glutathione Redox Reactions I	4.00
Gluconeogenesis I	9.21	Superoxide Radicals Degradation	3.98
Atherosclerosis Signaling	8.53	IGF-1 Signaling	3.90
TCA Cycle II (Eukaryotic)	8.50	Regulation of eIF4 and p70S6K Signaling	3.87
ILK Signaling	8.36	Tryptophan Degradation III (Eukaryotic)	3.69
Intrinsic Prothrombin Activation Pathway	7.29	Isoleucine Degradation I	3.69
Cdc42 Signaling	7.28	CCR3 Signaling in Eosinophils	3.64
Production of Nitric Oxide and Reactive Oxygen Species in Macrophages	7.28	Sertoli Cell-Sertoli Cell Junction Signaling	3.60
Ephrin Receptor Signaling	7.10	Unfolded protein response	3.56
Virus Entry via Endocytic Pathways	6.88	Thrombin Signaling	3.56
Protein Ubiquitination Pathway	6.87	PPARα/RXRα Activation	3.45
Huntington's Disease Signaling	6.59	Xenobiotic Metabolism Signaling	3.45
Oxidative Phosphorylation	6.43	Pentose Phosphate Pathway	3.44
Epithelial Adherens Junction Signaling	6.43	Role of Tissue Factor in Cancer	3.43
Caveolar-mediated Endocytosis Signaling	6.27	Ethanol Degradation II	3.36
phagosome maturation	6.14	mTOR Signaling	3.32
Glycogen Degradation II	6.02	GDP-glucose Biosynthesis	3.32
Lipid Antigen Presentation by CD1	5.99	Androgen Signaling	3.30
Agrin Interactions at Neuromuscular Junction	5.90	Myc Mediated Apoptosis Signaling	3.24
Rac Signaling	5.89	Methylglyoxal Degradation III	3.23
G Beta Gamma Signaling	5.63	Neuroprotective Role of THOP1 in Alzheimer's Disease	3.22
fMLP Signaling in Neutrophils	5.63	Glutathione-mediated Detoxification	3.21
CDK5 Signaling	5.59	Axonal Guidance Signaling	3.16
p70S6K Signaling	5.58	Synaptic Long Term Potentiation	3.06
Ephrin B Signaling	5.42	14-3-3-mediated Signaling	3.06
Glycogen Degradation III	5.34	Semaphorin Signaling in Neurons	3.02
Fcγ Receptor-mediated Phagocytosis in Macrophages and Monocytes	5.31	Glucose and Glucose-1-phosphate Degradation	3.02
		Aspartate Degradation II	3.02

Supplemental Table 5. Enriched Ingenuity Canonical Pathways among 725 Human Distal Aortic Proteins (FDR<0.001)

	-log(B-H p-value)		-log(B-H p-value)
Acute Phase Response Signaling	22.80	IGF-1 Signaling	5.26
LXR/RXR Activation	20.90	Phospholipase C Signaling	5.26
Integrin Signaling	19.90	Axonal Guidance Signaling	5.16
Complement System	18.60	Extrinsic Prothrombin Activation Pathway	5.12
Clathrin-mediated Endocytosis Signaling	18.00	Huntington's Disease Signaling	4.93
FXR/RXR Activation	16.80	Germ Cell-Sertoli Cell Junction Signaling	4.87
Actin Cytoskeleton Signaling	16.80	Glutaryl-CoA Degradation	4.78
RhoGDI Signaling	15.80	Glycogen Degradation III	4.78
Glycolysis I	15.50	Thrombin Signaling	4.78
Signaling by Rho Family GTPases	14.40	Noradrenaline and Adrenaline Degradation	4.73
RhoA Signaling	13.70	Breast Cancer Regulation by Stathmin1	4.68
Regulation of Actin-based Motility by Rho	13.60	Ephrin B Signaling	4.68
Gluconeogenesis I	12.00	Protein Ubiquitination Pathway	4.57
Actin Nucleation by ARP-WASP Complex	11.70	Tryptophan Degradation III (Eukaryotic)	4.43
Remodeling of Epithelial Adherens Junctions	11.30	Agrin Interactions at Neuromuscular Junction	4.34
Intrinsic Prothrombin Activation Pathway	9.84	14-3-3-mediated Signaling	4.33
ILK Signaling	9.81	Sertoli Cell-Sertoli Cell Junction Signaling	4.26
Caveolar-mediated Endocytosis Signaling	9.71	IL-12 Signaling and Production in Macrophages	4.26
Coagulation System	8.42	Neuroprotective Role of THOP1 in Alzheimer's Disease	4.05
Epithelial Adherens Junction Signaling	7.88	Hepatic Fibrosis / Hepatic Stellate Cell Activation	3.99
Atherosclerosis Signaling	7.87	Pentose Phosphate Pathway	3.99
Ephrin Receptor Signaling	7.61	FAK Signaling	3.94
Cdc42 Signaling	7.36	Lipid Antigen Presentation by CD1	3.90
Production of Nitric Oxide and Reactive Oxygen Species in Macrophages	7.27	CCR3 Signaling in Eosinophils	3.89
Virus Entry via Endocytic Pathways	7.16	Unfolded protein response	3.85
phagosome maturation	6.64	Role of Tissue Factor in Cancer	3.56
G Beta Gamma Signaling	6.45	Myc Mediated Apoptosis Signaling	3.51
ERK/MAPK Signaling	6.34	Androgen Signaling	3.44
Rac Signaling	6.18	Cellular Effects of Sildenafil (Viagra)	3.44
p70S6K Signaling	5.97	Ethanol Degradation II	3.26
fMLP Signaling in Neutrophils	5.96	ERK5 Signaling	3.22
Regulation of Cellular Mechanics by Calpain Protease	5.96	Isoleucine Degradation I	3.22
PI3K/AKT Signaling	5.84	Synaptic Long Term Potentiation	3.22
CDK5 Signaling	5.84	Semaphorin Signaling in Neurons	3.19
Paxillin Signaling	5.84	Sucrose Degradation V (Mammalian)	3.19
Protein Kinase A Signaling	5.70	Superoxide Radicals Degradation	3.19
NRF2-mediated Oxidative Stress Response	5.64	Cardiac β-adrenergic Signaling	3.18
Mitochondrial Dysfunction	5.59	Dopamine Receptor Signaling	3.17
Fcγ Receptor-mediated Phagocytosis in Macrophages and Monocytes	5.47	P2Y Purigenic Receptor Signaling Pathway	3.17
Glycogen Degradation II	5.29	Gαi Signaling	3.10
α-Adrenergic Signaling	5.28	eNOS Signaling	3.09
HIPPO signaling	5.28	Pentose Phosphate Pathway (Oxidative Branch)	3.00

Supplemental Table 6. Regression Models of Association Between Individual Proteins and Extent of Surface Area Involve with Fibrous Plaque (FP) or Normal Intima (NL) in Human LAD Arterial Samples (top 100 proteins). In models of %FP, the r FP% fraction includes fatty streaks (FS) and NML intima. Likewise, in models of % NL, the non-NL faction includes both FP an FS. Accordingly, we modeled both %FP and %NL separately. We also classified samples into three level ordinal categories o extent of FP and extent of NL and performed ordinal logistic regression (Ord LR). This approach is less statistically powerful, makes fewer distributional assumptions about the measures of extent of disease. In addition, we used MANOVA to jointly m the distribution of %FP, %FS and %NL. P-values and q-values ≤0.05 are highlighted in green and pink respectively. **Proteins i bold (n=21) are also included in the top 100 AA proteins**

			MANOVA (%FP,%FS)		GLM (%FP)			Ord LR (%FP)			GLM (% NML)			Ord LR (%NML)		
Uniprot ID	Protein	Gene	*p-value*	*q-value*	*beta*	*p-value*	*q-value*	*beta*	*p-value*	*q-value*	*beta*	*p-value*	*q-value*	*beta*	*p-value*	*q-value*
P07858	**Cathepsin B**	**CTSB**	9.3E-09	5.5E-06	16.5	2.4E-08	1.0E-05	-1.9	2.2E-05	1.5E-02	-20.1	1.0E-08	7.4E-06	2.3	9.8E-06	5.8E-03
P24821	**Tenascin**	**TNC**	2.1E-08	6.3E-06	2.3	1.2E-08	1.0E-05	-0.3	7.1E-05	2.4E-02	-2.6	9.9E-08	3.6E-05	0.3	2.8E-04	4.2E-02
Q15063	**Periostin**	**POSTN**	1.1E-06	2.1E-04	1.9	2.9E-06	7.5E-04	-0.2	3.8E-04	3.0E-02	-2.4	4.1E-07	9.9E-05	0.2	1.3E-04	2.5E-02
P04114	**Apolipoprotein B-100**	**APOB**	3.5E-06	5.3E-04	0.6	3.1E-05	3.7E-03	-0.1	9.3E-04	4.5E-02	-0.9	6.6E-07	1.2E-04	0.1	8.0E-04	7.9E-02
P07996	Thrombospondin-1	THBS1	6.3E-06	7.5E-04	2.7	3.3E-04	2.0E-02	-0.3	2.8E-03	8.6E-02	-4.3	9.2E-07	1.3E-04	0.4	1.3E-03	9.5E-02
P13796	**Plastin-2**	LCP1	1.4E-05	1.2E-03	6.5	3.6E-06	7.5E-04	-0.7	2.0E-04	3.0E-02	-6.9	4.2E-05	3.7E-03	0.5	9.4E-04	7.9E-02
P07339	**Cathepsin D**	**CTSD**	1.7E-05	1.3E-03	11.9	4.9E-06	8.3E-04	-1.4	2.6E-03	8.6E-02	-12.9	3.9E-05	3.7E-03	1.4	2.5E-03	1.1E-01
Q9UBR2	**Cathepsin Z**	**CTSZ**	1.3E-05	1.2E-03	29.6	2.0E-05	2.7E-03	-3.9	2.2E-04	3.0E-02	-37.3	5.0E-06	6.0E-04	2.7	8.7E-04	7.9E-02
P50895	**Basal cell adhesion molecule**	**BCAM**	4.4E-04	2.2E-02	-3.3	4.3E-02	4.0E-01	0.6	1.6E-02	2.3E-01	7.0	1.9E-04	1.4E-02	-1.0	4.1E-05	1.2E-02
P40261	Nicotinamide N-methyltransferase	NNMT	3.1E-04	1.7E-02	27.3	6.3E-05	6.6E-03	-3.7	3.0E-04	3.0E-02	-22.6	6.5E-03	1.2E-01	2.2	5.8E-03	1.2E-01
P13760	HLA class II HC Ag, DRB1-4 beta	HLA-DRB1	3.0E-04	1.7E-02	18.2	7.5E-05	7.0E-03	-1.9	8.4E-04	4.5E-02	-19.2	4.7E-04	2.6E-02	1.5	9.0E-03	1.5E-01
P40121	**Macrophage-capping protein**	**CAPG**	5.1E-04	2.2E-02	13.4	1.0E-04	8.5E-03	-1.8	1.4E-04	3.0E-02	-13.1	1.6E-03	5.9E-02	1.3	1.6E-03	1.0E-01
O43866	**CD5 antigen-like**	CD5L	5.0E-04	2.2E-02	11.7	1.3E-04	9.9E-03	-1.4	4.1E-04	3.0E-02	-12.4	6.7E-04	3.2E-02	0.9	6.2E-03	1.2E-01
P35442	**Thrombospondin-2**	**THBS2**	8.4E-04	2.9E-02	2.3	3.4E-03	1.1E-01	-0.3	8.1E-03	1.7E-01	-3.5	1.6E-04	1.3E-02	0.2	1.0E-02	1.5E-01
P07998	Ribonuclease pancreatic	RNASE1	2.8E-04	1.7E-02	73.8	1.7E-04	1.2E-02	-4.8	2.1E-02	2.4E-01	-45.5	5.7E-02	3.5E-01	2.8	1.4E-01	3.3E-01
O14773	Tripeptidyl-peptidase 1	TPP1	7.7E-04	2.9E-02	20.8	1.8E-04	1.2E-02	-3.6	3.7E-04	3.0E-02	-16.3	1.6E-02	2.0E-01	1.6	1.1E-02	1.5E-01
P01871	**Ig mu chain C region**	IGHM	8.3E-04	2.9E-02	2.2	4.6E-04	2.3E-02	-0.2	2.7E-03	8.6E-02	-2.7	3.7E-04	2.4E-02	0.2	2.8E-03	1.1E-01
P22105	Tenascin-X	TNXB	9.1E-04	3.0E-02	2.4	4.6E-04	2.3E-02	-0.3	4.9E-04	3.0E-02	-2.9	4.3E-04	2.6E-02	0.2	3.4E-03	1.1E-01
Q15582	TGFBI ig-h3	TGFBI	4.3E-03	9.5E-02	2.9	1.2E-03	5.6E-02	-0.4	4.4E-04	3.0E-02	-3.1	3.8E-03	8.9E-02	0.3	3.0E-03	1.1E-01
P13667	Protein disulfide-isomerase A4	PDIA4	1.5E-03	4.1E-02	16.5	4.5E-04	2.3E-02	-1.7	3.5E-03	1.0E-01	-18.2	1.2E-03	5.1E-02	1.4	4.3E-03	1.1E-01
P04004	**Vitronectin**	**VTN**	2.5E-03	6.2E-02	3.5	2.0E-02	3.2E-01	-0.4	3.1E-02	2.5E-01	-6.1	5.7E-04	3.0E-02	0.5	1.0E-02	1.5E-01
P14618	Pyruvate kinase PKM	PKM	1.7E-02	1.9E-01	3.4	6.5E-03	1.8E-01	-0.6	9.2E-04	4.5E-02	-3.9	8.5E-03	1.5E-01	0.4	3.7E-03	1.1E-01
P09960	Leukotriene A-4 hydrolase	LTA4H	9.6E-04	3.0E-02	6.0	5.4E-02	4.6E-01	-0.7	1.0E-01	3.7E-01	1.9	6.2E-01	6.6E-01	-0.3	3.5E-01	4.2E-01
P00450	**Ceruloplasmin**	**CP**	1.1E-03	3.2E-02	2.6	7.9E-03	2.0E-01	-0.4	1.1E-02	1.9E-01	-0.5	6.7E-01	6.8E-01	0.0	8.2E-01	5.7E-01
P04844	Ribophorin-2	RPN2	3.7E-03	8.4E-02	13.8	2.8E-03	1.0E-01	-1.7	5.2E-03	1.4E-01	-17.7	1.1E-03	5.1E-02	1.5	3.0E-03	1.1E-01
Q08380	Galectin-3-binding protein	LGALS3BP	5.7E-03	1.1E-01	6.4	8.8E-03	2.2E-01	-0.6	2.0E-02	2.4E-01	-9.2	1.3E-03	5.3E-02	0.7	1.3E-02	1.8E-01
P08519	Apolipoprotein(a)	LPA	6.5E-03	1.2E-01	23.3	1.5E-02	2.7E-01	-3.0	7.8E-03	1.7E-01	-35.8	1.5E-03	5.6E-02	2.8	8.0E-03	1.4E-01
Q03135	Caveolin-1	CAV1	4.6E-03	9.8E-02	-10.0	2.5E-03	9.4E-02	2.0	1.6E-03	6.9E-02	12.3	1.8E-03	6.1E-02	-1.1	3.8E-03	1.1E-01
P07900	Heat shock protein HSP 90-alpha	HSP90AA1	1.6E-03	4.3E-02	1.6	1.2E-01	6.0E-01	0.0	8.1E-01	6.7E-01	1.0	4.1E-01	5.9E-01	-0.1	1.6E-01	3.5E-01
P30153	PP2A subunit A isoform PR65-alpha	PPP2R1A	2.0E-03	5.1E-02	0.4	8.9E-01	8.8E-01	-0.1	8.9E-01	6.8E-01	7.8	3.4E-02	2.8E-01	-0.7	3.2E-02	2.2E-01
P12955	Xaa-Pro dipeptidase	PEPD	6.8E-03	1.2E-01	32.3	2.1E-03	9.3E-02	-3.2	9.6E-03	1.8E-01	-35.3	4.8E-03	1.0E-01	2.6	1.6E-02	1.9E-01
O15511	Actin-related protein 2/3 complex subunit 5	ARPC5	6.8E-03	1.2E-01	30.5	2.3E-03	9.4E-02	-3.9	2.1E-03	8.6E-02	-21.2	8.0E-02	4.0E-01	2.0	6.2E-02	2.8E-01
P48163	NADP-dependent malic enzyme	ME1	9.4E-03	1.5E-01	-5.2	2.3E-02	3.3E-01	0.8	4.3E-02	2.9E-01	8.1	2.2E-03	7.2E-02	-1.0	3.8E-03	1.1E-01
P01023	**Alpha-2-macroglobulin**	**A2M**	9.9E-03	1.5E-01	1.7	3.3E-03	1.1E-01	-0.3	2.2E-03	8.6E-02	-1.8	6.0E-03	1.2E-01	0.1	2.8E-02	2.1E-01
Q8WX93	Palladin	PALLD	2.1E-02	2.2E-01	-2.6	9.8E-02	5.5E-01	0.6	1.2E-02	2.0E-01	4.9	6.6E-03	1.2E-01	-0.6	2.2E-03	1.1E-01
Q6NZI2	Polymerase I and transcript release factor	PTRF	1.3E-02	1.7E-01	-5.9	1.9E-02	3.2E-01	1.6	2.5E-03	8.6E-02	8.7	3.2E-03	8.7E-02	-0.9	5.8E-03	1.2E-01
O43396	Thioredoxin-like protein 1	TXNL1	8.0E-03	1.4E-01	45.9	2.5E-03	9.4E-02	-4.8	6.4E-03	1.5E-01	-33.4	6.7E-02	3.8E-01	2.5	9.2E-02	2.8E-01
P27169	**Serum paraoxonase/arylesterase 1**	**PON1**	1.1E-02	1.5E-01	6.9	2.8E-02	3.4E-01	-0.6	8.2E-02	3.5E-01	-11.1	2.6E-03	7.8E-02	1.0	3.1E-02	2.2E-01

Q9NZN4	EH domain-containing protein 2	EHD2	3.1E-03	7.4E-02	-1.2	2.0E-01	6.9E-01	0.2	4.7E-02	2.9E-01	3.3	2.6E-03	7.8E-02	-0.3	5.6E-03	1.2E-01
P00352	Retinal dehydrogenase 1	ALDH1A1	1.4E-02	1.7E-01	-1.9	6.5E-03	1.8E-01	0.3	2.8E-03	8.6E-02	2.3	5.4E-03	1.1E-01	-0.2	8.1E-03	1.4E-01
Q13885	Tubulin beta-2A chain	TUBB2A	8.5E-03	1.4E-01	-0.8	8.1E-02	5.3E-01	0.1	2.7E-02	2.5E-01	1.6	2.8E-03	8.1E-02	-0.1	1.1E-02	1.5E-01
P09543	2',3'-cyclic-nucleotide 3'-phosphodiesterase	CNP	1.1E-02	1.5E-01	-8.7	7.5E-03	2.0E-01	2.3	8.9E-03	1.7E-01	11.4	3.2E-03	8.7E-02	-0.9	2.7E-02	2.1E-01
P62158	Calmodulin	CALM1	3.6E-02	2.8E-01	-6.3	8.8E-02	5.4E-01	1.2	5.3E-02	3.0E-01	11.1	1.1E-02	1.7E-01	-1.5	3.4E-03	1.1E-01
Q07065	Cytoskeleton-associated protein 4	CKAP4	2.6E-02	2.4E-01	14.6	1.0E-02	2.4E-01	-2.2	5.4E-03	1.4E-01	-16.9	1.2E-02	1.7E-01	1.8	3.5E-03	1.1E-01
Q9BQE3	Tubulin alpha-1C chain	TUBA1C	8.7E-03	1.4E-01	-1.0	1.2E-01	6.0E-01	0.2	5.1E-02	2.9E-01	2.1	3.6E-03	8.9E-02	-0.2	2.6E-02	2.1E-01
P02545	Adenylyl cyclase-associated protein 1	CAP1	1.1E-02	1.5E-01	-1.6	8.9E-02	5.4E-01	0.3	4.6E-02	2.9E-01	3.2	3.6E-03	8.9E-02	-0.3	4.3E-03	1.1E-01
P61160	Actin-related protein 2	ACTR2	1.2E-02	1.6E-01	10.6	3.8E-03	1.2E-01	-1.1	2.0E-02	2.4E-01	-11.5	8.3E-03	1.5E-01	0.6	1.3E-01	3.2E-01
P10768	S-formylglutathione hydrolase	ESD	1.4E-02	1.7E-01	-5.7	5.1E-02	4.5E-01	0.8	4.7E-02	2.9E-01	10.0	3.8E-03	8.9E-02	-0.9	4.2E-03	1.1E-01
P55268	Cell division control protein 42 homolog	CDC42	4.1E-02	2.8E-01	-1.5	3.4E-02	3.6E-01	0.3	1.8E-02	2.4E-01	2.1	1.2E-02	1.7E-01	-0.3	3.9E-03	1.1E-01
P98095	Fibulin-2	FBLN2	1.6E-02	1.8E-01	3.3	2.6E-02	3.4E-01	-0.4	2.9E-02	2.5E-01	-5.0	4.1E-03	9.1E-02	0.3	3.5E-02	2.3E-01
P07602	Prosaposin	PSAP	1.5E-02	1.7E-01	23.5	4.2E-03	1.3E-01	-2.4	1.1E-02	1.9E-01	-24.7	1.2E-02	1.7E-01	1.9	2.0E-02	2.0E-01
P50395	Rab GDP dissociation inhibitor beta	GDI2	3.5E-02	2.7E-01	4.9	2.8E-02	3.4E-01	-0.9	4.3E-03	1.2E-01	-6.7	1.0E-02	1.7E-01	0.7	4.8E-03	1.1E-01
Q14108	Lysosome membrane protein 2	SCARB2	1.6E-02	1.8E-01	21.8	9.1E-02	5.4E-01	-2.7	4.5E-02	2.9E-01	-42.3	5.1E-03	1.1E-01	4.3	4.8E-03	1.1E-01
P13489	Ribonuclease inhibitor	RNH1	4.9E-03	1.0E-01	3.2	1.5E-01	6.1E-01	-0.4	2.6E-01	4.9E-01	1.9	4.8E-01	6.3E-01	-0.1	5.7E-01	5.0E-01
P06756	Integrin alpha-V	ITGAV	6.6E-03	1.2E-01	29.7	5.4E-03	1.6E-01	-2.5	3.7E-02	2.6E-01	-14.9	2.5E-01	5.1E-01	1.0	3.3E-01	4.2E-01
P52566	Rho GDP-dissociation inhibitor 2	ARHGDIB	2.7E-02	2.4E-01	11.3	1.1E-02	2.4E-01	-1.5	5.4E-03	1.4E-01	-7.3	1.8E-01	4.6E-01	0.5	2.1E-01	3.7E-01
P53396	ATP-citrate synthase	ACLY	2.4E-02	2.3E-01	-8.9	3.0E-02	3.5E-01	2.4	3.0E-02	2.5E-01	13.2	6.2E-03	1.2E-01	-2.0	8.4E-03	1.4E-01
Q15746	Myosin light chain kinase, smooth muscle	MYLK	3.2E-02	2.6E-01	-1.6	3.5E-01	7.4E-01	0.7	1.4E-02	2.1E-01	4.5	2.2E-02	2.3E-01	-0.5	6.9E-03	1.3E-01
P12111	**Collagen alpha-3(VI) chain**	**COL6A3**	6.8E-02	3.2E-01	0.6	2.0E-02	3.2E-01	-0.1	7.1E-03	1.6E-01	-0.6	5.8E-02	3.6E-01	0.0	7.4E-02	2.8E-01
P00488	**Coagulation factor XIII A chain**	**F13A1**	1.2E-01	3.8E-01	3.8	4.1E-02	4.0E-01	-0.6	7.6E-03	1.7E-01	-4.0	7.1E-02	3.9E-01	0.3	9.0E-02	2.8E-01
O43852	Calumenin	CALU	2.9E-02	2.6E-01	30.0	7.7E-03	2.0E-01	-3.0	2.3E-02	2.4E-01	-28.2	3.6E-02	2.9E-01	2.5	3.9E-02	2.4E-01
P49327	Protein CutA	CUTA	4.6E-02	2.8E-01	-0.6	2.5E-02	3.4E-01	0.1	2.2E-02	2.4E-01	0.7	1.6E-02	2.0E-01	-0.1	8.3E-03	1.4E-01
P31146	**Coronin-1A**	**CORO1A**	4.7E-02	2.8E-01	7.8	1.4E-02	2.6E-01	-1.0	8.3E-03	1.7E-01	-6.6	7.9E-02	4.0E-01	0.6	5.4E-02	2.8E-01
Q9BXN1	Asporin	ASPN	3.1E-02	2.6E-01	11.4	1.1E-02	2.4E-01	-1.4	8.9E-03	1.7E-01	-12.9	1.6E-02	2.0E-01	0.9	4.3E-02	2.5E-01
Q15847	Adipogenesis regulatory factor	ADIRF	1.1E-01	3.8E-01	-12.9	4.8E-02	4.2E-01	1.8	8.3E-02	3.5E-01	15.1	5.1E-02	3.4E-01	-2.0	9.1E-03	1.5E-01
P02649	**Apolipoprotein E**	**APOE**	3.3E-02	2.7E-01	3.0	3.2E-02	3.5E-01	-0.3	7.8E-02	3.5E-01	-4.4	9.2E-03	1.6E-01	0.3	6.9E-02	2.8E-01
P31949	Protein S100-A11	S100A11	2.7E-02	2.4E-01	6.6	9.4E-03	2.3E-01	-0.5	1.0E-01	3.7E-01	-4.7	1.3E-01	4.3E-01	0.2	3.5E-01	4.2E-01
P08294	Extracellular superoxide dismutase [Cu-Zn]	SOD3	9.7E-03	1.5E-01	1.0	7.5E-01	8.6E-01	-0.1	8.6E-01	6.8E-01	6.2	9.5E-02	4.2E-01	-0.4	2.2E-01	3.7E-01
P43121	Cell surface glycoprotein MUC18	MCAM	5.2E-02	2.9E-01	-2.7	9.8E-02	5.5E-01	0.5	3.6E-02	2.6E-01	4.6	1.6E-02	2.0E-01	-0.5	9.9E-03	1.5E-01
P20231	Tryptase beta-2	TPSB2	3.2E-02	2.6E-01	6.4	2.1E-02	3.2E-01	-0.6	6.2E-02	3.2E-01	-8.4	1.0E-02	1.7E-01	0.5	5.6E-02	2.8E-01
P62258	14-3-3 protein epsilon	YWHAE	1.6E-02	1.8E-01	-1.2	6.6E-01	8.3E-01	0.2	5.4E-01	6.0E-01	7.1	3.2E-02	2.7E-01	-0.8	1.0E-02	1.5E-01
Q04828	Aldo-keto reductase family 1 member C1	AKR1C1	3.5E-02	2.7E-01	-4.4	1.0E-02	2.4E-01	0.7	1.9E-02	2.4E-01	4.6	2.7E-02	2.6E-01	-0.4	6.5E-02	2.8E-01
P02656	Apolipoprotein C-III	APOC3	3.7E-02	2.8E-01	-20.2	3.2E-02	3.5E-01	2.9	7.6E-02	3.5E-01	28.4	1.1E-02	1.7E-01	-1.7	1.2E-01	3.1E-01
P12277	Creatine kinase B-type	CKB	1.0E-01	3.6E-01	-3.2	9.0E-02	5.4E-01	0.6	2.8E-02	2.5E-01	4.8	3.2E-02	2.7E-01	-0.5	1.1E-02	1.5E-01
Q01518	Prelamin-A/C	LMNA	1.1E-02	1.5E-01	2.7	1.1E-01	5.6E-01	-0.2	2.3E-01	4.9E-01	0.7	7.2E-01	6.9E-01	-0.2	2.1E-01	3.7E-01
Q969G5	Coronin-1B	CORO1B	2.1E-02	2.2E-01	-4.4	2.2E-01	7.1E-01	0.8	9.2E-02	3.5E-01	10.7	1.1E-02	1.7E-01	-0.9	1.7E-02	1.9E-01
P14625	Endoplasmin	HSP90B1	2.3E-02	2.3E-01	4.7	1.6E-02	2.8E-01	-0.7	1.1E-02	1.9E-01	-2.3	3.2E-01	5.4E-01	0.1	4.9E-01	4.8E-01
Q16527	Cysteine and glycine-rich protein 2	CSRP2	2.7E-02	2.4E-01	-6.7	1.2E-02	2.5E-01	0.8	2.3E-02	2.4E-01	8.0	1.1E-02	1.7E-01	-0.6	2.7E-02	2.1E-01
P12110	Collagen alpha-2(VI) chain	COL6A2	8.0E-02	3.3E-01	1.8	3.3E-02	3.5E-01	-0.3	1.2E-02	2.0E-01	-2.1	3.6E-02	2.9E-01	0.2	3.5E-02	2.3E-01
Q7Z7G0	Target of Nesh-SH3	ABI3BP	4.4E-02	2.8E-01	-3.9	5.9E-02	4.8E-01	0.6	3.1E-02	2.5E-01	6.1	1.2E-02	1.7E-01	-0.5	1.6E-02	1.9E-01
P10643	Complement component C7	C7	4.5E-02	2.8E-01	5.7	1.3E-02	2.5E-01	-0.5	8.9E-02	3.5E-01	-5.1	5.8E-02	3.6E-01	0.2	3.3E-01	4.2E-01
Q96CX2	Chloride intracellular channel protein 6	CLIC6	4.2E-02	2.8E-01	11.1	1.3E-02	2.5E-01	-1.3	2.8E-02	2.5E-01	-8.7	1.0E-01	4.3E-01	0.7	1.2E-01	3.2E-01
Q99715	Collagen alpha-1(XII) chain	COL12A1	1.4E-02	1.7E-01	0.5	3.7E-01	7.5E-01	-0.1	3.6E-01	5.4E-01	-1.7	1.3E-02	1.8E-01	0.1	8.1E-02	2.8E-01
P62942	Peptidyl-prolyl cis-trans isomerase FKBP1A	FKBP1A	4.8E-02	2.8E-01	-10.8	7.4E-02	5.2E-01	1.1	2.0E-01	4.6E-01	17.6	1.4E-02	1.8E-01	-1.2	5.9E-02	2.8E-01
P19105	Myosin regulatory light chain 12A	MYL12A	2.2E-01	4.5E-01	-1.4	9.1E-02	5.4E-01	0.3	1.4E-02	2.1E-01	1.5	1.1E-01	4.3E-01	-0.1	1.2E-01	3.2E-01
Q16853	Membrane primary amine oxidase	AOC3	4.3E-02	2.8E-01	-2.2	2.3E-02	3.3E-01	0.4	1.4E-02	2.1E-01	2.8	1.5E-02	2.0E-01	-0.3	2.8E-02	2.1E-01
P30040	Endoplasmic reticulum resident protein 29	ERP29	5.0E-02	2.9E-01	29.3	1.4E-02	2.7E-01	-2.7	7.2E-02	3.4E-01	-26.0	6.9E-02	3.8E-01	1.6	1.7E-01	3.5E-01
P09382	Galectin-1	LGALS1	5.7E-02	2.9E-01	-1.7	2.9E-01	7.2E-01	0.5	6.0E-02	3.2E-01	4.0	2.8E-02	2.7E-01	-0.5	1.4E-02	1.8E-01
Q16658	Fascin	FSCN1	4.3E-02	2.8E-01	18.0	1.4E-02	2.7E-01	-1.9	4.5E-02	2.9E-01	-19.7	2.5E-02	2.5E-01	1.3	8.8E-02	2.8E-01
P27824	Calnexin	CANX	3.2E-02	2.6E-01	6.6	1.5E-02	2.7E-01	-0.8	3.5E-02	2.6E-01	-4.0	2.3E-01	5.0E-01	0.1	7.0E-01	5.5E-01
P29401	Transketolase	TKT	8.7E-02	3.3E-01	-1.2	4.1E-01	7.6E-01	0.2	3.3E-01	5.4E-01	3.4	5.1E-02	3.4E-01	-0.5	1.5E-02	1.9E-01
P60981	Destrin	DSTN	6.8E-02	3.2E-01	-2.0	3.5E-01	7.4E-01	0.4	2.1E-01	4.7E-01	5.2	3.7E-02	2.9E-01	-0.6	1.6E-02	1.9E-01
P00736	**Complement C1r subcomponent**	**C1R**	2.2E-02	2.2E-01	4.7	2.1E-02	3.2E-01	-0.7	1.6E-02	2.3E-01	-2.0	4.2E-01	6.0E-01	0.1	7.2E-01	5.5E-01

Q12765	Utrophin	UTRN	1.7E-01	4.2E-01	-4.9	4.1E-01	7.6E-01	1.3	1.7E-01	4.4E-01	12.1	8.5E-02	4.1E-01	-1.8	1.6E-02	1.9E-01
P30048	Peroxiredoxin III	PRDX3	4.3E-02	2.8E-01	-13.6	2.2E-02	3.3E-01	1.0	2.1E-01	4.7E-01	16.9	1.6E-02	2.0E-01	-1.1	1.1E-01	3.0E-01
P15088	Mast cell carboxypeptidase A	CPA3	1.6E-01	4.2E-01	6.8	1.5E-01	6.3E-01	-1.2	4.5E-02	2.9E-01	-10.8	5.6E-02	3.5E-01	1.2	1.6E-02	1.9E-01
O60888	Fatty acid synthase	FASN	4.6E-02	2.8E-01	-7.3	1.7E-01	6.4E-01	1.0	1.9E-01	4.6E-01	14.7	1.7E-02	2.0E-01	-1.3	2.6E-02	2.1E-01
P35555	Fibrillin-1	FBN1	1.0E-01	3.7E-01	0.9	8.2E-02	5.3E-01	-0.2	1.7E-02	2.3E-01	-1.3	3.3E-02	2.8E-01	0.1	2.4E-02	2.1E-01
P17858	ATP-dependent 6-phosphofructokinase, liver type	PFKL	8.3E-02	3.3E-01	10.1	4.4E-02	4.0E-01	-1.6	1.7E-02	2.3E-01	-5.6	3.5E-01	5.6E-01	0.4	4.0E-01	4.5E-01
Q8NBX0	UV excision repair protein RAD23 homolog A	RAD23A	2.5E-01	4.5E-01	30.5	1.0E-01	5.5E-01	-5.0	1.7E-02	2.3E-01	-33.8	1.3E-01	4.3E-01	3.2	8.5E-02	2.8E-01

Supplemental Table 7. Regression Models of Association Between Individual Proteins and Extent of Surface Area Involve with Fibrous Plaque (FP) or Normal (NML) in Human Abdominal Aorta Samples (top 100 proteins). In models of %FP, the r FP% fraction includes fatty streaks (FS) and NML intima. Likewise, in models of % NML, the non-NML faction includes both F and FS. Accordingly, we modeled both %FP and %NML separately. We also classified samples into three level ordinal catego of extent of FP and extent of NML and performed ordinal logistic regression (Ord LR). This approach is less statistically powe but makes fewer distributional assumptions about the measures of extent of disease. In addition, we used MANOVA to joint model the distribution of %FP, %FS, and %NML. P-values and q-values ≤0.05 are highlighted in green and pink respectively. **Proteins in bold (n=21) are also included in the top 100 LAD proteins**.

			MANOVA (%FP,%FS)		GLM (%FP)			Ord LR (%FP)			GLM (% NML)			Ord LR (%NML)		
Uniprot ID	Protein	Gene	*p-value*	*q-value*	*beta*	*p-value*	*q-value*	*beta*	*p-value*	*q-value*	*beta*	*p-value*	*q-value*	*beta*	*p-value*	*q-va*
P04114	**Apolipoprotein B-100**	APOB	4.08E-15	1.64E-12	1.01	4.17E-16	1.42E-13	-0.11	6.33E-05	1.13E-02	-0.71	2.08E-04	2.82E-02	0.05	2.32E-02	4.19
P02649	**Apolipoprotein E**	APOE	2.64E-14	5.31E-12	9.39	4.77E-15	8.12E-13	-0.72	3.96E-04	2.45E-02	-8.79	9.69E-07	4.72E-04	0.53	3.88E-03	4.19
O43866	**CD5 antigen-like**	CD5L	2.28E-13	3.06E-11	23.47	2.16E-14	2.45E-12	-3.57	6.57E-06	2.35E-03	-17.32	2.20E-04	2.82E-02	0.97	2.49E-02	4.19
P00747	Plasminogen	PLG	5.98E-12	6.01E-10	7.58	1.48E-12	1.26E-10	-0.56	1.42E-03	3.05E-02	-4.55	5.14E-03	1.43E-01	0.19	1.35E-01	5.04
P19823	Inter-alpha-trypsin	ITIH2	9.60E-11	7.72E-09	10.63	3.94E-11	2.68E-09	-0.92	8.50E-04	3.05E-02	-5.77	1.71E-02	2.61E-01	0.32	1.00E-01	4.76
P07339	**Cathepsin D**	CTSD	2.08E-09	1.11E-07	21.06	2.59E-10	1.37E-08	-1.67	3.20E-03	4.29E-02	-18.24	1.72E-04	2.82E-02	1.07	1.86E-02	4.19
P40121	**Macrophage-capping protein**	CAPG	4.22E-10	2.83E-08	23.61	2.82E-10	1.37E-08	-1.43	7.37E-03	6.43E-02	-25.64	1.48E-06	4.72E-04	2.57	1.96E-03	4.19
P01892	HLA class I HC Ag, A-2 alpha	HLA-A	3.97E-09	1.77E-07	20.85	4.47E-10	1.90E-08	-1.76	4.80E-04	2.45E-02	-16.10	1.02E-03	5.59E-02	1.05	1.50E-02	4.19
P27169	**Serum paraoxonase 1**	PON1	2.22E-09	1.11E-07	19.28	5.05E-10	1.91E-08	-1.62	9.99E-03	6.76E-02	-11.51	1.23E-02	2.18E-01	0.42	3.21E-01	6.30
P00739	Haptoglobin-related protein	HPR	9.08E-09	3.04E-07	14.51	1.11E-09	3.79E-08	-1.30	3.52E-03	4.29E-02	-10.60	2.40E-03	7.80E-02	0.85	1.74E-02	4.19
P24821	**Tenascin**	TNC	1.21E-08	3.46E-07	2.23	1.40E-09	4.34E-08	-0.11	1.90E-02	8.04E-02	-1.79	8.55E-04	5.59E-02	0.08	8.27E-02	4.70
P07858	**Cathepsin B**	CTSB	1.07E-08	3.32E-07	17.11	1.80E-09	5.10E-08	-1.00	1.52E-02	7.52E-02	-11.05	8.26E-03	1.76E-01	0.59	1.45E-01	5.17
P01871	**Ig mu chain C region**	IGHM	5.90E-09	2.37E-07	6.48	1.99E-09	5.21E-08	-0.77	1.10E-04	1.22E-02	-3.53	2.71E-02	3.02E-01	0.18	1.51E-01	5.17
P13796	**Plastin-2**	LCP1	1.96E-08	5.25E-07	11.39	2.32E-09	5.64E-08	-0.60	1.15E-02	6.76E-02	-9.18	9.26E-04	5.59E-02	0.58	4.32E-02	4.59
P05090	Apolipoprotein D	APOD	7.04E-09	2.57E-07	23.52	2.15E-08	4.29E-07	-1.90	9.70E-04	3.05E-02	-7.87	2.04E-01	5.95E-01	0.22	6.12E-01	7.29
P04003	C4b-binding protein	C4BPA	6.70E-08	1.50E-06	6.27	8.23E-09	1.87E-07	-0.46	3.30E-03	4.29E-02	-4.96	1.64E-03	6.98E-02	0.36	1.08E-02	4.19
P00734	Prothrombin	F2	5.62E-08	1.33E-06	10.31	1.82E-08	3.86E-07	-0.67	1.06E-02	6.76E-02	-5.57	3.80E-02	3.20E-01	0.41	8.28E-02	4.70
P01023	**Alpha-2-macroglobulin**	A2M	2.34E-08	5.89E-07	2.87	2.26E-07	3.50E-06	-0.28	1.45E-03	3.05E-02	-0.62	4.42E-01	7.70E-01	0.00	9.33E-01	8.06
P05546	Heparin cofactor 2	SERPIND	3.92E-07	7.16E-06	27.74	7.47E-08	1.41E-06	-1.90	6.08E-03	5.88E-02	-17.35	2.04E-02	2.90E-01	0.67	2.67E-01	6.04
P20742	Pregnancy zone protein	PZP	1.38E-07	2.92E-06	26.87	1.63E-07	2.77E-06	-2.17	2.20E-02	8.33E-02	-10.27	1.70E-01	5.85E-01	0.10	8.52E-01	7.90
P01031	Complement C5	C5	9.55E-07	1.60E-05	7.22	1.46E-07	2.61E-06	-0.65	3.59E-03	4.29E-02	-6.37	1.14E-03	5.59E-02	0.40	2.01E-02	4.19
P02647	Apolipoprotein A-I	APOA1	2.07E-07	3.97E-06	7.40	1.86E-07	3.01E-06	-0.81	2.17E-03	3.64E-02	-3.01	1.45E-01	5.32E-01	-0.01	9.20E-01	8.06
P04179	Superoxide dismutase	SOD2	1.90E-07	3.81E-06	55.81	2.58E-07	3.81E-06	-3.31	1.62E-02	7.64E-02	-20.26	1.99E-01	5.95E-01	0.17	8.79E-01	7.96
P02671	Fibrinogen alpha chain	FGA	1.32E-06	2.12E-05	3.47	2.79E-07	3.95E-06	-0.23	1.09E-02	6.76E-02	-2.10	3.15E-02	3.10E-01	0.09	2.24E-01	5.97
Q9UJ70	N-acetyl-D-glucosamine kinase	NAGK	3.50E-06	4.42E-05	70.08	5.24E-07	7.14E-06	-4.04	5.13E-02	1.22E-01	-59.67	2.68E-03	8.14E-02	2.25	2.05E-01	5.91
O14791	Apolipoprotein L1	APOL1	2.61E-06	3.62E-05	33.46	5.64E-07	7.39E-06	-2.76	1.13E-02	6.76E-02	-20.07	3.72E-02	3.20E-01	0.87	3.16E-01	6.29
P55268	Laminin subunit beta-2	LAMB2	5.70E-07	9.96E-06	-2.91	2.90E-06	2.74E-05	0.23	9.12E-03	6.76E-02	0.59	5.08E-01	8.10E-01	-0.03	6.17E-01	7.29
P02675	Fibrinogen beta chain	FGB	2.92E-06	3.91E-05	1.15	6.85E-07	8.40E-06	-0.06	2.28E-02	8.33E-02	-0.67	4.47E-02	3.43E-01	0.03	2.32E-01	5.99
P35442	**Thrombospondin-2**	THBS2	4.77E-06	5.81E-05	5.24	6.91E-07	8.40E-06	-0.39	3.55E-03	4.29E-02	-4.11	6.38E-03	1.52E-01	0.25	3.54E-02	4.59
P04080	Cystatin-B	CSTB	3.52E-06	4.42E-05	47.93	8.58E-07	1.01E-05	-4.84	1.72E-03	3.43E-02	-27.51	4.96E-02	3.51E-01	0.29	7.69E-01	7.66
O14818	Proteasome subunit alpha type-7	PSMA7	7.03E-06	7.85E-05	88.12	1.08E-06	1.23E-05	-5.38	2.07E-02	8.04E-02	-63.83	1.34E-02	2.29E-01	1.73	3.78E-01	6.54
P02679	Fibrinogen gamma	FGG	5.91E-06	6.93E-05	2.44	1.21E-06	1.33E-05	-0.14	2.33E-02	8.33E-02	-1.50	3.78E-02	3.20E-01	0.07	2.14E-01	5.94
P04004	**Vitronectin**	VTN	6.03E-06	6.93E-05	7.65	1.28E-06	1.37E-05	-0.62	7.66E-03	6.53E-02	-7.42	8.44E-04	5.59E-02	0.41	2.38E-02	4.19
Q9NZU5	LIM and cysteine-rich domains protein 1	LMCD1	2.29E-06	3.41E-05	-7.02	1.57E-06	1.62E-05	0.82	4.61E-04	2.45E-02	2.88	1.72E-01	5.85E-01	-0.20	1.70E-01	5.37
P11047	Laminin subunit gamma-1	LAMC1	2.28E-06	3.41E-05	-3.59	6.39E-05	4.63E-04	0.29	2.03E-02	8.04E-02	-0.14	9.13E-01	8.64E-01	0.00	9.74E-01	8.08
P98160	Basement membrane-specific heparan sulfate	HSPG2	2.44E-06	3.50E-05	-1.03	2.30E-06	2.31E-05	0.14	8.44E-04	3.05E-02	0.38	2.28E-01	6.32E-01	-0.03	2.61E-01	6.04
P0C0L5	Complement C4-B	C4B	1.77E-05	1.83E-04	3.14	2.83E-06	2.74E-05	-0.21	1.97E-02	8.04E-02	-2.29	1.66E-02	2.60E-01	0.14	6.14E-02	4.70
P05155	Plasma protease C1 inhibitor	SERPING 1	2.68E-05	2.69E-04	11.82	5.01E-06	4.56E-05	-0.94	1.56E-02	7.52E-02	-7.73	3.61E-02	3.20E-01	0.50	6.90E-02	4.70
P11216	Glycogen phosphorylase, brain	PYGB	3.11E-05	3.02E-04	-8.84	5.09E-06	4.56E-05	1.29	1.36E-04	1.22E-02	7.49	6.19E-03	1.52E-01	-0.54	8.86E-03	4.19
Q15124	Phosphoglucomutase-like protein 5	PGM5	3.16E-05	3.02E-04	-4.59	6.29E-06	5.48E-05	0.51	2.19E-03	3.64E-02	4.33	2.44E-03	7.80E-02	-0.26	2.00E-02	4.19
O00159	Unconventional myosin-Ic	MYO1C	8.01E-06	8.70E-05	-5.81	4.43E-05	3.51E-04	0.60	4.68E-03	4.79E-02	0.67	7.42E-01	8.46E-01	-0.02	8.83E-01	7.96
O15230	Laminin subunit alpha-5	LAMA5	8.97E-06	9.49E-05	-2.00	4.07E-05	3.30E-04	0.17	1.58E-02	7.52E-02	0.27	6.94E-01	8.46E-01	-0.01	8.63E-01	7.92
P02792	Ferritin light chain	FTL	7.19E-05	6.42E-04	13.07	2.71E-05	2.31E-04	-0.60	1.33E-01	1.91E-01	-14.43	8.40E-04	5.59E-02	0.80	2.17E-02	4.19
Q14315	Filamin-C	FLNC	1.98E-04	1.59E-03	-2.67	3.54E-05	2.94E-04	0.33	2.37E-03	3.68E-02	1.96	3.11E-02	3.10E-01	-0.11	9.75E-02	4.76
P08133	Annexin A6	ANXA6	5.29E-05	4.95E-04	-4.62	5.31E-05	4.11E-04	0.52	1.08E-02	6.76E-02	1.39	3.91E-01	7.52E-01	-0.07	5.45E-01	7.03
P01024	Complement C3	C3	2.13E-04	1.68E-03	1.78	5.90E-05	4.46E-04	-0.11	5.49E-02	1.26E-01	-0.96	1.24E-01	5.01E-01	0.05	2.86E-01	6.14
P52209	6-phosphogluconate dehydrogenase,	PGD	1.76E-04	1.47E-03	19.04	6.06E-05	4.48E-04	-0.77	1.96E-01	2.32E-01	-9.25	1.69E-01	5.85E-01	0.19	7.16E-01	7.49
P02768	Serum albumin	ALB	7.09E-05	6.42E-04	0.24	6.86E-05	4.86E-04	-0.02	1.81E-02	8.03E-02	-0.07	3.99E-01	7.52E-01	0.00	4.40E-01	6.77
Q9UBR2	**Cathepsin Z**	**CTSZ**	1.96E-04	1.59E-03	33.51	7.45E-05	5.12E-04	-2.14	3.35E-02	9.66E-02	-37.34	1.43E-03	6.52E-02	1.49	1.01E-01	4.76
P21333	Filamin-A	FLNA	1.10E-04	9.59E-04	-0.50	7.52E-05	5.12E-04	0.05	9.91E-03	6.76E-02	0.18	3.26E-01	7.06E-01	-0.01	3.69E-01	6.54
P08603	Complement factor H	CFH	4.27E-04	2.85E-03	2.85	8.70E-05	5.80E-04	-0.21	3.07E-02	9.31E-02	-2.60	1.04E-02	2.03E-01	0.13	8.81E-02	4.70
Q15063	**Periostin**	**POSTN**	4.00E-04	2.82E-03	2.23	9.40E-05	6.05E-04	-0.19	1.07E-02	6.76E-02	-2.18	6.10E-03	1.52E-01	0.11	6.75E-02	4.70
P01042	Kininogen-1	KNG1	3.26E-04	2.38E-03	10.38	9.43E-05	6.05E-04	-0.98	1.13E-02	6.76E-02	-5.50	1.43E-01	5.30E-01	0.18	4.84E-01	6.91
Q8N2S1	Latent-transforming growth factor beta-binding protein 4	LTBP4	2.29E-04	1.77E-03	-5.71	1.08E-04	6.83E-04	0.54	1.32E-02	7.15E-02	2.35	2.59E-01	6.54E-01	-0.06	7.04E-01	7.46
P04196	Histidine-rich glycoprotein	HRG	6.63E-04	4.23E-03	8.46	1.42E-04	8.81E-04	-0.85	8.89E-03	6.76E-02	-7.85	1.13E-02	2.07E-01	0.34	1.29E-01	5.04

O76070	Gamma-synuclein	SNCG	7.68E-04	4.68E-03	15.28	1.47E-04	8.90E-04	-2.03	9.20E-04	3.05E-02	-11.71	3.77E-02	3.20E-01	0.70	9.01E-02	4.70
P16112	Aggrecan core protein	ACAN	1.49E-04	1.28E-03	-2.93	2.28E-04	1.27E-03	0.52	1.35E-03	3.05E-02	0.59	5.97E-01	8.16E-01	-0.01	8.66E-01	7.92
P00450	**Ceruloplasmin**	CP	3.74E-04	2.69E-03	4.15	1.68E-04	1.00E-03	-0.28	5.32E-02	1.25E-01	-1.73	2.66E-01	6.54E-01	0.07	5.15E-01	6.93
Q9NR12	PDZ and LIM domain protein 7	PDLIM7	8.75E-04	5.05E-03	-7.92	1.77E-04	1.04E-03	1.01	1.99E-03	3.64E-02	5.53	6.18E-02	3.84E-01	-0.52	1.85E-02	4.19
P19827	Inter-alpha-trypsin inhibitor heavy chain H1	ITIH1	1.09E-03	5.79E-03	6.68	2.16E-04	1.25E-03	-0.62	1.28E-02	7.15E-02	-5.58	2.70E-02	3.02E-01	0.32	8.01E-02	4.70
P35749	Myosin-11	MYH11	6.78E-04	4.26E-03	-0.33	2.24E-04	1.27E-03	0.03	1.54E-02	7.52E-02	0.16	1.99E-01	5.95E-01	-0.01	1.11E-01	4.79
P43121	Cell surface glycoprotein MUC18	MCAM	2.45E-04	1.86E-03	-3.74	4.66E-02	7.31E-02	0.36	1.80E-01	2.24E-01	-4.20	1.02E-01	4.54E-01	0.26	1.54E-01	5.17
P00740	Coagulation factor IX	F9	4.14E-04	2.85E-03	11.84	2.56E-04	1.40E-03	-0.95	2.28E-02	8.33E-02	-14.56	1.06E-03	5.59E-02	0.72	3.45E-02	4.59
P06312	Ig kappa chain V-IV region (Fragment)	IGKV4-1	2.61E-04	1.94E-03	19.67	7.48E-03	2.02E-02	-1.38	1.49E-01	2.05E-01	8.57	4.01E-01	7.52E-01	-0.74	3.02E-01	6.27
O43707	Alpha-actinin-4	ACTN4	1.07E-03	5.75E-03	-1.23	2.70E-04	1.46E-03	0.13	1.13E-02	6.76E-02	0.72	1.31E-01	5.04E-01	-0.04	2.07E-01	5.91
P12111	**Collagen alpha-3(VI)**	COL6A3	9.82E-04	5.56E-03	1.13	2.94E-04	1.56E-03	-0.06	1.40E-01	1.96E-01	-0.59	1.81E-01	5.91E-01	0.02	5.79E-01	7.20
P18206	Vinculin	VCL	1.06E-03	5.75E-03	-2.28	3.29E-04	1.72E-03	0.26	7.85E-03	6.53E-02	1.16	1.93E-01	5.95E-01	-0.08	2.03E-01	5.91
P30613	Pyruvate kinase PKLR	PKLR	1.28E-03	6.69E-03	65.77	6.80E-03	1.86E-02	-4.71	1.37E-01	1.95E-01	-	3.82E-04	4.07E-02	5.58	3.84E-02	4.59
Q96HC4	PDZ and LIM domain protein 5	PDLIM5	4.20E-04	2.85E-03	-6.65	1.05E-02	2.58E-02	1.22	6.69E-03	6.19E-02	-3.13	3.84E-01	7.52E-01	0.11	6.43E-01	7.34
P37837	Transaldolase	TALDO1	8.79E-04	5.05E-03	43.34	4.24E-04	2.19E-03	-2.18	9.85E-02	1.66E-01	-51.49	2.34E-03	7.80E-02	0.58	6.33E-01	7.33
P01834	Ig kappa chain C region	IGKC	4.33E-04	2.85E-03	3.37	4.14E-03	1.27E-02	-0.22	1.33E-01	1.91E-01	0.75	6.48E-01	8.31E-01	-0.12	3.17E-01	6.29
Q06828	Fibromodulin	FMOD	5.13E-04	3.32E-03	-5.23	3.45E-02	5.84E-02	0.76	5.50E-02	1.26E-01	-4.56	1.80E-01	5.91E-01	0.20	4.03E-01	6.60
P31146	**Coronin-1A**	CORO1A	2.53E-03	1.24E-02	15.69	5.55E-04	2.82E-03	-1.05	3.97E-02	1.07E-01	-13.97	2.70E-02	3.02E-01	0.49	2.78E-01	6.12
O43294	Transforming growth factor beta-1-induced transcript 1 protein	TGFB1I1	2.70E-03	1.31E-02	-5.48	5.90E-04	2.95E-03	0.44	5.06E-02	1.21E-01	3.81	8.70E-02	4.31E-01	-0.24	1.31E-01	5.04
P39060	Collagen alpha-1(XVIII) chain	COL18A1	2.07E-03	1.04E-02	-5.45	6.30E-04	3.11E-03	0.57	2.90E-02	9.09E-02	2.82	2.07E-01	5.96E-01	-0.04	8.12E-01	7.83
P06727	Apolipoprotein A-IV	APOA4	3.01E-03	1.41E-02	7.40	6.61E-04	3.21E-03	-0.91	1.15E-02	6.76E-02	-5.19	8.72E-02	4.31E-01	0.16	4.52E-01	6.79
P63244	Guanine nucleotide-	GNB2L1	2.88E-03	1.36E-02	28.04	6.73E-04	3.22E-03	-2.07	6.95E-02	1.39E-01	-26.09	2.26E-02	3.02E-01	0.73	3.67E-01	6.54
Q9Y490	Talin-1	TLN1	1.88E-03	9.58E-03	-1.45	7.12E-04	3.36E-03	0.21	3.45E-03	4.29E-02	0.65	2.82E-01	6.69E-01	-0.08	5.45E-02	4.70
P05156	Complement factor I	CFI	7.24E-04	4.48E-03	17.78	1.42E-03	5.95E-03	-0.77	2.59E-01	2.63E-01	-1.56	8.41E-01	8.58E-01	-0.30	5.86E-01	7.20
P00488	**Coagulation factor XIII** A chain	F13A1	3.57E-03	1.63E-02	9.72	7.67E-04	3.58E-03	-0.72	2.81E-02	8.97E-02	-8.01	4.64E-02	3.47E-01	0.54	8.38E-02	4.70
P01620	Ig kappa chain V-III region SIE	IGKV3-20	8.15E-04	4.89E-03	12.69	4.33E-03	1.31E-02	-0.53	3.02E-01	2.86E-01	1.84	7.67E-01	8.46E-01	-0.18	6.69E-01	7.44
P00736	**Complement C1r subcomponent**	C1R	3.35E-03	1.55E-02	11.46	8.30E-04	3.82E-03	-0.78	8.33E-02	1.57E-01	-7.05	1.41E-01	5.28E-01	0.03	9.23E-01	8.06
Q08431	Lactadherin	MFGE8	8.32E-04	4.92E-03	-3.70	3.63E-03	1.20E-02	0.43	2.02E-02	8.04E-02	-0.37	8.36E-01	8.58E-01	-0.01	9.32E-01	8.06
P59665	Neutrophil defensin 1	DEFA1	1.00E-03	5.60E-03	28.10	9.28E-04	4.21E-03	-3.00	1.24E-02	7.05E-02	-6.59	5.80E-01	8.16E-01	-0.02	9.83E-01	8.08
Q14112	Nidogen-2	NID2	4.44E-03	1.94E-02	28.59	1.04E-03	4.66E-03	-3.01	5.49E-03	5.45E-02	-26.02	3.14E-02	3.10E-01	1.73	5.85E-02	4.70
P50895	**Basal cell adhesion molecule**	BCAM	1.05E-03	5.75E-03	-5.67	1.99E-03	7.62E-03	0.51	4.69E-02	1.19E-01	0.41	8.72E-01	8.64E-01	-0.01	9.38E-01	8.06
Q96PD5	N-acetylmuramoyl-L-alanine amidase	PGLYRP2	2.77E-03	1.33E-02	13.60	1.09E-03	4.83E-03	-1.19	2.75E-02	8.97E-02	-5.84	3.16E-01	7.06E-01	0.12	7.72E-01	7.67
P12109	Collagen alpha-1(VI) chain	COL6A1	4.92E-03	2.13E-02	2.64	1.14E-03	4.96E-03	-0.21	7.63E-02	1.48E-01	-1.81	1.10E-01	4.70E-01	0.09	2.66E-01	6.04
Q99497	Protein deglycase DJ-1	PARK7	2.55E-02	6.17E-02	-9.80	6.84E-03	1.86E-02	2.08	1.29E-03	3.05E-02	8.74	8.05E-02	4.21E-01	-0.70	5.58E-02	4.70
P05062	Fructose-bisphosphate aldolase B	ALDOB	2.26E-02	5.85E-02	-7.17	8.01E-03	2.12E-02	1.50	1.30E-03	3.05E-02	7.92	3.29E-02	3.10E-01	-0.49	7.12E-02	4.70
Q9BXR6	Complement factor H-related protein 5	CFHR5	5.32E-03	2.23E-02	28.81	1.31E-03	5.66E-03	-1.34	2.10E-01	2.38E-01	-18.32	1.43E-01	5.30E-01	0.06	9.48E-01	8.08
Q13361	Microfibrillar-associated protein 5	MFAP5	6.17E-03	2.45E-02	33.64	1.41E-03	5.95E-03	-2.13	1.08E-01	1.72E-01	-28.59	5.05E-02	3.51E-01	-0.71	4.89E-01	6.91
P46952	3-hydroxyanthranilate 3,4-dioxygenase	HAAO	3.23E-02	7.13E-02	-14.05	8.90E-03	2.23E-02	5.09	1.42E-03	3.05E-02	12.53	9.08E-02	4.31E-01	-0.84	1.12E-01	4.80
P08758	Annexin A5	ANXA5	5.21E-03	2.20E-02	-6.24	1.46E-03	6.07E-03	0.94	6.86E-03	6.19E-02	3.50	2.01E-01	5.95E-01	-0.33	9.23E-02	4.70
Q13418	Integrin-linked protein kinase	ILK	1.68E-03	8.65E-03	-7.10	1.48E-03	6.07E-03	0.87	8.57E-03	6.76E-02	1.61	6.06E-01	8.16E-01	-0.01	9.75E-01	8.08
P21291	Cysteine and glycine-rich protein 1	CSRP1	6.65E-03	2.57E-02	-6.17	1.55E-03	6.27E-03	0.83	1.20E-02	6.92E-02	4.34	1.10E-01	4.70E-01	-0.29	1.33E-01	5.04
P10909	Clusterin	CLU	6.62E-03	2.57E-02	6.63	1.70E-03	6.81E-03	-0.35	1.94E-01	2.32E-01	-6.35	2.97E-02	3.10E-01	0.32	1.37E-01	5.04
P00738	Haptoglobin	HP	4.41E-03	1.94E-02	1.15	1.82E-03	7.20E-03	-0.07	8.10E-02	1.54E-01	-0.47	3.59E-01	7.32E-01	0.05	2.05E-01	5.91
Q92747	Actin-related protein 2/3 complex subunit 1A	ARPC1A	8.33E-03	2.93E-02	-85.33	1.92E-03	7.50E-03	13.45	4.31E-03	4.57E-02	66.51	8.16E-02	4.21E-01	-1.70	5.24E-01	6.95
P51884	Lumican	LUM	8.38E-03	2.93E-02	6.76	1.98E-03	7.62E-03	-0.71	1.78E-02	8.03E-02	-4.82	1.13E-01	4.73E-01	0.15	4.72E-01	6.89

Supplemental Table 8. Up-Regulated Proteins in LAD Fibrous Plaque Samples (n=15) Compared with Normal LAD Samples (n=30). Samples were selected using patho-proteomic phenotyping designed to integrate pathologist assessment of extent of disease and CAM deconvolution of global protein profiles (fold-change = mean FP/ mean NL).

Uniprot ID	Protein	Gene	Fold change	q-value
P24821	Tenascin	TNC	13.04	1.08E-03
P07996	Thrombospondin-1	THBS1	10.05	2.06E-03
P13796	Plastin-2	LCP1	3.87	9.80E-04
P04114	Apolipoprotein B-100	APOB	3.65	6.26E-04
P07858	Cathepsin B	CTSB	3.63	3.13E-04
P40121	Macrophage-capping protein	CAPG	2.72	6.89E-03
P35442	Thrombospondin-2	THBS2	2.69	4.40E-04
P13760	HLA class II histocompatibility antigen, DRB1-4 beta chain	HLA-DRB1	2.57	1.02E-02
P05783	Keratin, type I cytoskeletal 18	KRT18	2.55	4.20E-02
P27169	Serum paraoxonase/arylesterase 1	PON1	2.21	3.75E-02
Q9UBR2	Cathepsin Z	CTSZ	2.20	9.53E-04
P01871	Ig mu chain C region	IGHM	2.15	8.14E-03
P31146	Coronin-1A	CORO1A	2.13	1.22E-02
O43866	CD5 antigen-like	CD5L	2.10	1.22E-02
P08519	Apolipoprotein(a)	LPA	1.97	1.08E-02
Q15063	Periostin	POSTN	1.94	5.47E-04
P01031	Complement C5	C5	1.89	1.58E-02
Q15582	Transforming growth factor-beta-induced protein ig-h3	TGFBI	1.86	2.41E-03
P02649	Apolipoprotein E	APOE	1.79	1.28E-02
P40261	Nicotinamide N-methyltransferase	NNMT	1.74	1.08E-02
Q8IUX7	Adipocyte enhancer-binding protein 1	AEBP1	1.71	4.77E-03

Supplemental Table 9. Down-Regulated Proteins in LAD Fibrous Plaque Samples (n=15) Compared with Normal LAD Samples (n=30). Samples were selected using patho-proteomic phenotyping designed to integrate pathologist assessment of extent of disease and CAM deconvolution of global protein profiles. (For down regulated proteins Fold-change = -1* mean NL/mean FP.)

Uniprot ID	Protein	Gene	Fold-change	q-value
P07197	Neurofilament medium polypeptide	NEFM	-5.70	3.42E-02
P49327	Fatty acid synthase	FASN	-5.40	1.55E-05
P15090	Fatty acid-binding protein, adipocyte	FABP4	-3.58	6.87E-03
P07196	Neurofilament light polypeptide	NEFL	-3.27	2.45E-02
Q96Q06	Perilipin-4	PLIN4	-2.53	2.90E-04
P09543	2',3'-cyclic-nucleotide 3'-phosphodiesterase	CNP	-2.50	2.77E-04
P33121	Long-chain-fatty-acid--CoA ligase 1	ACSL1	-2.41	4.90E-04
P11586	C-1-tetrahydrofolate synthase, cytoplasmic	MTHFD1	-2.28	1.55E-05
O60240	Perilipin-1	PLIN1	-2.24	3.13E-04
P22695	Cytochrome b-c1 complex subunit 2, mitochondrial	UQCRC2	-2.19	3.13E-04
P23634	Plasma membrane calcium-transporting ATPase 4	ATP2B4	-2.18	2.77E-04
Q68CZ2	Tensin-3	TNS3	-2.17	2.22E-03
Q05469	Hormone-sensitive lipase	LIPE	-2.16	1.36E-03
O43301	Heat shock 70 kDa protein 12A	HSPA12A	-2.13	4.90E-04
Q86TX2	Acyl-coenzyme A thioesterase 1	ACOT1	-2.11	9.01E-04
Q16363	Laminin subunit alpha-4	LAMA4	-2.10	4.90E-04
O43175	D-3-phosphoglycerate dehydrogenase	PHGDH	-2.09	2.77E-04
Q16698	2,4-dienoyl-CoA reductase, mitochondrial	DECR1	-2.08	5.47E-04
P11532	Dystrophin	DMD	-2.07	5.47E-04
P16930	Fumarylacetoacetase	FAH	-2.05	9.53E-04
Q02952	A-kinase anchor protein 12	AKAP12	-2.03	3.13E-04
Q9UN36	Protein NDRG2	NDRG2	-2.02	2.06E-03
Q9HBL0	Tensin-1	TNS1	-2.01	5.58E-04
P21695	Glycerol-3-phosphate dehydrogenase [NAD(+)], cytoplasmic	GPD1	-1.99	1.96E-04
Q9BSJ8	Extended synaptotagmin-1	ESYT1	-1.98	1.07E-03
O75112	LIM domain-binding protein 3	LDB3	-1.98	1.70E-02
P49748	Very long-chain specific acyl-CoA dehydrogenase, mitochondrial	ACADVL	-1.96	4.41E-04
P53396	ATP-citrate synthase	ACLY	-1.95	2.06E-03
O95810	Serum deprivation-response protein	SDPR	-1.95	5.67E-04
P48163	NADP-dependent malic enzyme	ME1	-1.95	3.46E-03
P31323	cAMP-dependent protein kinase type II-beta regulatory subunit	PRKAR2B	-1.94	2.05E-02
Q99685	Monoglyceride lipase	MGLL	-1.94	1.55E-03
Q13683	Integrin alpha-7	ITGA7	-1.90	3.46E-03
Q2UY09	Collagen alpha-1(XXVIII) chain	COL28A1	-1.90	1.92E-03
P46821	Microtubule-associated protein 1B	MAP1B	-1.90	4.59E-03
Q96JY6	PDZ and LIM domain protein 2	PDLIM2	-1.89	3.61E-03
O75390	Citrate synthase, mitochondrial	CS	-1.88	1.88E-03
P13804	Electron transfer flavoprotein subunit alpha, mitochondrial	ETFA	-1.87	2.77E-04
P21397	Amine oxidase [flavin-containing] A	MAOA	-1.87	5.24E-04
Q6YN16	Hydroxysteroid dehydrogenase-like protein 2	HSDL2	-1.86	5.47E-04

P31930	Cytochrome b-c1 complex subunit 1, mitochondrial	UQCRC1	-1.86	1.10E-03
P23141	Liver carboxylesterase 1	CES1	-1.86	9.39E-03
Q9BTV4	Transmembrane protein 43	TMEM43	-1.84	1.08E-03
Q15836	Vesicle-associated membrane protein 3	VAMP3	-1.82	1.86E-03
Q14112	Nidogen-2	NID2	-1.81	5.47E-04
Q13011	Delta(3,5)-Delta(2,4)-dienoyl-CoA isomerase, mitochondrial	ECH1	-1.81	4.59E-03
Q99798	Aconitate hydratase, mitochondrial	ACO2	-1.80	1.96E-04
P09622	Dihydrolipoyl dehydrogenase, mitochondrial	DLD	-1.80	3.88E-04
P11177	Pyruvate dehydrogenase E1 component subunit beta, mitochondrial	PDHB	-1.80	1.08E-03
P14854	Cytochrome c oxidase subunit 6B1	COX6B1	-1.79	6.94E-04
Q96AM1	Mas-related G-protein coupled receptor member F	MRGPRF	-1.79	7.86E-03
P17540	Creatine kinase S-type, mitochondrial	CKMT2	-1.79	4.43E-02
P35611	Alpha-adducin	ADD1	-1.78	2.15E-03
P07451	Carbonic anhydrase 3	CA3	-1.78	1.08E-02
P27816	Microtubule-associated protein 4	MAP4	-1.78	1.28E-02
P06737	Glycogen phosphorylase, liver form	PYGL	-1.78	2.34E-02
Q02218	2-oxoglutarate dehydrogenase, mitochondrial	OGDH	-1.77	1.24E-02
P07099	Epoxide hydrolase 1	EPHX1	-1.77	4.10E-02
Q9UHD8	Septin-9	SEP9	-1.76	1.68E-03
P50213	Isocitrate dehydrogenase [NAD] subunit alpha, mitochondrial	IDH3A	-1.74	5.06E-03
P10620	Microsomal glutathione S-transferase 1	MGST1	-1.73	2.06E-03
Q16891	MICOS complex subunit MIC60	IMMT	-1.72	2.88E-03
P51911	Calponin-1	CNN1	-1.71	1.88E-03
Q6PCB0	von Willebrand factor A domain-containing protein 1	VWA1	-1.71	1.70E-02
P21399	Cytoplasmic aconitate hydratase	ACO1	-1.71	7.94E-03
P30084	Enoyl-CoA hydratase, mitochondrial	ECHS1	-1.71	1.36E-03
Q01082	Spectrin beta chain, non-erythrocytic 1	SPTBN1	-1.71	5.24E-04
O43491	Band 4.1-like protein 2	EPB41L2	-1.71	7.31E-03

Supplemental Table 10. Predicted Upstream Master Regulators for Up- and Down-Regulated Fibrous Plaque Proteins

A. LAD Samples

Overrepresented Pathways with Consistent Evidence of Activation or Inhibition

Upstream Regulator	Molecule Type	p-value of overlap	Predicted Activation	Activation z-score
INSR	kinase	8.56E-16	Inhibited	-2.493
PPARG	ligand-dependent nuclear receptor	2.42E-13	Inhibited	-2.805
PPARA	ligand-dependent nuclear receptor	4.22E-10	Inhibited	-3.060
TNF	cytokine	2.64E-07	Activated	3.043

Overrepresented Pathways without Consistent Evidence of Activation or Inhibition

Upstream Regulator	Molecule Type	p-value of overlap	Predicted Activation	Activation z-score
TP53	transcription regulator	5.60E-08	n/a	-0.723
MGEA5	enzyme	2.40E-06	n/a	0.302
PTEN	phosphatase	2.48E-06	n/a	-0.950
ESR2	ligand-dependent nuclear receptor	1.61E-05	n/a	-0.239
MYC	transcription regulator	2.34E-04	n/a	0.000
ERBB2	kinase	4.20E-04	n/a	n/a*
TGFB1	growth factor	1.79E-03	n/a	0.720

* not enough information in the Ingenuity database to estimate

B. AA Samples

Overrepresented Pathways with Consistent Evidence of Activation or Inhibition

Upstream Regulator	Molecule Type	p-value of overlap	Predicted Activation	Activation z-score
TGFB1	growth factor	8.53E-11	Inhibited	-3.147
APOE	transporter	4.53E-09	Inhibited	-2.611
APP	other	2.76E-06	Activated	2.148
TNF	cytokine	1.92E-05	Activated	2.192
IL1B	cytokine	2.31E-05	Activated	2.676
MGEA5	enzyme	9.02E-04	Activated	2.714
IL6	cytokine	1.05E-03	Activated	2.195

Overrepresented Pathways without Consistent Evidence of Activation or Inhibition

Upstream Regulator	Molecule Type	p-value of overlap	Predicted Activation	Activation z-score
TP53	transcription regulator	5.16E-11	n/a	-1.918
HRAS	enzyme	7.29E-11	n/a	0.617
MYC	transcription regulator	8.34E-08	n/a	-0.650
MYCN	transcription regulator	3.17E-07	n/a	1.612

PRL	cytokine	1.02E-05	n/a	0.818
JUN	transcription regulator	2.60E-05	n/a	0.859
AR	ligand-dependent nuclear receptor	5.86E-05	n/a	-0.816
MAPK1	kinase	7.29E-05	n/a	0.000
KRAS	enzyme	7.39E-05	n/a	-0.043
NFKBIA	transcription regulator	2.55E-04	n/a	1.310
HTT	transcription regulator	4.65E-04	n/a	0.447
ESR1	ligand-dependent nuclear receptor	1.03E-03	n/a	0.905
SP1	transcription regulator	1.84E-03	n/a	0.342
ERBB2	kinase	3.98E-03	n/a	-1.154
SMARCA4	transcription regulator	4.67E-03	n/a	-1.949
STAT3	transcription regulator	6.15E-03	n/a	1.680
FOS	transcription regulator	1.22E-02	n/a	-1.069
CTNNB1	transcription regulator	1.32E-02	n/a	0.000

Up-stream regulators common to both territories are indicated in **bold**

Supplemental Table 11. Up-Regulated Proteins in Fibrous Plaque Enriched AA Samples (n=7) Compared with Normal AA Samples (n=15). Samples were selected using patho-proteomic phenotyping designed to integrate pathologist assessment of extent of disease and CAM deconvolution of global protein profiles (fold-change = mean FP/ mean NL).

Uniprot ID	Protein	Gene	Fold-change	q-value
P04114	Apolipoprotein B-100	APOB	11.68	4.87E-03
P13796	Plastin-2	LCP1	9.22	4.50E-04
P02675	Fibrinogen beta chain	FGB	6.03	1.73E-03
P07858	Cathepsin B	CTSB	5.99	4.84E-03
P00734	Prothrombin	F2	5.30	5.92E-04
P00738	Haptoglobin	HP	4.26	1.36E-03
P01892	HLA class I histocompatibility antigen, A-2 alpha chain	HLA-A	4.16	4.73E-03
P20742	Pregnancy zone protein	PZP	4.04	3.90E-02
P27169	Serum paraoxonase/arylesterase 1	PON1	4.04	3.42E-02
P19823	Inter-alpha-trypsin inhibitor heavy chain H2	ITIH2	4.00	7.61E-04
P40121	Macrophage-capping protein	CAPG	3.88	1.09E-02
P35442	Thrombospondin-2	THBS2	3.82	1.36E-03
P00488	Coagulation factor XIII A chain	F13A1	3.77	5.86E-03
P01031	Complement C5	C5	3.64	5.07E-03
P02679	Fibrinogen gamma chain	FGG	3.53	3.90E-03
P04003	C4b-binding protein alpha chain	C4BPA	3.45	1.24E-03
P00739	Haptoglobin-related protein	HPR	3.41	5.26E-03
P31146	Coronin-1A	CORO1A	3.30	3.13E-05
P05090	Apolipoprotein D	APOD	3.29	2.90E-04
P24821	Tenascin	TNC	3.17	2.70E-03
P05546	Heparin cofactor 2	SERPIND1	3.12	1.03E-02
P02649	Apolipoprotein E	APOE	3.06	2.06E-04
Q14624	Inter-alpha-trypsin inhibitor heavy chain H4	ITIH4	3.04	3.70E-04
P02671	Fibrinogen alpha chain	FGA	3.03	1.26E-03
P52209	6-phosphogluconate dehydrogenase, decarboxylating	PGD	2.99	4.57E-02
P05155	Plasma protease C1 inhibitor	SERPING1	2.85	1.08E-04
P00747	Plasminogen	PLG	2.73	4.08E-04
P0C0L5	Complement C4-B	C4B	2.72	3.13E-05
Q9BXR6	Complement factor H-related protein 5	CFHR5	2.64	2.00E-02
O43866	CD5 antigen-like	CD5L	2.63	1.62E-02
O14791	Apolipoprotein L1	APOL1	2.58	3.29E-02
P00736	Complement C1r subcomponent	C1R	2.56	3.13E-02
P02792	Ferritin light chain	FTL	2.54	4.01E-04
Q9UBR2	Cathepsin Z	CTSZ	2.51	1.40E-02
P19827	Inter-alpha-trypsin inhibitor heavy chain H1	ITIH1	2.50	1.95E-05
P18428	Lipopolysaccharide-binding protein	LBP	2.48	1.02E-04
P01871	Ig mu chain C region	IGHM	2.43	2.07E-02
P04196	Histidine-rich glycoprotein	HRG	2.41	1.52E-06
P20700	Lamin-B1	LMNB1	2.40	1.62E-02
P04179	Superoxide dismutase [Mn], mitochondrial	SOD2	2.36	1.04E-03
P61626	Lysozyme C	LYZ	2.31	1.72E-02
P02794	Ferritin heavy chain	FTH1	2.21	5.16E-04
Q96PD5	N-acetylmuramoyl-L-alanine amidase	PGLYRP2	2.16	1.40E-02

P07358	Complement component C8 beta chain	C8B	2.15	3.93E-02
P01023	Alpha-2-macroglobulin	A2M	2.11	8.38E-04
P07339	Cathepsin D	CTSD	2.05	4.12E-03
P59665	Neutrophil defensin 1	DEFA1	2.04	1.75E-02
P01877	Ig alpha-2 chain C region	IGHA2	2.02	2.90E-03
P05156	Complement factor I	CFI	1.98	8.48E-03
P08603	Complement factor H	CFH	1.98	6.41E-06
Q14764	Major vault protein	MVP	1.97	2.54E-02
P00740	Coagulation factor IX	F9	1.88	1.16E-02
P00751	Complement factor B	CFB	1.85	1.94E-02
P13671	Complement component C6	C6	1.85	7.56E-03
P01594	Ig kappa chain V-I region AU		1.84	4.49E-02
P00450	Ceruloplasmin	CP	1.83	7.34E-05
P10643	Complement component C7	C7	1.82	1.97E-03
P04004	Vitronectin	VTN	1.81	9.08E-04
Q9UJ70	N-acetyl-D-glucosamine kinase	NAGK	1.80	3.61E-02
O14818	Proteasome subunit alpha type-7	PSMA7	1.79	1.75E-02
P01042	Kininogen-1	KNG1	1.79	1.84E-03

Supplemental Table 12. Down-Regulated Proteins in Fibrous Plaque Enriched AA Samples (n=7) Compared with Normal AA Samples (n=15). Samples were selected using patho-proteomic phenotyping designed to integrate pathologist assessment of extent of disease and CAM deconvolution of global protein profiles. (For down regulated proteins Fold-change = -1* mean NL/mean FP)

Uniprot ID	Protein	Gene	Fold-change	q-value
Q8N2S1	Latent-transforming growth factor beta-binding protein 4	LTBP4	-6.38	4.00E-07
P55083	Microfibril-associated glycoprotein 4	MFAP4	-4.92	6.64E-05
Q7Z4I7	LIM and senescent cell antigen-like-containing domain protein 2	LIMS2	-4.47	5.95E-05
P17661	Desmin	DES	-4.36	1.95E-05
P46821	Microtubule-associated protein 1B	MAP1B	-4.11	4.00E-07
P11216	Glycogen phosphorylase, brain form	PYGB	-3.74	7.51E-07
Q9HBL0	Tensin-1	TNS1	-3.72	1.73E-05
Q9H223	EH domain-containing protein 4	EHD4	-3.69	1.52E-06
Q0ZGT2	Nexilin	NEXN	-3.62	5.65E-05
P16112	Aggrecan core protein	ACAN	-3.55	6.64E-05
Q14315	Filamin-C	FLNC	-3.54	7.34E-05
Q53GG5	PDZ and LIM domain protein 3	PDLIM3	-3.48	1.22E-05
P50895	Basal cell adhesion molecule	BCAM	-3.46	1.77E-06
O00151	PDZ and LIM domain protein 1	PDLIM1	-3.37	4.28E-05
O43175	D-3-phosphoglycerate dehydrogenase	PHGDH	-3.31	4.90E-06
O00159	Unconventional myosin-Ic	MYO1C	-3.19	3.56E-06
P53814	Smoothelin	SMTN	-3.14	7.75E-07
P29536	Leiomodin-1	LMOD1	-3.12	5.80E-07
Q7Z7G0	Target of Nesh-SH3	ABI3BP	-3.05	1.55E-04
Q8WX93	Palladin	PALLD	-3.05	3.56E-06
P60660	Myosin light polypeptide 6	MYL6	-3.03	2.64E-04
Q9NR12	PDZ and LIM domain protein 7	PDLIM7	-2.98	4.12E-05
Q01082	Spectrin beta chain, non-erythrocytic 1	SPTBN1	-2.86	2.07E-04
Q9Y4G6	Talin-2	TLN2	-2.84	3.06E-05
Q96A00	Protein phosphatase 1 regulatory subunit 14A	PPP1R14A	-2.82	3.88E-05
Q8IVN8	Somatomedin-B and thrombospondin type-1 domain-containing protein	SBSPON	-2.79	1.87E-05
Q15746	Myosin light chain kinase, smooth muscle	MYLK	-2.77	5.54E-06
Q9NVD7	Alpha-parvin	PARVA	-2.69	5.54E-06
Q9NZU5	LIM and cysteine-rich domains protein 1	LMCD1	-2.68	1.08E-05
Q9UMS6	Synaptopodin-2	SYNPO2	-2.68	1.53E-04
P19105	Myosin regulatory light chain 12A	MYL12A	-2.57	1.95E-05
P17655	Calpain-2 catalytic subunit	CAPN2	-2.50	1.26E-04
Q96HC4	PDZ and LIM domain protein 5	PDLIM5	-2.48	5.89E-05
O75112	LIM domain-binding protein 3	LDB3	-2.48	3.29E-04
Q07954	Prolow-density lipoprotein receptor-related protein 1	LRP1	-2.47	9.83E-05
Q9BX66	Sorbin and SH3 domain-containing protein 1	SORBS1	-2.45	4.10E-04
Q9BZQ8	Protein Niban	FAM129A	-2.45	3.34E-04
Q15942	Zyxin	ZYX	-2.40	8.03E-06
Q9UGI8	Testin	TES	-2.39	3.47E-05
O94875	Sorbin and SH3 domain-containing protein 2	SORBS2	-2.38	1.85E-04
O14974	Protein phosphatase 1 regulatory subunit 12A	PPP1R12A	-2.38	2.97E-05

Q15365	Poly(rC)-binding protein 1	PCBP1	-2.37	2.20E-04
P09651	Heterogeneous nuclear ribonucleoprotein A1	HNRNPA1	-2.37	6.11E-03
P16615	Sarcoplasmic/endoplasmic reticulum calcium ATPase 2	ATP2A2	-2.36	4.13E-04
P48059	LIM and senescent cell antigen-like-containing domain protein 1	LIMS1	-2.33	8.29E-04
Q14BN4	Sarcolemmal membrane-associated protein	SLMAP	-2.30	5.89E-05
Q8WUP2	Filamin-binding LIM protein 1	FBLIM1	-2.27	1.33E-04
P51911	Calponin-1	CNN1	-2.26	6.30E-04
Q93052	Lipoma-preferred partner	LPP	-2.26	9.77E-05
O43294	Transforming growth factor beta-1-induced transcript 1 protein	TGFB1I1	-2.25	6.93E-04
Q14204	Cytoplasmic dynein 1 heavy chain 1	DYNC1H1	-2.24	1.66E-03
Q05682	Caldesmon	CALD1	-2.24	2.94E-04
Q16836	Hydroxyacyl-coenzyme A dehydrogenase, mitochondrial	HADH	-2.22	6.78E-04
O15061	Synemin	SYNM	-2.21	1.72E-02
Q9BTV4	Transmembrane protein 43	TMEM43	-2.21	1.16E-03
Q9Y696	Chloride intracellular channel protein 4	CLIC4	-2.21	5.54E-06
P43121	Cell surface glycoprotein MUC18	MCAM	-2.18	1.28E-05
P09104	Gamma-enolase	ENO2	-2.17	3.96E-04
Q13976	cGMP-dependent protein kinase 1	PRKG1	-2.16	3.88E-04
Q03252	Lamin-B2	LMNB2	-2.15	1.03E-02
Q13813	Spectrin alpha chain, non-erythrocytic 1	SPTAN1	-2.14	5.45E-04
Q15019	Septin-2	2-Sep	-2.11	1.58E-03
Q15124	Phosphoglucomutase-like protein 5	PGM5	-2.08	1.36E-03
Q9UBX5	Fibulin-5	FBLN5	-2.08	9.44E-04
P02511	Alpha-crystallin B chain	CRYAB	-2.06	7.93E-03
O14558	Heat shock protein beta-6	HSPB6	-2.05	9.05E-05
P13861	cAMP-dependent protein kinase type II-alpha regulatory subunit	PRKAR2A	-2.05	2.43E-04
P53708	Integrin alpha-8	ITGA8	-2.02	1.15E-03
P27816	Microtubule-associated protein 4	MAP4	-2.01	3.71E-04
O15230	Laminin subunit alpha-5	LAMA5	-2.01	7.86E-04
P20073	Annexin A7	ANXA7	-2.01	4.50E-03
P55268	Laminin subunit beta-2	LAMB2	-2.01	9.55E-04
Q03135	Caveolin-1	CAV1	-1.98	2.33E-03
Q96AC1	Fermitin family homolog 2	FERMT2	-1.95	6.78E-04
Q01995	Transgelin	TAGLN	-1.95	7.34E-05
Q14240	Eukaryotic initiation factor 4A-II	EIF4A2	-1.93	4.44E-03
P08670	Vimentin	VIM	-1.92	3.35E-04
Q92599	Septin-8	8-Sep	-1.92	1.68E-02
Q9NZN4	EH domain-containing protein 2	EHD2	-1.92	1.66E-03
Q04917	14-3-3 protein eta	YWHAH	-1.89	1.16E-03
Q00577	Transcriptional activator protein Pur-alpha	PURA	-1.89	1.73E-04
Q9UBI6	Guanine nucleotide-binding protein G(I)/G(S)/G(O) subunit gamma-12	GNG12	-1.88	2.96E-03
Q13555	Calcium/calmodulin-dependent protein kinase type II subunit gamma	CAMK2G	-1.88	5.82E-03
P30084	Enoyl-CoA hydratase, mitochondrial	ECHS1	-1.87	2.10E-02
Q08257	Quinone oxidoreductase	CRYZ	-1.87	7.25E-04
Q16555	Dihydropyrimidinase-related protein 2	DPYSL2	-1.86	7.75E-07
Q96S97	Myeloid-associated differentiation marker	MYADM	-1.85	1.68E-04
Q16181	Septin-7	7-Sep	-1.85	5.25E-03
Q9H4M9	EH domain-containing protein 1	EHD1	-1.84	1.71E-03
Q8WUM4	Programmed cell death 6-interacting	PDCD6IP	-1.84	9.46E-03

	protein			
Q15847	Adipogenesis regulatory factor	ADIRF	-1.84	8.01E-03
P11047	Laminin subunit gamma-1	LAMC1	-1.84	5.83E-04
Q9NZN3	EH domain-containing protein 3	EHD3	-1.83	3.53E-03
P36871	Phosphoglucomutase-1	PGM1	-1.81	2.31E-03
P05388	60S acidic ribosomal protein P0	RPLP0	-1.79	2.10E-03
Q6NZI2	Polymerase I and transcript release factor	PTRF	-1.78	2.41E-03
P12277	Creatine kinase B-type	CKB	-1.77	1.09E-02
P31150	Rab GDP dissociation inhibitor alpha	GDI1	-1.76	7.96E-03
P62140	Serine/threonine-protein phosphatase PP1-beta catalytic subunit	PPP1CB	-1.76	6.41E-03
P35749	Myosin-11	MYH11	-1.75	3.46E-04
Q9UL25	Ras-related protein Rab-21	RAB21	-1.73	4.72E-03
P21333	Filamin-A	FLNA	-1.73	3.57E-04
Q969G5	Protein kinase C delta-binding protein	PRKCDBP	-1.73	1.18E-02
P39060	Collagen alpha-1(XVIII) chain	COL18A1	-1.72	3.46E-04
P63167	Dynein light chain 1, cytoplasmic	DYNLL1	-1.70	3.39E-04
Q63ZY3	KN motif and ankyrin repeat domain-containing protein 2	KANK2	-1.70	1.38E-02

Supplementary Table 13. Overlap of Patho-Proteomic Fibrous Plaque Proteins in Human LAD (n=99) and AA (n=99) Samples Twelve proteins were significantly (q<=0.05) up-regulated in fibrous plaque enriched samples compared to normal samples in both the LAD and AA. With the exception of cathepsin Z, all of the up-regulated proteins were also identified as fibrous plaque proteins in both LAD and AA using CAM. Similarly, seven proteins were significantly down-regulated in fibrous plaque samples compared to normal.

			LAD		AA		
Uniprot ID	Protein	Gene	Fold-change	q-value	Fold-change	q-value	
P24821	Tenascin	TNC	13.04	1.08E-03	3.17	2.70E-03	up-regulated
P04114	Apolipoprotein B-100	APOB	3.65	6.26E-04	11.68	4.87E-03	
P13796	Plastin-2	LCP1	3.87	9.80E-04	9.22	4.50E-04	
P07858	Cathepsin B	CTSB	3.63	3.13E-04	5.99	4.84E-03	
P40121	Macrophage-capping protein	CAPG	2.72	6.89E-03	3.88	1.09E-02	
P35442	Thrombospondin-2	THBS2	2.69	4.40E-04	3.82	1.36E-03	
P01031	Complement C5	C5	1.89	1.58E-02	3.64	5.07E-03	
P31146	Coronin-1A	CORO1A	2.13	1.22E-02	3.30	3.13E-05	
P02649	Apolipoprotein E	APOE	1.79	1.28E-02	3.06	2.06E-01	
O43866	CD5 antigen-like	CD5L	2.10	1.22E-02	2.63	1.62E-02	
Q9UBR2	Cathepsin Z	CTSZ	2.20	9.53E-04	2.51	1.40E-02	
P01871	Ig mu chain C region	IGHM	2.15	8.14E-03	2.43	2.07E-02	
P46821	Microtubule-associated protein 1B	MAP1B	-1.90	4.59E-03	-4.11	4.00E-07	down-regulated
Q9HBI0	Tensin-1	TNS1	-2.01	5.58E-04	-3.72	1.73E-05	
O43175	D-3-phosphoglycerate dehydrogenase	PHGDH	-2.09	2.77E-04	-3.31	4.90E-06	
O75112	LIM domain-binding protein 3	LDB3	-1.98	1.70E-02	-2.48	3.29E-04	
P51911	Calponin-1	CNN1	-1.71	1.88E-03	-2.26	6.30E-04	
P27816	Microtubule-associated protein 4	MAP4	-1.78	1.28E-02	-2.01	3.71E-04	
P30084	Enoyl-CoA hydratase, mitochondrial	ECHS1	-1.71	1.36E-03	-1.87	2.10E-02	

Proteomic Architecture of Human Coronary and Aortic Atherosclerosis

Herrington David M[1]*, Mao Chunhong[2], Parker Sarah[3], Fu Zongming[4], Yu Guoqiang[5], Chen Lulu[5], Venkatraman Vidya[3], Fu Yi[5], Wang Yizhi[5], Howard Tim[6], Goo Jun[7], Zhao CF[1], Liu Yongming[8], Saylor Georgia[1], Athas Grace[9], Troxclair Dana[9], Hixson James[7]*, Vander Heide Richard[9]*, Wang Yue[4]*,Van Eyk Jennifer[3]* (*contributed equally)

Supplemental Figures

Table of Contents

Supplemental Figure 1a. Enriched GO:Biological Process Terms From Human LAD and AA Proteins
GO enrichment analysis was performed using 944 LAD proteins (left half of the plot – blue) and 725 AA proteins (right half of the plot – purple) that were included for subsequent analysis. GO terms with Bonferroni adjusted p-value <0.05 in either anatomic territory are presented.

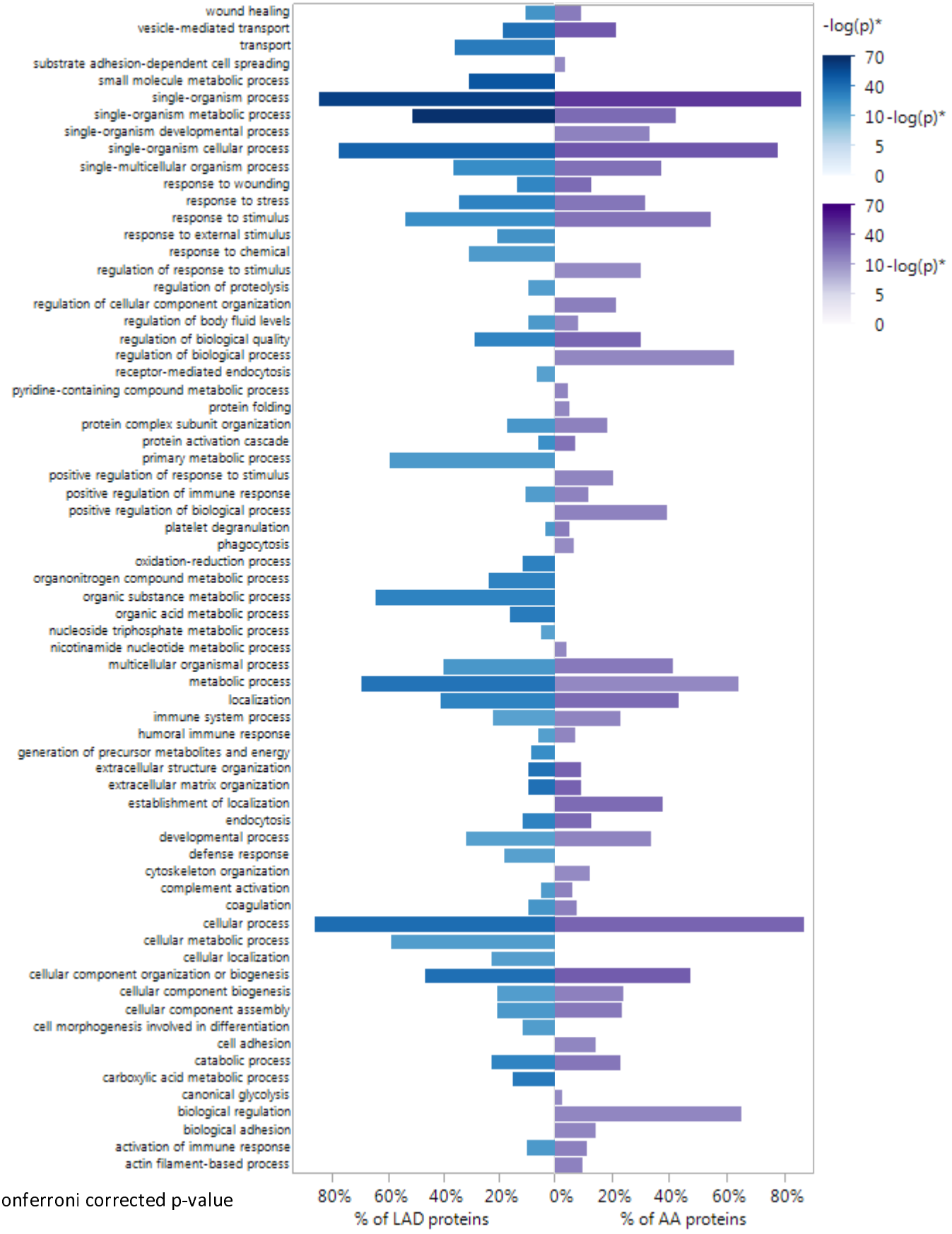

* Bonferroni corrected p-value

Supplemental Figure 1b. Enriched GO:Molecular Function Terms From Human LAD and AA Proteins
GO term enrichment analysis was performed using 944 LAD proteins (left half of the plot – blue) and 725 AA proteins (right half of the plot – purple) that were included for subsequent analysis. GO terms with Bonferroni adjusted p-value <0.05 in either anatomic territory are presented.

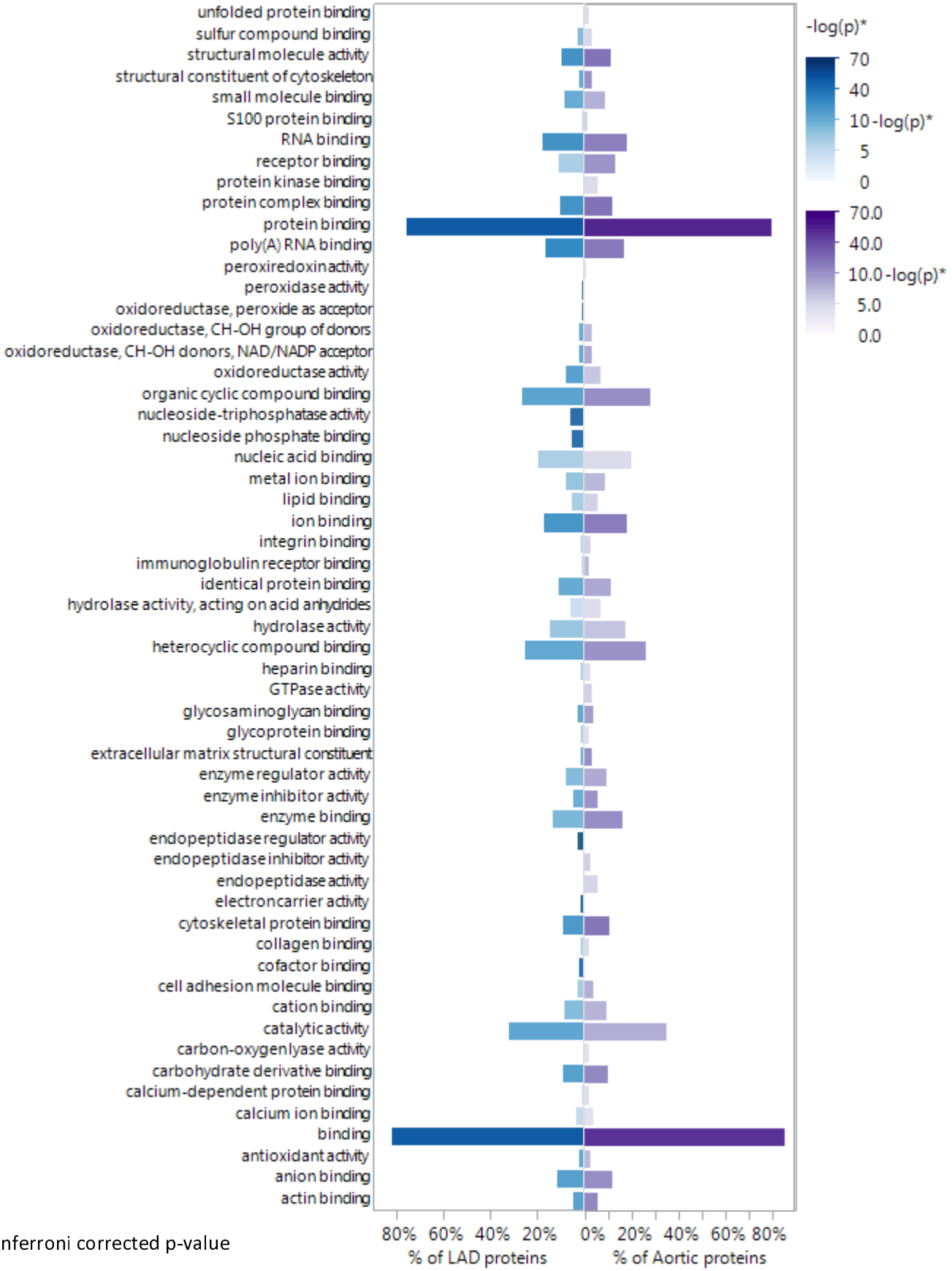

* Bonferroni corrected p-value

Supplemental Figure 1c. Enriched GO:Cellular Component Terms From Human LAD and AA Proteins
GO term enrichment analysis was performed using 944 LAD proteins (left half of the plot – blue) and 725 AA proteins (right half of the plot – purple) that were included for subsequent analysis. GO terms with Bonferroni adjusted p-value <0.05 in either anatomic territory are presented.

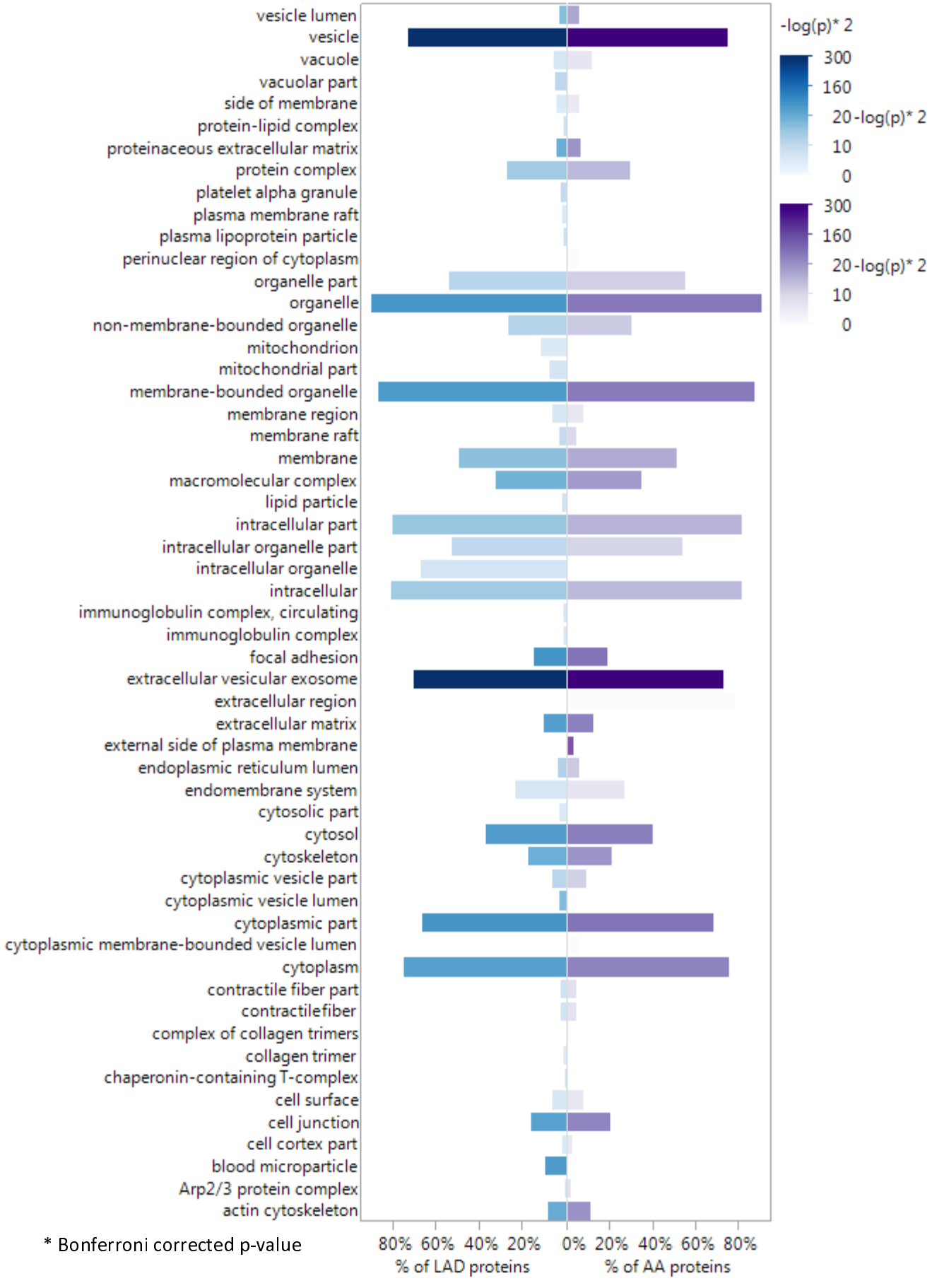

* Bonferroni corrected p-value

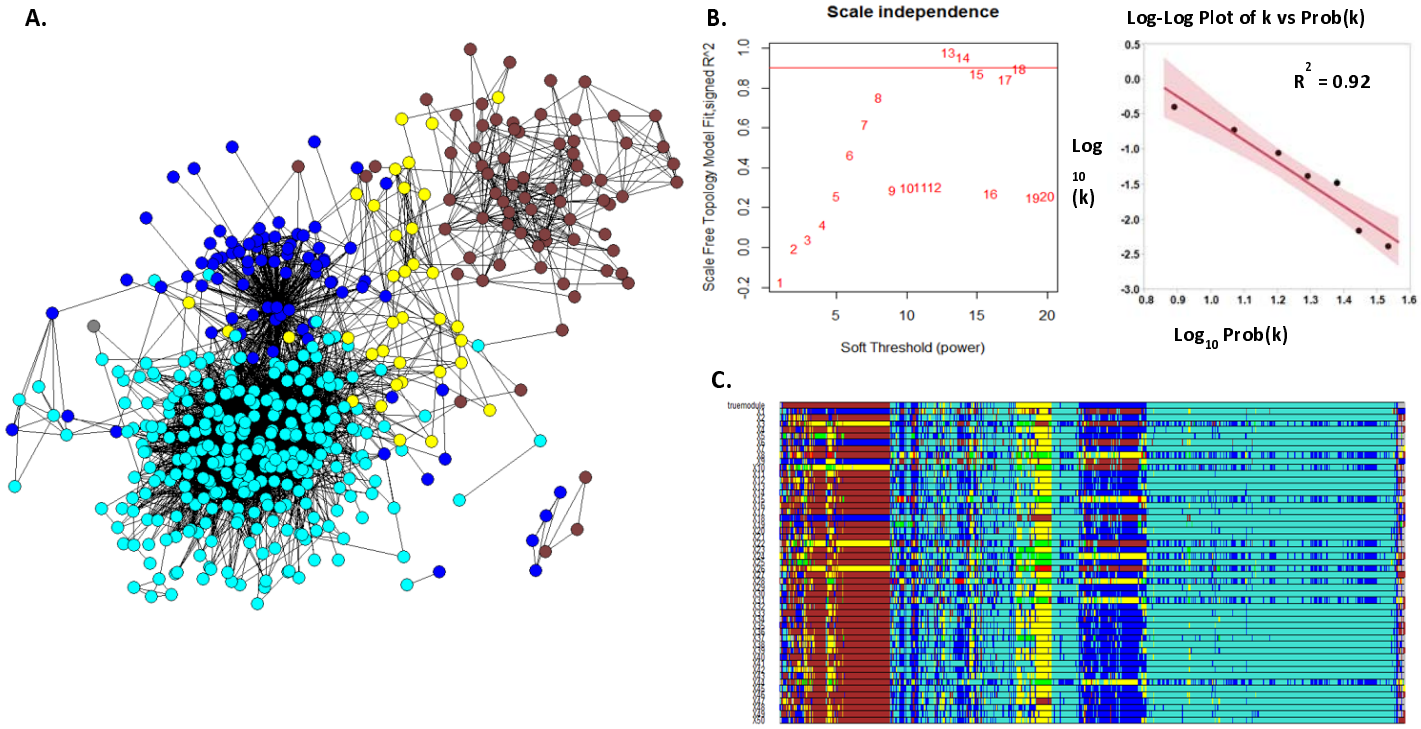

Supplemental Figure 2. Weighted Co-Expression Network Analysis of Human Abdominal Aortic (AA) Proteins A. Adjacency map of AA proteins color coded by module assignment based on hierarchical clustering of the topological overlap matrix (TOM)-based dissimilarity measure. For clarity of presentation only nodes (proteins) with at least one edge (adjacency measure (k)) > 98%tile are shown. B. Left panel shows that scale-free topology is well approximated when the adjacency power parameter β= 8. Right panel shows the log-log plot of adjacency (k) vs prob(k) with β= 8, supporting a power-law relationship in the connectivity of the expressed proteins. C. Module assignment for fifty 90% random samples of the data illustrating the overall stability of the modular structure of the protein expression patterns. Colors are assigned according cluster size which may vary with each random sample. As a result actual color assignment may vary from run to run, but module membership remains relatively stable.

Supplemental Figure 3. Number of identifiable proteins from human LAD and AA arterial samples. a. All samples (n=99 samples from each territory). Left Venn diagram: proteins detected at least once in any sample according to anatomic territory; Right Venn diagram: proteins detected in >50% of the samples. GO term analysis of the LAD only proteins indicated significant enrichment of mitochondrial proteins (p-values: unambiguous proteins = 1.8e-28; proteins with <50% missingness = 1.7e-6) b. Nomal samples only (n=30 from each territory). Left Venn diagram: proteins detected at least once in any sample according to anatomic territory; Right Venn diagram: proteins detected in >50% of the samples. GO term analysis of the LAD only proteins indicated significant enrichment of mitochondrial proteins (p-values: unambiguous proteins = 1.0e-13; proteins with <50% missingness p-value = 1.9e-12)

a. All Samples (LAD: n=99; AA: n=99)

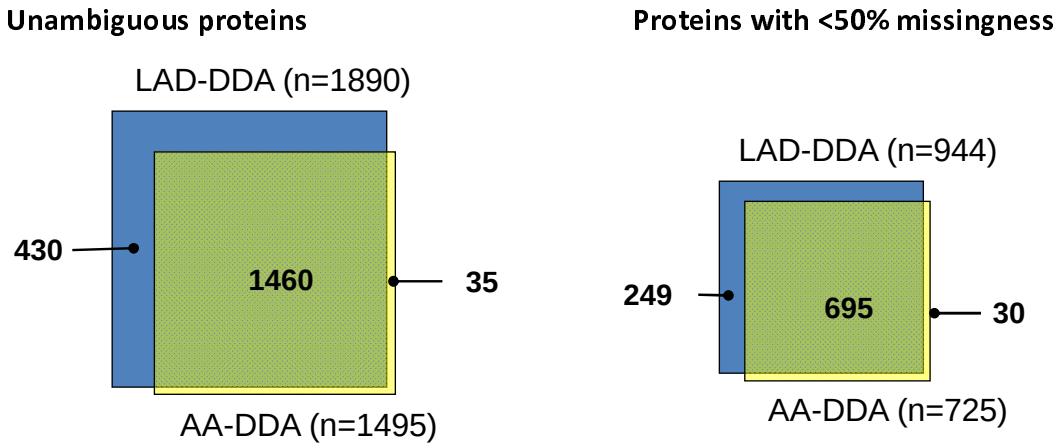

b. Normal Samples only (LAD: n=30; AA: n=30)

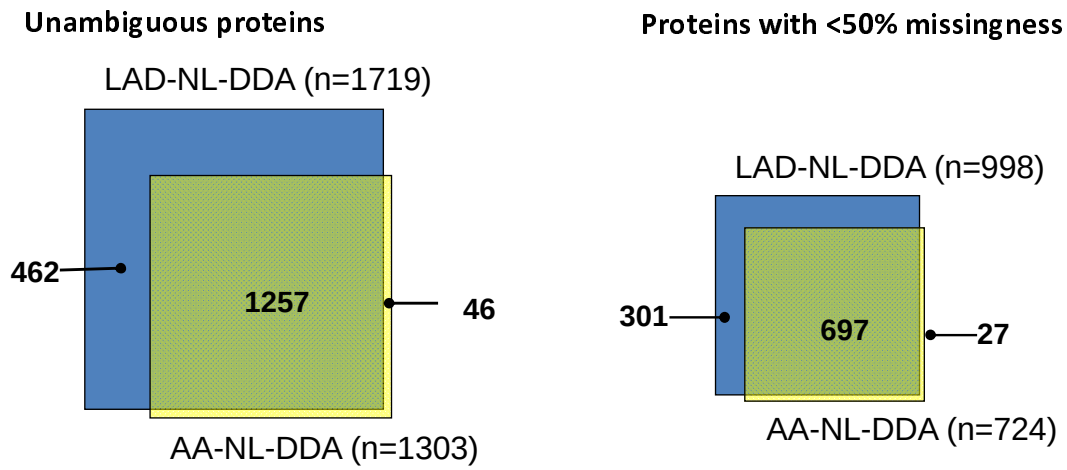

Supplemental Figure 4. Comparison of Mitochondrial Proteins in Normal LAD and AA Samples. Data independent MS (SWATH) analysis of completely normal LAD and AA samples (n=15 from each anatomic location) with adjustment for age, sex, MYH11, RABA7A, TERA, G6PI. Mean fold-difference = 6% (AA>LAD), p= 0.01.

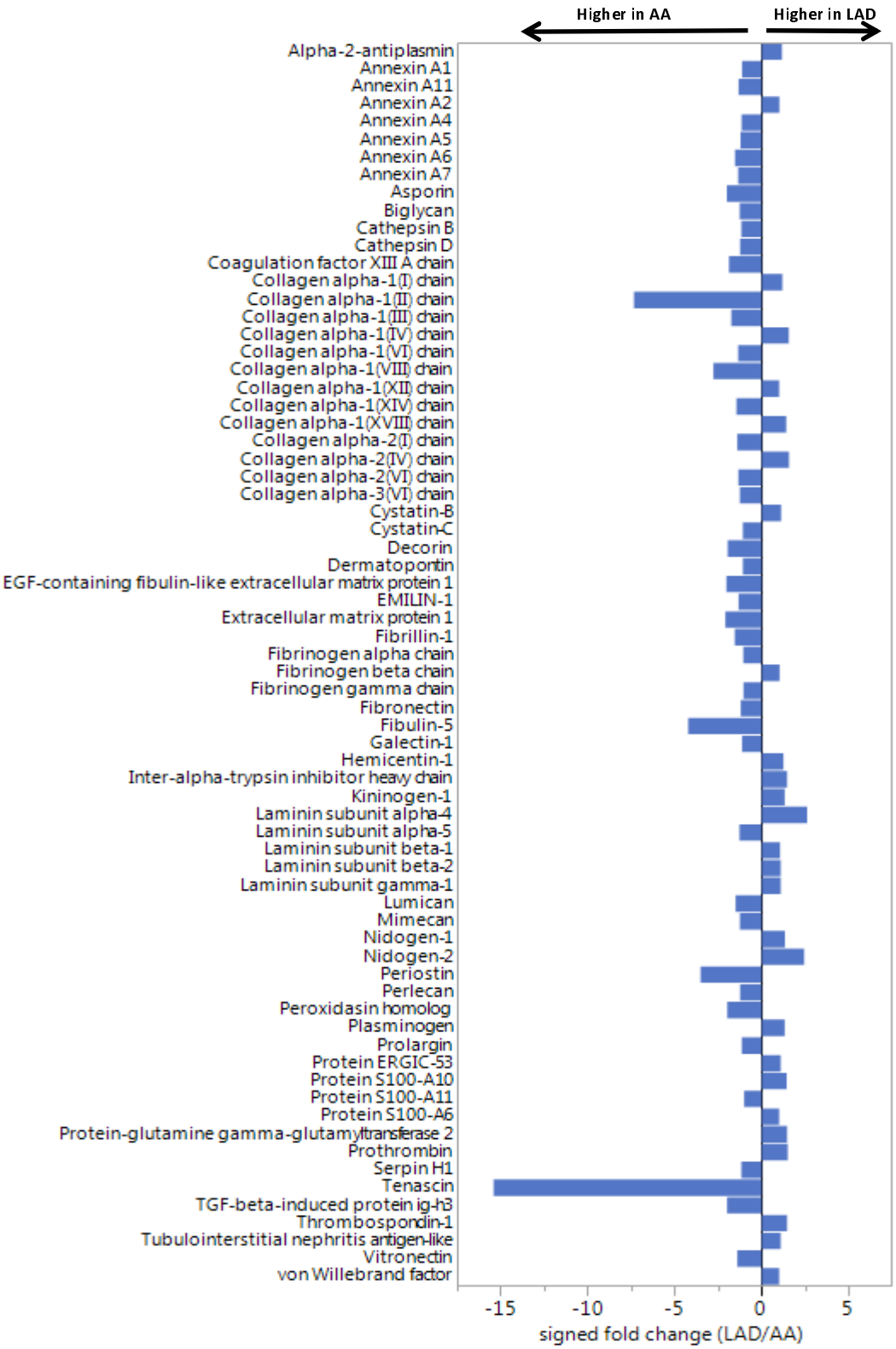

Supplemental Figure 5. Elastic Net Modelling of Proteins Predicting Presence or Absence of Fibrous Plaque in LAD (N=99) Samples. Graphs: Misclassification and AUC across a range of lambdas for two typical elastic net models predicting presence of fibrous plaque. Red points indicate the mean and bars indicate the SE for the estimate of misclassification or AUC across 10-folds in a cross-fold validation scheme. Numbers across the top indicate the number of variables (proteins) remaining in the model as the model progresses fr the most inclusive (left) to the most parsimonious (right).

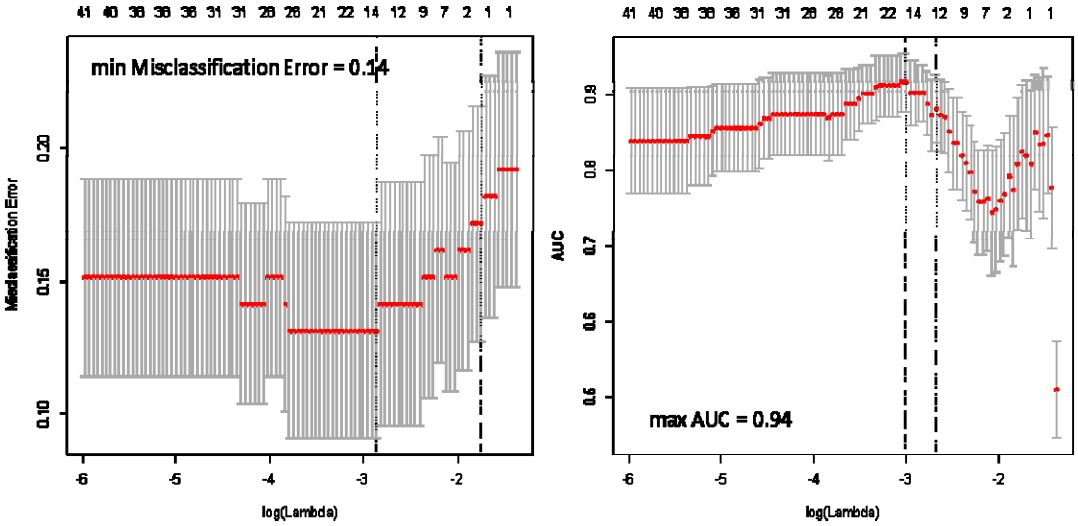

Table: Models were developed using cross-fold validation to select the lambdas optimizing AUC or misclassification. To minimize the effect of chance in selecting folds for the cross-fold validation each model was run 100 times and the selected proteins and their respective beta coefficients were recorded. The table indicates the number of times each protein was selected in each of 100 models and the mean beta for the subset of models where the protein in question was included. Proteins included in 10 or more models are indicated by bold in the # of models columns. Several highly correlated proteins competed for entry into these models.

			Maximizing AUC		Minimizing Misclassification	
Uniprot ID	Protein	Gene	# of models	mean *beta*	# of models	mean *beta*
P24821	Tenascin	TNC	**98**	0.2186	**99**	0.4057
O43852	Calumenin	CALU	**39**	1.2896	**76**	0.3454
Q8NBX0	Saccharopine dehydrogenase-like oxidoreductase	SCCPDH	**39**	0.9419	**46**	0.5198
O43866	CD5 antigen-like	CD5L	**39**	0.8716	**69**	0.2865
O14773	Tripeptidyl-peptidase 1	TPP1	**39**	0.7078	**76**	0.1898
Q15063	Periostin	POSTN	**39**	0.5949	**93**	0.1174
P07602	Prosaposin	PSAP	**39**	0.4851	**48**	0.2585
P13760	HLA class II histocompatibility antigen, DRB1-4 beta chain	HLA-DRB1	**39**	0.4804	**99**	0.1096
Q9UBR2	Cathepsin Z	CTSZ	**39**	0.2781	**85**	0.1031
Q6NZI2	Polymerase I and transcript release factor	PTRF	**39**	-0.9566	**46**	-0.5423
P07998	Ribonuclease pancreatic	RNASE1	**38**	0.0979	**23**	0.1233
P09543	2',3'-cyclic-nucleotide 3'-phosphodiesterase	CNP	**38**	-0.2526	**26**	-0.2877
Q03135	Caveolin-1	CAV1	**38**	-0.2749	**45**	-0.1503
P07858	Cathepsin B	CTSB	**32**	0.0764	**95**	0.0270
P04114	Apolipoprotein B-100	APOB	**21**	0.3371	**11**	0.5460
Q16853	Membrane primary amine oxidase	AOC3	**19**	-0.0698	**10**	-0.0813
P40261	Nicotinamide N-methyltransferase	NNMT	**17**	0.4705	8	0.9733
Q13200	26S proteasome non-ATPase regulatory subunit 2	PSMD2	**15**	-0.6538	6	-1.8703
P11586	C-1-tetrahydrofolate synthase, cytoplasmic	MTHFD1	**13**	-0.1454	3	-1.2007
P50395	Rab GDP dissociation inhibitor beta	GDI2	8	0.6810	3	2.5022
P63241	Eukaryotic translation initiation factor 5A-1	EIF5A	8	-0.7468	3	-3.2132
P08237	ATP-dependent 6-phosphofructokinase, muscle type	PFKM	7	0.5024	3	1.7951
Q06828	Fibromodulin	FMOD	7	-2.3252	3	-7.3673
P09960	Leukotriene A-4 hydrolase	LTA4H	6	0.9809	3	2.6087
P04844	Dolichyl-diphosphooligosaccharide--protein glycosyltransferase subunit 2	RPN2	2	3.3432	1	14.3237
P34932	Heat shock 70 kDa protein 4	HSPA4	2	5.1045	1	20.5268
P49908	Selenoprotein P	SEPP1	2	-5.0315	1	-17.3829
P52209	6-phosphogluconate dehydrogenase, decarboxylating	PGD	2	-3.5218	1	-10.0906
P84157	Matrix-remodeling-associated protein 7	MXRA7	2	-4.9994	1	-19.5041
O95834	Echinoderm microtubule-associated protein-like 2	EML2	1	2.4512	1	3.3472
P14174	Macrophage migration inhibitory factor	MIF	1	-2.0485	1	-3.4632

P21926	CD9 antigen	CD9	1	-0.8408	1	-1.0123
P28482	Mitogen-activated protein kinase 1	MAPK1	1	3.6737	1	4.5044
P43652	Afamin	AFM	1	2.9634	1	3.4717

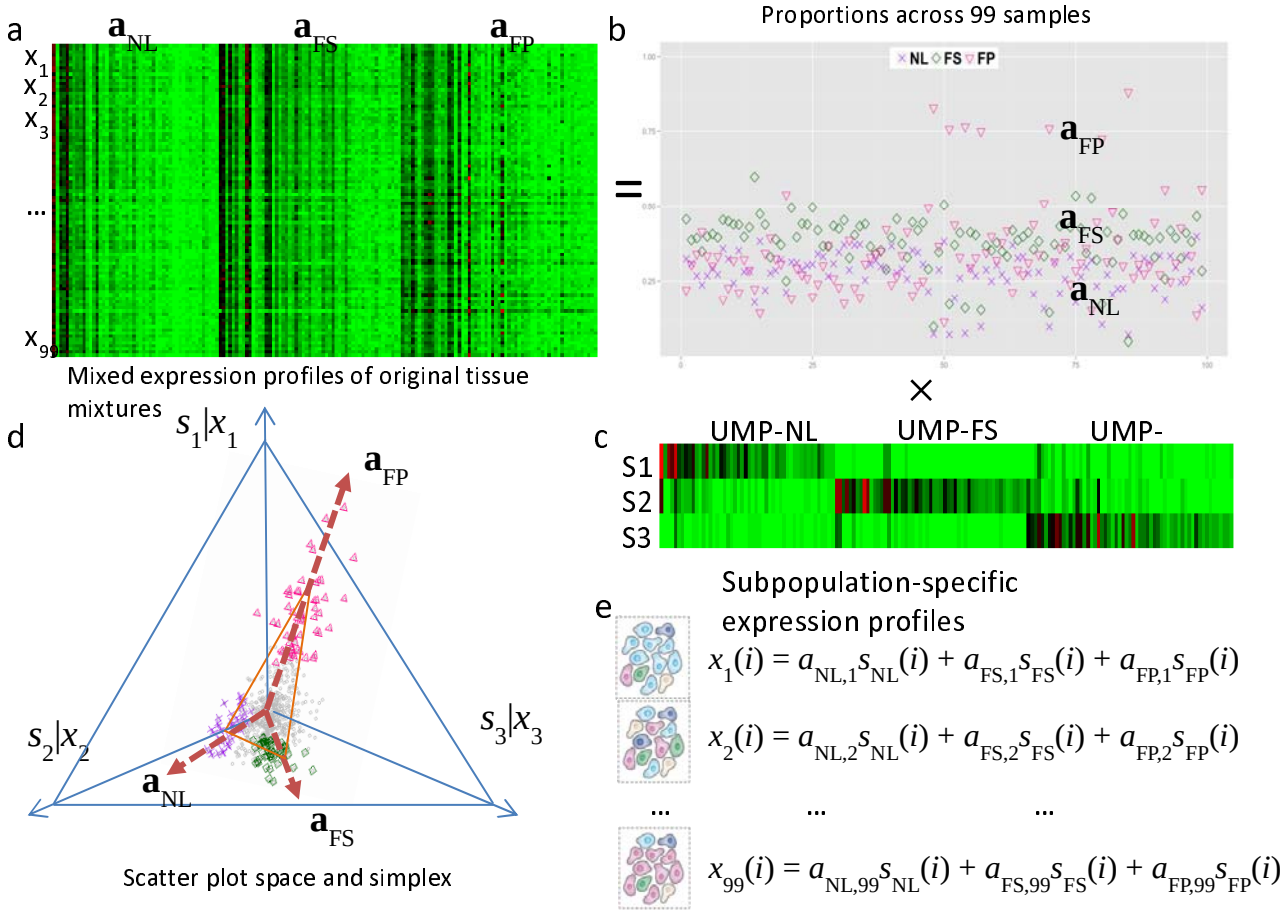

Supplementary Figure 6 Convex Analysis of Mixtures of AA Protein Data. a. Heatmap of mixed expressions of upregulated marker proteins (UMP) in 99 AA samples. b. Estimated proportions of NL, FS, and FP across 99 AA samples. Note: The AA data only supported identification of three vertices compared with four vertices in the LAD data. c. Heatmap of subpopulation-specific expressions of upregulated marker proteins. d. Geometry of the mixing operation in scatter space that produces a compressed and rotated scatter simplex whose vertices host subpopulation-specific upregulated marker proteins and correspond to mixing proportions. e. Mathematical description on the protein expression readout of multiple distinct subpopulations.

Supplemental Figure 7. Convex Analysis of Mixtures (CAM) Identified Upregulated Fibrous Plaque Marker Proteins for LAD (n=99) and AA (n=99) Samples.

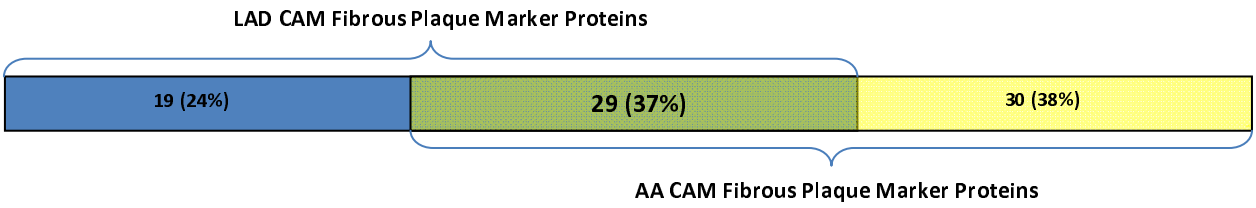

LAD Only			LAD and AA			AA Only		
UniprotID	*Protein*	*Gene*	*UniprotID*	*Protein*	*Gene*	*UniprotID*	*Protein*	*Gene*
Q8IUX7	Adipocyte enhancer-binding protein 1	AEBP1	P04114	Apolipoprotein B-100	APOB	P01023	Alpha-2-macroglobulin	A2M
P01024	Complement C3	C3	P02649	Apolipoprotein E	APOE	P02765	Alpha-2-HS-glycoprotein	AHSG
P07358	Complement component C8 beta chain	C8B	O14791	Apolipoprotein L1	APOL1	P05090	Apolipoprotein D	APOD
P07360	Complement component C8 gamma chain	C8G	P00736	Complement C1r subcomponent	C1R	P0C0L5	Complement C4-B	C4B
Q99715	Collagen alpha-1(XII) chain	COL12A1	P04003	C4b-binding protein alpha chain	C4BPA	P00751	Complement factor B	CFB
Q9UBR2	Cathepsin Z	CTSZ	P01031	Complement C5	C5	Q9BXR6	Complement factor H-related protein 5	CFHR5
P02751	Fibronectin	FN1	P10643	Complement component C7	C7	P00450	Ceruloplasmin	CP
P13760	HLA class II HCAg, DRB1-4 beta chain	HLA-DRB1	P40121	Macrophage-capping protein	CAPG	P59665	Neutrophil defensin 1	DEFA1
Q92743	Serine protease HTRA1	HTRA1	O43866	CD5 antigen-like	CD5L	P00488	Coagulation factor XIII A chain	F13A1
P35858	IGF-binding protein complex acid labile subunit	IGFALS	P08603	Complement factor H	CFH	P00734	Prothrombin	F2
P05783	Keratin, type I cytoskeletal 18	KRT18	P05156	Complement factor I	CFI	P02671	Fibrinogen alpha chain	FGA
P08519	Apolipoprotein(a)	LPA	P31146	Coronin-1A	CORO1A	P02794	Ferritin heavy chain	FTH1
P01620	Ig kappa chain V-III region SIE	none	P07858	Cathepsin B	CTSB	P02792	Ferritin light chain	FTL
Q15063	Periostin	POSTN	P07339	Cathepsin D	CTSD	P69905	Hemoglobin subunit alpha	HBA1
P34096	Ribonuclease 4	RNASE4	P02675	Fibrinogen beta chain	FGB	P69891	Hemoglobin subunit gamma-1	HBG1
P06702	Protein S100-A9	S100A9	P02679	Fibrinogen gamma chain	FGG	P01892	HLA class I HCAg, A-2 alpha chain	HLA-A
Q15582	TGFB-induced protein Ig-h3	TGFBI	P01871	Ig mu chain C region	IGHM	P00739	Haptoglobin	HP
P07996	Thrombospondin-1	THBS1	P19827	Inter-alpha-trypsin inhibitor heavy chain H1	ITIH1	P00739	Haptoglobin-related protein	HPR
P04004	Vitronectin	VTN	P19823	Inter-alpha-trypsin inhibitor heavy chain H2	ITIH2	P04196	Histidine-rich glycoprotein	HRG
			P18428	Lipopolysaccharide-binding protein	LBP	P01877	Ig alpha-2 chain C region	IGHA2
			P13796	Plastin-2	LCP1	P06312	Ig kappa chain V-IV region (Fragment)	IGKV4-1
			P61626	Lysozyme C	LYZ	Q14624	Inter-alpha-trypsin inhibitor heavy chain H4	ITIH4
			P40261	Nicotinamide N-methyltransferase	NNMT	P01042	Kininogen-1	KNG1
			Q96PD5	N-acetylmuramoyl-L-alanine amidase	PGLYRP2	P20700	Lamin-B1	LMNB1
			P27169	Serum paraoxonase/arylesterase 1	PON1	P01594	Ig kappa chain V-I region AU	none
			P05546	Heparin cofactor 2	SERPIND1	P52209	6-phosphogluconate dehydrogenase, decarboxylating	PGD
			P02730	Band 3 anion transport protein	SLC4A1	P00747	Plasminogen	PLG
			P35442	Thrombospondin-2	THBS2	P20742	Pregnancy zone protein	PZP
			P24821	Tenascin	TNC	P05155	Plasma protease C1 inhibitor	SERPING1
						P04179	Superoxide dismutase [Mn], mitochondrial	SOD2

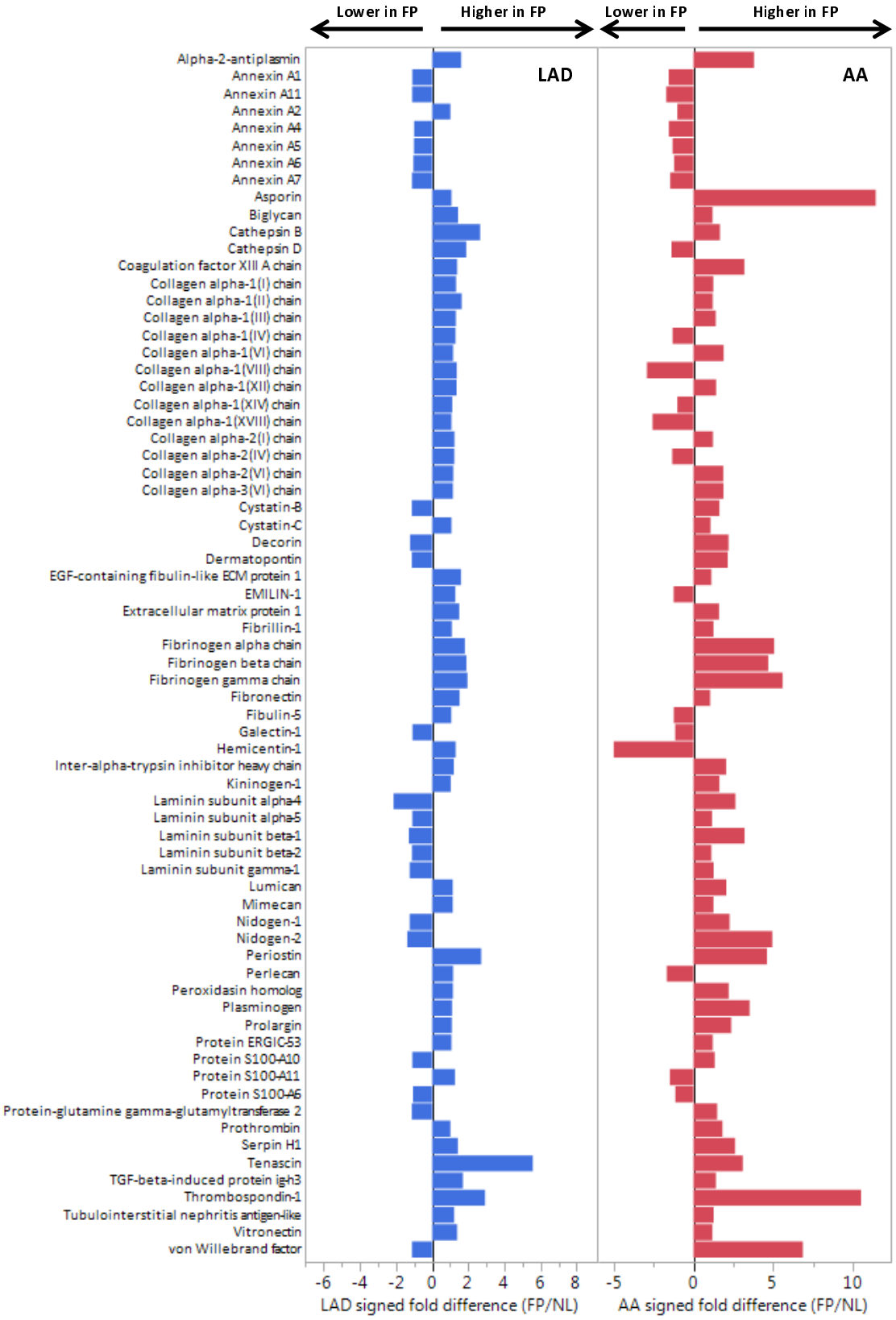

Supplemental Figure 8. Comparison of Extracellular Matrix Proteins in FP vs NL Samples in LAD and AA Samples Data independent acquisition (SWATH) analysis was used to compare a targeted set of mitochondrial proteins in LAD (FP n=15; NL n=30) and AA (FP n=9; NL n=18) samples after adjustment for age, sex, MYH11, RABA7A, TERA, G6PI. Histogram bars indicate relative difference between FP and NL samples in each anatomic location. LAD Mean FP/NL = 1.25, MANOVA p-value = 0.02; AA Mean FP/NL = 1.78, p-value = 0.017

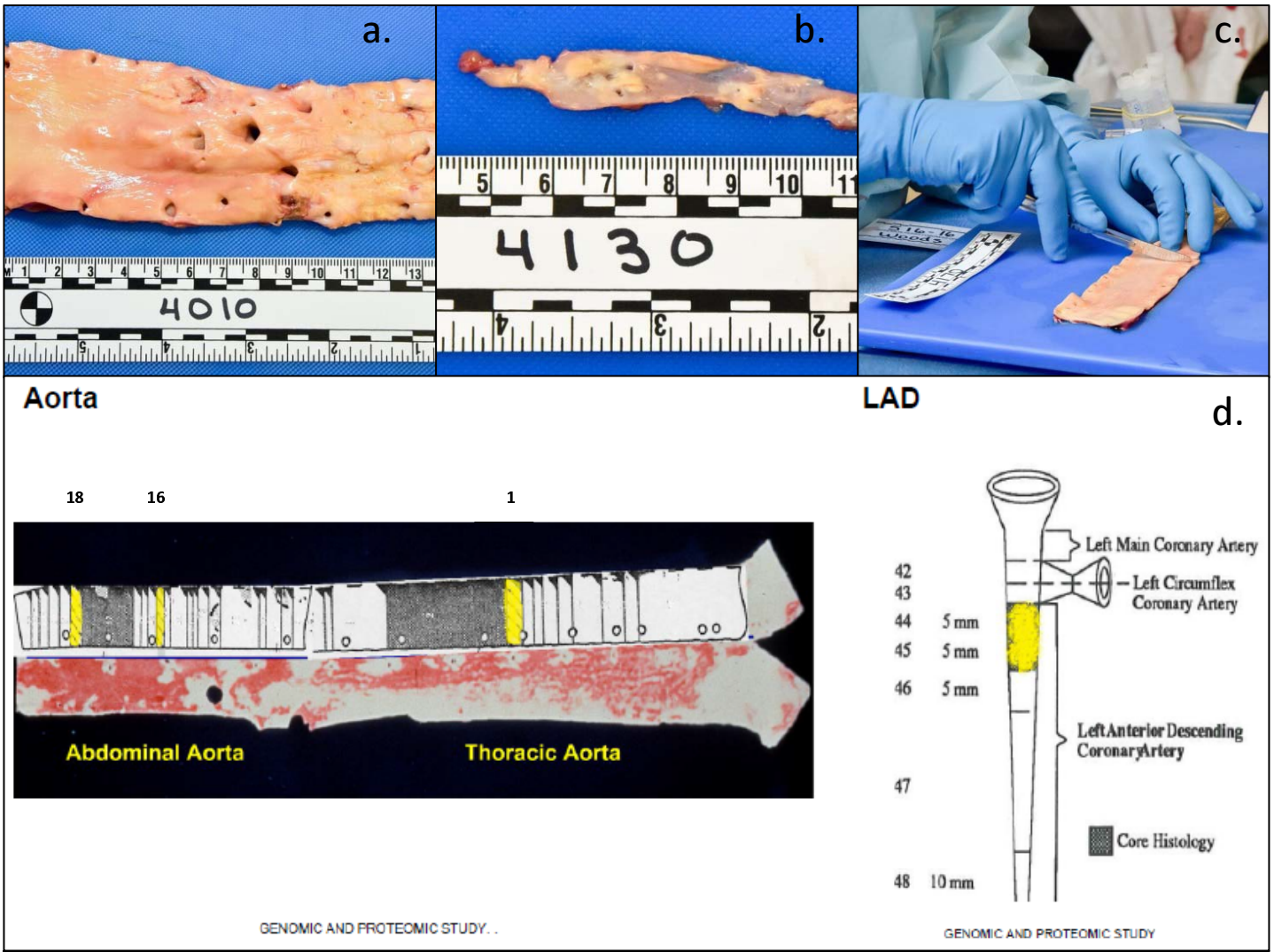

Supplemental Figure 9. Arterial Sample Acquisition: **a**.) distal aorta; **b**.) left anterior descending (LAD) coronary artery; **c**.) collection of a gram of tissue from the distal aortic specimen; **d**.) Standardized locations for sample collection. Specimens were obtained from Sections 1, 16, 18, 44 and 45 (indicated in yellow) for all autopsies. These locations correspond to locations originally established and used for the Pathobiological Determinants of Atherosclerosis in Youth study[29].

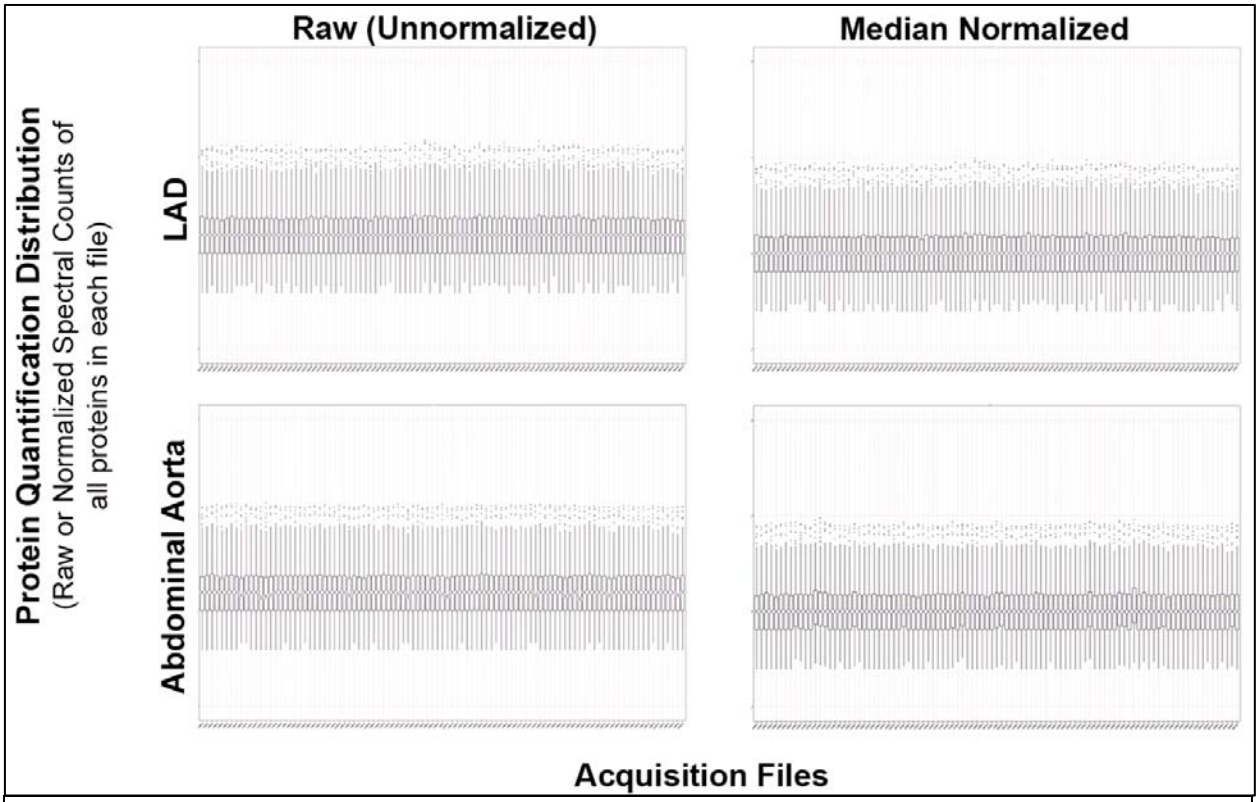

Supplemental Figure 10. Acquisition and Protein Quantification Quality Control (QC). QC was assessed by plotting the distribution in the form of a box and whisker plot of protein quantitation values for all identified proteins across all acquired specimen. Notches represent the 95% confidence interval of the median, and files with unaligned notches represent substantially different quantitative distributions. Using this approach, while the LAD files all had nicely aligned quantitative distributions of raw spectral counts with overlapping medians for all files (upper left panel), the aorta samples had some acquisitions with uneven quantitative distribution. For aorta

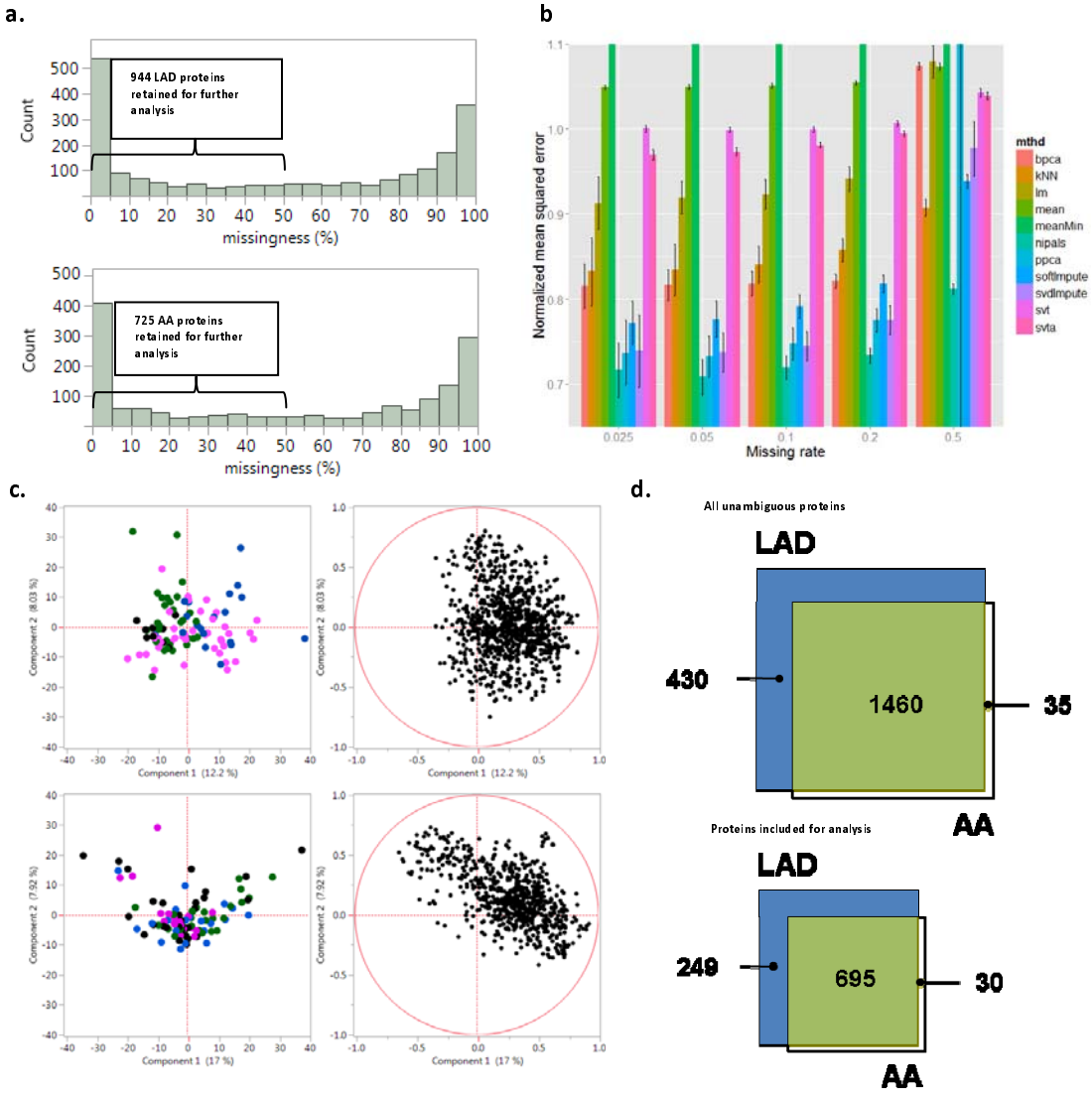

Supplemental Figure 11. Data missingness, imputation, batch affects and anatomic overlap. a.) Distribution of missingness for the LAD and AA data. The most common value for missingness was 0% in both the LAD and AA. However, there was a range of missingness including some unambiguously identified protein groups that were only present in a minority of samples. Missingness encoded models did not identify any proteins with >50% missingness that were significantly associated with disease status. b.) Using proteins with complete data (0% missingness) data sets simulating various rates (2.5%-50.0%), and types (random, inversely proportional with mean signal intensity) of missingness were used to test 11 different matrix completion methods. Based on the low normalized mean squared error, the NPIALS method was selected for imputation. c.) PCA analysis with color encoding for different protein extraction batches did not identify important batch effects or extreme outliers. d.) Proportional Venn diagrams indicating the overlap in identified and analyzed proteins in the LAD and AA territories.

REFERENCES

1. Hanzawa, H., *et al.* Combined Plasma and Tissue Proteomic Study of Atherogenic Model Mouse: Approach To Elucidate Molecular Determinants in Atherosclerosis Development. *Journal of proteome research* **14**, 4257-4269 (2015).

2. Jing, L., *et al.* Discovery of biomarker candidates for coronary artery disease from an APOE-knock out mouse model using iTRAQ-based multiplex quantitative proteomics. *Proteomics* **11**, 2763-2776 (2011).

3. Mayr, M., *et al.* Proteomic and metabolomic analyses of atherosclerotic vessels from apolipoprotein E-deficient mice reveal alterations in inflammation, oxidative stress, and energy metabolism. *Arteriosclerosis, thrombosis, and vascular biology* **25**, 2135-2142 (2005).

4. Fach, E.M., *et al.* In vitro biomarker discovery for atherosclerosis by proteomics. *Molecular & cellular proteomics : MCP* **3**, 1200-1210 (2004).

5. Conway, J.P. & Kinter, M. Proteomic and transcriptomic analyses of macrophages with an increased resistance to oxidized low density lipoprotein (oxLDL)-induced cytotoxicity generated by chronic exposure to oxLDL. *Molecular & cellular proteomics : MCP* **4**, 1522-1540 (2005).

6. Olson, F.J., *et al.* Consistent differences in protein distribution along the longitudinal axis in symptomatic carotid atherosclerotic plaques. *Biochemical and biophysical research communications* **401**, 574-580 (2010).

7. Liang, W., *et al.* Distinctive proteomic profiles among different regions of human carotid plaques in men and women. *Scientific reports* **6**, 26231 (2016).

8. Didangelos, A., *et al.* Extracellular matrix composition and remodeling in human abdominal aortic aneurysms: a proteomics approach. *Molecular & cellular proteomics : MCP* **10**, M111.008128 (2011).

9. Porcelli, B., *et al.* Proteomic analysis of atherosclerotic plaque. *Biomedicine & pharmacotherapy = Biomedecine & pharmacotherapie* **64**, 369-372 (2010).

10. Lepedda, A.J., *et al.* A proteomic approach to differentiate histologically classified stable and unstable plaques from human carotid arteries. *Atherosclerosis* **203**, 112-118 (2009).

11. de la Cuesta, F., *et al.* A proteomic focus on the alterations occurring at the human atherosclerotic coronary intima. *Molecular & cellular proteomics : MCP* **10**, M110.003517 (2011).

12. Bagnato, C., *et al.* Proteomics analysis of human coronary atherosclerotic plaque: a feasibility study of direct tissue proteomics by liquid chromatography and tandem mass spectrometry. *Molecular & cellular proteomics : MCP* **6**, 1088-1102 (2007).

13. Didangelos, A., *et al.* Proteomics characterization of extracellular space components in the human aorta. *Molecular & cellular proteomics : MCP* **9**, 2048-2062 (2010).

14. Mayr, M., *et al.* Proteomics, metabolomics, and immunomics on microparticles derived from human atherosclerotic plaques. *Circulation. Cardiovascular genetics* **2**, 379-388 (2009).

15. Viiri, L.E., *et al.* Smooth muscle cells in human atherosclerosis: proteomic profiling reveals differences in expression of Annexin A1 and mitochondrial proteins in carotid disease. *Journal of molecular and cellular cardiology* **54**, 65-72 (2013).

16. Fredman, G., *et al.* An imbalance between specialized pro-resolving lipid mediators and pro-inflammatory leukotrienes promotes instability of atherosclerotic plaques. *Nature communications* **7**, 12859 (2016).

17. Preil, S.A., *et al.* Quantitative Proteome Analysis Reveals Increased Content of Basement Membrane Proteins in Arteries From Patients With Type 2 Diabetes Mellitus and Lower Levels Among Metformin Users. *Circulation. Cardiovascular genetics* **8**, 727-735 (2015).

18. Maleki, S., *et al.* Mesenchymal state of intimal cells may explain higher propensity to ascending aortic aneurysm in bicuspid aortic valves. *Scientific reports* **6**, 35712 (2016).

19. Gene Ontology Consortium: going forward. *Nucleic acids research* **43**, D1049-1056 (2015).

20. Carter, S.L., Brechbuhler, C.M., Griffin, M. & Bond, A.T. Gene co-expression network topology provides a framework for molecular characterization of cellular state. *Bioinformatics (Oxford, England)* **20**, 2242-2250 (2004).

21. Jeong, H., Tombor, B., Albert, R., Oltvai, Z.N. & Barabasi, A.L. The large-scale organization of metabolic networks. *Nature* **407**, 651-654 (2000).

22. Bergmann, S., Ihmels, J. & Barkai, N. Similarities and differences in genome-wide expression data of six organisms. *PLoS biology* **2**, E9 (2004).

23. Mitchell, M. *Complexity: A Guided Tour*, (Oxford University Press, New York, New York, 2009).

24. Gao, J., Barzel, B. & Barabasi, A.L. Universal resilience patterns in complex networks. *Nature* **536**, 238 (2016).

25. Creixell, P., Schoof, E.M., Erler, J.T. & Linding, R. Navigating cancer network attractors for tumor-specific therapy. *Nature biotechnology* **30**, 842-848 (2012).

26. Mitra, K., Carvunis, A.R., Ramesh, S.K. & Ideker, T. Integrative approaches for finding modular structure in biological networks. *Nature reviews. Genetics* **14**, 719-732 (2013).

27. Ideker, T. & Krogan, N.J. Differential network biology. *Molecular systems biology* **8**, 565 (2012).

28. Boccaletti, S., Latora, V., Moreno, Y., Chavez, M. & Hwang, D. Complex Networks: Structure and Dynamics *Physics Reports* **424**, 175-308 (2006).

29. Mercer, J.R., *et al.* DNA damage links mitochondrial dysfunction to atherosclerosis and the metabolic syndrome. *Circulation research* **107**, 1021-1031 (2010).

30. Sergin, I., *et al.* Exploiting macrophage autophagy-lysosomal biogenesis as a therapy for atherosclerosis. *Nature communications* **8**, 15750 (2017).

31. Chen, Q., Smith, C.Y., Bailey, K.R., Wennberg, P.W. & Kullo, I.J. Disease location is associated with survival in patients with peripheral arterial disease. *Journal of the American Heart Association* **2**, e000304 (2013).

32. Kullo, I.J. & Leeper, N.J. The genetic basis of peripheral arterial disease: current knowledge, challenges, and future directions. *Circulation research* **116**, 1551-1560 (2015).

33. Hansson, G.K. Inflammation, atherosclerosis, and coronary artery disease. *The New England journal of medicine* **352**, 1685-1695 (2005).

34. Tabas, I. The role of endoplasmic reticulum stress in the progression of atherosclerosis. *Circulation research* **107**, 839-850 (2010).

35. Strong, J.P.*, et al.* Prevalence and extent of atherosclerosis in adolescents and young adults: implications for prevention from the Pathobiological Determinants of Atherosclerosis in Youth Study. *Jama* **281**, 727-735 (1999).

36. Chambers, M.C.*, et al.* A cross-platform toolkit for mass spectrometry and proteomics. *Nature biotechnology* **30**, 918-920 (2012).

37. Craig, R. & Beavis, R.C. TANDEM: matching proteins with tandem mass spectra. *Bioinformatics (Oxford, England)* **20**, 1466-1467 (2004).

38. Geer, L.Y.*, et al.* Open mass spectrometry search algorithm. *Journal of proteome research* **3**, 958-964 (2004).

39. Elias, J.E. & Gygi, S.P. Target-decoy search strategy for increased confidence in large-scale protein identifications by mass spectrometry. *Nature methods* **4**, 207-214 (2007).

40. Apweiler, R.*, et al.* UniProt: the Universal Protein knowledgebase. *Nucleic acids research* **32**, D115-119 (2004).

41. Keller, A., Eng, J., Zhang, N., Li, X.J. & Aebersold, R. A uniform proteomics MS/MS analysis platform utilizing open XML file formats. *Molecular systems biology* **1**, 2005.0017 (2005).

42. Keller, A., Nesvizhskii, A.I., Kolker, E. & Aebersold, R. Empirical statistical model to estimate the accuracy of peptide identifications made by MS/MS and database search. *Analytical chemistry* **74**, 5383-5392 (2002).

43. Shteynberg, D.*, et al.* iProphet: multi-level integrative analysis of shotgun proteomic data improves peptide and protein identification rates and error estimates. *Molecular & cellular proteomics : MCP* **10**, M111.007690 (2011).

44. Nesvizhskii, A.I., Keller, A., Kolker, E. & Aebersold, R. A statistical model for identifying proteins by tandem mass spectrometry. *Analytical chemistry* **75**, 4646-4658 (2003).

45. Vogel, C. & Marcotte, E.M. Label-free protein quantitation using weighted spectral counting. *Methods in molecular biology (Clifton, N.J.)* **893**, 321-341 (2012).

46. Vizcaino, J.A.*, et al.* The PRoteomics IDEntifications (PRIDE) database and associated tools: status in 2013. *Nucleic acids research* **41**, D1063-1069 (2013).

47. Cand`es, E. & Recht, B. Exact Matrix Completion via Convex Optimization. *Foundations of Computational mathematics* **9.6**, 717-772 (2009).

48. Zhang, B. & Horvath, S. A general framework for weighted gene co-expression network analysis. *Statistical applications in genetics and molecular biology* **4**, Article17 (2005).

49. Buettner, F.*, et al.* Computational analysis of cell-to-cell heterogeneity in single-cell RNA-sequencing data reveals hidden subpopulations of cells. *Nature biotechnology* **33**, 155-160 (2015).

50. Lake, B.B.*, et al.* Neuronal subtypes and diversity revealed by single-nucleus RNA sequencing of the human brain. *Science (New York, N.Y.)* **352**, 1586-1590 (2016).

51. Guintivano, J., Aryee, M.J. & Kaminsky, Z.A. A cell epigenotype specific model for the correction of brain cellular heterogeneity bias and its application to age, brain region and major depression. *Epigenetics* **8**, 290-302 (2013).

52. Kuhn, A., Thu, D., Waldvogel, H.J., Faull, R.L. & Luthi-Carter, R. Population-specific expression analysis (PSEA) reveals molecular changes in diseased brain. *Nature methods* **8**, 945-947 (2011).

53. Rahmani, E.*, et al.* Sparse PCA corrects for cell type heterogeneity in epigenome-wide association studies. *Nature methods* **13**, 443-445 (2016).

54. Chan, T., Ma, W., Chi, C. & Wang, Y. A convex analysis framework for blind separation of non-negative sources. *IEEE Trans Signal Processing* **56**, 5120-5134 (2008).

55. Wang, N.*, et al.* Mathematical modelling of transcriptional heterogeneity identifies novel markers and subpopulations in complex tissues. *Scientific reports* **6**, 18909 (2016).

56. Chen, L.*, et al.* CAM-CM: a signal deconvolution tool for in vivo dynamic contrast-enhanced imaging of complex tissues. *Bioinformatics (Oxford, England)* **27**, 2607-2609 (2011).

57. Chen, L.*, et al.* Tissue-specific compartmental analysis for dynamic contrast-enhanced MR imaging of complex tumors. *IEEE transactions on medical imaging* **30**, 2044-2058 (2011).

58. Frey, B.J. & Dueck, D. Clustering by passing messages between data points. *Science (New York, N.Y.)* **315**, 972-976 (2007).

59. Boyle, E.I.*, et al.* GO::TermFinder--open source software for accessing Gene Ontology information and finding significantly enriched Gene Ontology terms associated with a list of genes. *Bioinformatics (Oxford, England)* **20**, 3710-3715 (2004).

60. Supek, F., Bosnjak, M., Skunca, N. & Smuc, T. REVIGO summarizes and visualizes long lists of gene ontology terms. *PloS one* **6**, e21800 (2011).

61. Hu, J.X., Thomas, C.E. & Brunak, S. Network biology concepts in complex disease comorbidities. *Nature reviews. Genetics* **17**, 615-629 (2016).

62. Hudson, N.J., Dalrymple, B.P. & Reverter, A. Beyond differential expression: the quest for causal mutations and effector molecules. *BMC genomics* **13**, 356 (2012).

63. Zhang, B.*, et al.* DDN: a caBIG(R) analytical tool for differential network analysis. *Bioinformatics (Oxford, England)* **27**, 1036-1038 (2011).

64. Tian, Y.*, et al.* Knowledge-fused differential dependency network models for detecting significant rewiring in biological networks. *BMC systems biology* **8**, 87 (2014).

65. Tian, Y.*, et al.* KDDN: an open-source Cytoscape app for constructing differential dependency networks with significant rewiring. *Bioinformatics (Oxford, England)* **31**, 287-289 (2015).